Curriculum Vitae

Name: Susan L. Mercer

Degree and Date to be Conferred: Ph.D., 2008

Collegiate Institutions Attended:

Seton Hill University, Greensburg, PA 15601 – **2000-2004**
B.S. awarded May 2004
Major: Chemistry
Minor: Forensic Science

University of Maryland, Baltimore, Baltimore, MD 21201 – **2004-2008**
Ph.D. awarded August 2008
Major: Pharmaceutical Sciences
Focus: Medicinal Chemistry

Professional Publications:

1. Koek W, Chen W, **Mercer SL**, Coop A, France CP. Discriminative stimulus effects of gamma-hydroxybutyrate (GHB): role of training dose. *J. Pharmacol. Exp. Ther.* **2006**; 317(1): 409-417.

2. **Mercer SL**, Hassan HE, Cunningham CW, Eddington ND, Coop A. Opioids and efflux transporters. Part 1: P-Glycoprotein substrate activity of N-substituted analogs of meperidine. *Bioorg. Med. Chem. Lett.* **2007**; 17(5): 1160-1162.

3. Koek W, **Mercer SL**, Coop A. Cataleptic effects of GHB, its precursor GBL, and $GABA_B$ agonists: differential antagonism by CGP35348. *Psychopharmacology* **2007**; 192(3): 407-414.

4. Cunningham CW, **Mercer SL**, Hassan HE, Traynor JR, Eddington ND, Coop A. Opioids and efflux transporters. Part 2: P-Glycoprotein substrate activity of 3- and 6-substituted morphine analogs. *J Med.Chem.* **2008**; 51(7): 2316-2320.

5. **Mercer SL**, Shaikh J, Traynor JR, Matsumoto RR, Coop A. Nitrile analogs of meperidine as high affinity and selective sigma-1 receptor ligands. *Eur. J. Med. Chem.* **2008**; 43(6): 1304-1308.

6. **Mercer SL**, Cunningham CW, Eddington ND, Coop A. Opioids and efflux transporters. Part 3: P-glycoprotein substrate activity of 3-hydroxyl addition to meperidine analogs. *Bioorg. Med. Chem. Lett.* **2008**; 18(12): 3638-3640.

7. Hassan HE, **Mercer SL**, Cunningham CW, Coop A, Eddington ND. Evaluation of the P- glycoprotein affinity status of a series of novel and currently available morphine analogs: comparative study with meperidine analogs to identify opioids with minimal P-gp interactions. *Int. J. Pharmaceutics.* Accepted.

8. **Mercer SL** and Coop A. Opioid analgesics and P-glycoprotein efflux transporters: A potential systems-level contribution to analgesic tolerance. *Curr. Top. Med. Chem.* In Review.

Selected Professional Abstracts:

1. **SL Mercer**, CW Cunningham, HE Hassan, ND Eddington, A Coop. The Relative Activity of Meperidine Analogs as P-glycoprotein Substrates. University of Maryland, Baltimore, School of Pharmacy Annual Research Day. Baltimore, MD. May **2006**.

2. CW Cunningham, **SL Mercer**, HE Hassan, ND Eddington, A Coop. Effect of 3- and 6-Substitution on P-gp substrate activity of morphine analogs. University of Maryland, Baltimore, School of Pharmacy Annual Research Day. Baltimore, MD. May, **2006**.

3. **SL Mercer**, CW Cunningham, HE Hassan, ND Eddington, A Coop. The Relative Activity of Opioids as P-glycoprotein Substrates. Abstracts of the College on Problems of Drug Dependence. Scottsdale, AZ. June **2006**.

4. CW Cunningham, HE Hassan, **SL Mercer**, ND Eddington, A Coop. Diminished P-gp Substrate Activity of 3- and 6-Substituted Morphine Analogs. International Narcotics Research Conference. Minneapolis, MN. July, **2006**.

5. **SL Mercer**, CW Cunningham, HE Hassan, ND Eddington, A Coop. The Relative Activity of Meperidine Analogs as P-glycoprotein Substrates. International Narcotics Research Conference. Berlin, Germany. July **2007**.

6. **SL Mercer**, CW Cunningham, HE Hassan, ND Eddington, A Coop. The Relative Activity of Meperidine Analogs as P-glycoprotein Substrates. University of Maryland, Baltimore, School of Pharmacy Annual Research Day. Baltimore, MD. April **2008**.

7. TN Stephenson, **SL Mercer**, A Coop. UMB24 Analogs as Potential Methamphetamine Treatments. University of Maryland, Baltimore County (UMBC) Undergraduate Research and Creative Achievement Day. April **2008**.

8. **SL Mercer,** CW Cunningham, ND Eddington, A Coop. Synthesis and Characterization of Meperidine Analogs at the P-glycoprotein Efflux Transporter. National Medicinal Chemistry Symposium. Pittsburgh, PA. June **2008**.

9. CW Cunningham, **SL Mercer**, HE Hassan, JR Traynor, ND Eddington, A Coop. The Effect of 3- and 6-Substitution on the Substrate Activity of Morphine Analogs at P-glycoprotein. National Medicinal Chemistry Symposium. Pittsburgh, PA. June **2008**.

Professional Positions Held:

Assistant Professor
Lipscomb University College of Pharmacy
1 University Park Drive
Nashville, TN 37204
(Start Date: September 1, 2008)

Graduate Research Assistant
University of Maryland, School of Pharmacy
Department of Pharmaceutical Sciences
Baltimore, MD 21201
Mentor: Andrew Coop, Ph.D.
July 2004 – August 2008

Chemistry Lab Work-Study/ Lab Assistant.
Seton Hill University
Chemistry Department
Greensburg, PA 15601
Mentor: Susan Yochum, S.C., Ph.D.
August 2000 – May 2004

Summer Undergraduate Research Student
Howard Hughes Medical Institute Fellow
Case Western Reserve University, School of Medicine
Department of Pharmacology
Cleveland, OH 44106
Mentor: John Mieyal, Ph.D.
May 2002 – August 2002

Summer Internship Student
Bayer Corporation
OEM Coatings and Colorants Laboratory
Pittsburgh, PA 15210
Mentor: Patricia Jacobs, Ph.D.
May 2001 – August 2001

Current Committee Memberships:

American Association of Colleges of Pharmacy (AACP)

American Association of Pharmaceutical Scientists (AAPS)

American Chemical Society (ACS)

Tennessee Pharmacists Association (TPA)

Selected Leadership Positions:

American Chemical Society – Maryland Section (MD-ACS)
  Committee Chair – MD ACS Student Grants (2006-2008)
  Student Affiliate Liaison to the Executive Committee (2006-2008)
  Election Committee (2006)

Pharmaceutical Sciences Graduate Student Association
University of Maryland, Baltimore
  Graduate Student Association Representative (2006-2007)
  Vice-President (2005-2006)

American Association of Pharmaceutical Scientists – Student Chapter
University of Maryland, Baltimore
  Events Coordinator (2005-2006)

Seton Hill University SA-ACS Chemistry Club
  President (2002-2003 and 2003-2004)
  Secretary (2001-2002)

Selected Community Activities:

University of Maryland, Baltimore
  Pharmaceutical Sciences Graduate Program Steering Committee
    (2007-2008)
  Mentor for Exploration in Science Research Awareness Program (2007)
  Coordinator and Participant in Ronald McDonald House Dinner (2006)
  Tutor for "A Bridge to Academic Excellence" (2005)

Selected Special Awards:

National Medicinal Chemistry Symposium Travel Award (2008)
ACS Leadership Development Award (Younger Chemists Committee) (2008)
Pharmaceutical Sciences Competitive Departmental Predoctoral Fellowship and
  Merit Award (University of Maryland, School of Pharmacy) (2007-2008)

Abstract

Title of Dissertation: Synthesis and Characterization of Meperidine Analogs at

         the P-Glycoprotein Efflux Transporter

Susan L. Mercer, Doctor of Philosophy, 2008

Dissertation Directed by: Andrew Coop, Ph.D.

         Professor and Chair

         Department of Pharmaceutical Sciences

         University of Maryland, School of Pharmacy

         20 Penn Street, HSF II Room 543

         Baltimore, MD 21201 USA

   Chronic clinical pain remains poorly treated. The use of mu opioid analgesics is effective in treating chronic pain, but the rapid development of tolerance to the analgesic effects necessitates ever increasing doses to be administered. However, tolerance to the constipatory effects occurs at a slower rate, a condition we refer to as differential tolerance. There is a great need to develop opioids to which differential tolerance does not develop in order to reduce the severity of constipation. Our hypothesis is that the efflux transporter, P-glycoprotein (P-gp), contributes to the development of central tolerance by actively pumping morphine out of the CNS. P-gp is present at the BBB, morphine is a known P-gp substrate, and P-gp is up-regulated in morphine and oxycodone tolerant animals. As analgesia is primarily central and constipation is primarily peripheral, up-regulation of P-gp would be expected to lead to lower brain

concentrations of morphine compared to naïve animals; therefore, contributing to tolerance.

The design of opioids with decreased activity as P-gp substrates is anticipated to produce analgesics with reduced differential tolerance and therefore, diminished constipation. Meperidine, a moderately potent mu opioid receptor agonist causes less constipation than morphine clinically and has lower P-gp substrate activity than morphine. We have worked towards the optimization of meperidine by 1) employing opioid *N*-substituent SAR to increase its potency similar to morphine, 2) synthesizing isosteric replacements of the 4-ester to increase duration of action, and 3) introducing steric hinderance into the piperidine ring at the 2- and 6-positions to eliminate toxic metabolite formation. All analogs were analyzed for opioid receptor binding and P-gp substrate affinity. Results showed the optimal *N*-substituent was *N*-methyl; the ester was superior in the 4-position, and the introduction of a *m*-OH into the phenyl ring increased P-gp substrate affinity. Progress towards introducing steric hindrance is reported along with the strategy for their completion.

Additional work on the synthesis and development of 1) selective sigma-1 ligands for stimulant abuse and 2) a dual profile inhibitor of the S100β and p53 interaction involved in malignant melanoma is presented.

Synthesis and Characterization of Meperidine Analogs at the P-Glycoprotein Efflux Transporter

By

Susan L. Mercer

Dissertation submitted to the faculty of the Graduate School
of the University of Maryland, Baltimore in partial fulfillment
of the requirements for the degree of
Doctor of Philosophy
2008

UMI Number: 3337301

INFORMATION TO USERS

The quality of this reproduction is dependent upon the quality of the copy submitted. Broken or indistinct print, colored or poor quality illustrations and photographs, print bleed-through, substandard margins, and improper alignment can adversely affect reproduction.

In the unlikely event that the author did not send a complete manuscript and there are missing pages, these will be noted. Also, if unauthorized copyright material had to be removed, a note will indicate the deletion.

This work is dedicated to my parents,

Edward and Peggy Gillenberger, III

My sister, Chris Gillenberger

And my husband, Greg Mercer

For their unconditional love, support, and encouragement

Acknowledgments

I first and foremost would like to thank my advisor, Dr. Andrew Coop. His enduring support, guidance, and encouragement have fostered my development as a scientist. I am truly grateful that Andy has allowed me the freedom to explore additional scientific disciplines of personal interest so that I could truly become an interdisciplinary scientist and understand the many facets of drug design and discovery. Andy has been a great mentor, providing invaluable advice towards my career development, teaching me how to handle failure and how to celebrate success!

I thank my Ph.D. Committee Members, Dr. Sarah Michel, Dr. Edward Moreton, Dr. Amy Newman, and Dr. James Polli for their professional attention during my graduate training as well as their invaluable advice relating to career opportunities.

My time in graduate school has been made more enjoyable through working and interacting with my past and present labmates: Dr. Matthew Metcalf, Christopher Cunningham, Trudy Smith, Dr. Marilyn Matthews, and Lidiya Stavitskaya. Their support and constructive criticism of my work and future plans have encouraged me to work harder and excel as a scientist. I will truly miss our coffee breaks, group lunches, and trips to the pub to converse and celebrate the many milestones we have achieved individually and as a group.

I am thankful for having the opportunity to have worked and/or collaborated with Dr. Natalie Eddington, Dr. Alexander MacKerell, and Dr. Angela Wilks who have provided numerous learning opportunities and reality checks! Additionally, Drs. Kellie Hom and Julie Ray have provided excellent technical assistance in NMR and MS, respectively. Many thanks also go to the Drug Evaluation Committee for performing the

Table of Contents

List of Tables

Chapter 6

Chapter 7

List of Figures

Chapter 7

List of Schemes

Chapter 6

Chapter 7

List of Abbreviations

ABC	ATP-binding cassette
ADR	Adverse drug reaction
ATP	Adenosine triphosphate
BBB	Blood brain barrier
Caco-2	Epithelial human colon adenocarcinoma cell line
cat.	Catalytic amount
CHN	Combustion analysis
CNS	Central nervous system
CYP 3A4	cytochrome P450 3A4
δ	Delta opioid receptor
eq.	Equivalent
GABA	Gamma aminobutyric acid
GI	gastrointestinal
GPCR	G-protein coupled receptor
i.m.	Intramuscular route of administration
i.p.	Intraperatoneal route of administration
κ	Kappa opioid receptor
KO	Knockout
LLC-PK1	Pig kidney epithelial cells
μ	Mu opioid receptor
MDCK	Madine-Darby canine kidney epithelial cells
MDR	Multidrug resistance

mp	Melting point
MPE	Maximum possible effect
MS	Mass spectrophotometry
NMDA	N-methyl-D-aspartate
NMR	Nuclear magnetic resonance
NSAIDs	Non-steroidal anti-inflammatory drugs
P-gp	P-glycoprotein
p.o.	Oral route of administration
QSAR	Quantitative structure activity relationship
SAR	Structure-activity relationship
S.E.M.	Standard error of mean
TLC	Thin-layer chromatography

.

Chapter 1

Opioid Analgesics: Mechanism of Action, Side Effects and Current

Implications in Research

A portion of this chapter is currently under review for publication in *Current Topics in Medicinal Chemistry* as: Mercer, S. L.; Coop, A. Opioid Analgesics and P-Glycoprotein Efflux Transporters: A Potential Systems-Level Contribution to Analgesic Tolerance.

1.1   Introduction to Analgesics

Chronic clinical pain remains poorly treated. A number of drug classes are currently used to relieve pain, including non-steroidal anti-inflammatory drugs (NSAIDs), anesthetics, N-methyl-D-aspartate (NMDA) receptor antagonists and opioids. NDAIDs primarily have a peripheral site of action and are useful for the treatment of mild to moderate pain, while producing an anti-inflammatory effect; whereas, anesthetics (local or general) inhibit pain transmission through the inhibition of voltage-regulated sodium and potassium channels. These agents, however, are highly sedative or toxic when used in the appropriate dose needed for chronic or acute pain relief. NMDA receptor antagonists, such as ketamine, inhibit the action of the NMDA receptor producing a dissociative analgesia.[1] Current research is investigating other receptor systems which may operate by novel mechanisms resulting in analgesic effects. These include centrally acting α-adrenergic-,[2] cannabinoid-,[3] GABA-,[4] and nicotinic-[5] receptor agonists as well as N-type calcium channel blockers such as Ziconotide.[6] Despite these efforts, opioids remain the standard analgesics of choice in the clinical management of chronic and severe pain.

1.2   History of Opioids

One of the oldest recorded medications is the use of the juice (opium in Greek) or latex from the unripe seed pods of the poppy *Papaver Somniferum*. The writing of Theophrastus around 200 B.C. describes the use of opium in medicine; however, there is evidence that opium was used in the Sumerian culture as early as 3500 B.C. Opium was initially used as a tonic or it was smoked until Surtürner, a pharmacist, isolated an

alkaloid from opium in 1803. He named the alkaloid morphine (**1**) (Figure 1.1) after Morpheus, the Greek god of dreams. Other medically important alkaloids were later isolated from the latex of opium poppies to include codeine (**2**), thebaine, and papaverine. Morphine (**1**) was among the first isolated compounds to undergo structural modifications. The 3-ethyl ether- and diacetyl-morphine analogs were soon synthesized and are commonly known today as codeine (**2**) and heroin (**5**), respectively. Interestingly, heroin (**5**) was initially marketed as a nonaddicting analgesic, antidiarrheal and antitussive agent in 1898.

The use of terms opiate and opioid requires some clarification. The term opiate was used extensively until the 1980s to describe any natural or synthetic agent that was derived from morphine or any compound structurally related to morphine. However, a nomenclature change was prompted in the mid-1970s with the discovery of peptides in the brain which exhibited pharmacological actions similar to morphine. The peptides were not related to morphine structurally, but their pharmacological actions were similar to morphine. At this time, the term opioid was introduced, meaning opium- or morphine-like in terms of pharmacologic action. The broad group of opium alkaloids, synthetic derivatives related to the opium alkaloids, and the many naturally occurring and synthetic peptides with morphine-like pharmacologic effects are called opioids.[7] In addition to having pharmacologic effects similar to morphine a compound must be antagonized by an opioid antagonist such as naloxone to be classified an opioid. Neuronal-located proteins to which opioid agents bind and initiate a biologic response are called opioid receptors.

	R	R'
1	OH	OH
2	OMe	OH
3	OCOCH$_3$	OCOCH$_3$
4	OH	glucoronide
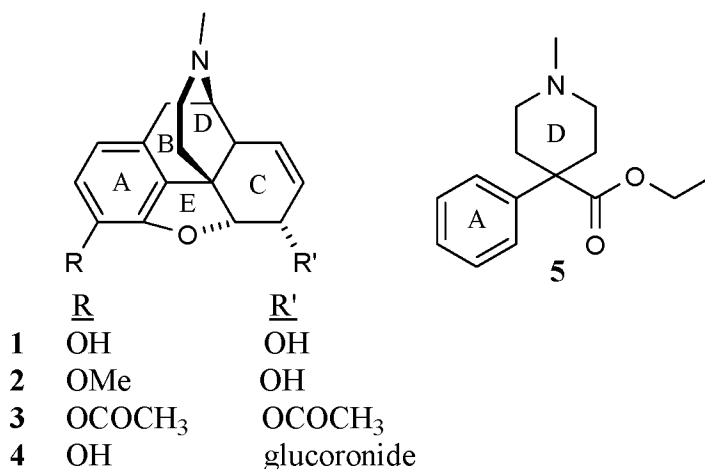
Figure 1.1. Structure of morphine (**1**), codeine (**2**), heroin (**3**), morphine-6-glucoronide (**4**), and meperidine (**5**). Letters in the ring, designate the ring classification in order to show how **5** is structurally related to **1**; ring D is the piperidine ring.

1.3   Opioid Receptor Subtypes and Pharmacological Actions

The mu opioid agonist morphine (**1**) continues to be the drug of choice for the treatment of severe pain due to its actions as an analgesic[8] and its ability to maintain patients in a state of "well-being".[9] Due to its analgesic effects, morphine is often used to treat terminal cancer patients[10, 11] and those suffering from AIDS.[12] However, mu opioid analgesics produce several undesired side effects including the development of tolerance, dependence,[13, 14] respiratory depression,[15] nausea,[16] and constipation.[17] It is reported that 10-30% of cancer patients treated with morphine receive inadequate treatment due to the presence of excessive undesired side effects, inadequate analgesia, or both.[18]

The pharmacological actions of opioids are a result of their interaction with the opioid receptors which are seven transmembrane domain, G-protein coupled receptors (GPCR) that are located in high concentrations in the brain and spinal cord.[19] Three subtypes have been cloned: mu (μ),[20] kappa (κ),[21] and delta (δ)[22, 23] and each has unique central pharmacological actions. Agonists of the μ receptor produce effects of analgesia,

euphoria, and respiratory depression, and are largely responsible for the physical dependence associated with opioids.[24] κ receptor agonists provide analgesia and show little dependence liability; however, they are poor therapeutic agents, as they produce intense dysphoric reactions.[25] Agonists at the δ receptor are also poor agents, as their activation produces convulsions as an undesirable side effect, at least in rodents.[26] Centrally active μ opioid agonists remain the primary choice in the clinical setting and methods are urgently required to reduce their side effects.

1.4 Opioid-Related Constipation and Current Treatments

In addition to opioids having central activity, μ opioid agonists also stimulate peripheral μ opioid receptors in the gastrointestinal (GI) tract inhibiting intestinal motility which is the primary cause for opioid-related constipation.[27] Constipation is considered the most common and often the most debilitating opioid adverse effect reported by patients.[28, 29] Persistent symptoms often impair quality of life measures[30] and some patients chose to discontinue analgesic therapy rather than experience the discomfort associated with the adverse effect.[31]

Stool softeners and laxatives are currently used to treat moderate constipation; however, they are less effective with more severe occurrences. Opioids that do not readily enter the central nervous system (CNS), such as loperamide (6) (Imodium®) (Figure 1.3) and diphenoxylate (7), are used as anti-diarrheal agents[31] and in the treatment of irritable bowel syndrome.[32] Due to their lack of central activity, such compounds do not produce the centrally-mediated effect of euphoria and therefore, have low abuse potential.[33] Loperamide and diphenoxylate reportedly do not enter the CNS

because they are too lipophilic to cross the BBB;[27, 33] however, new evidence suggests another mechanism which will be further described in Chapter 2.

Recent research has focused on the development of peripherally restricted μ opioid antagonists to selectively antagonize the μ opioid receptors in the GI tract. These agents are unable to penetrate the BBB due to their structural characteristics and therefore remain in the GI tract minimally impacting central opioid actions. Two agents currently under investigation include alvimopan (8) and methylnaltrexone (9) which are unable to cross the BBB due to the zwitterion and quaternary amine present in their respective structures.[31, 34, 35] Both compounds have moved forward to clinical trials. Phase III clinical trials on alvimopan, trade name Entereg, (GSK/Adolor) have been halted due to no difference between drug and placebo. Whereas the FDA just approved the New Drug Application for methylnaltrexone, trade name Relistor, (Wyeth/Progenics) for *s.c.* administration in April 2008.[36] While these agents may still find clinical usefulness, they ultimately add to an already increased patient drug regimen and will introduce further issues with compliance.
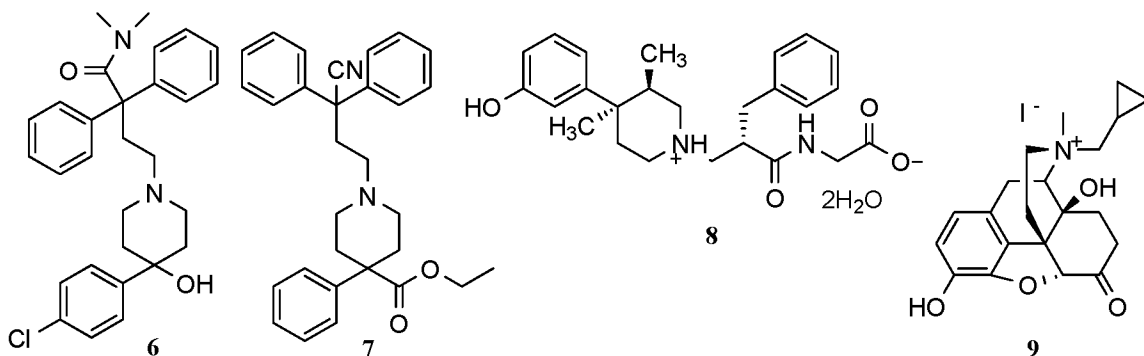
Figure 1.2. Structures of loperamide (**6**), diphenoxylate (**7**), alvimopan (**8**) and methylnaltrexone (**9**).

1.5   Opioid-Related Tolerance

Tolerance is the cellular or system level adaptations which cause the need for an increased dose of drug, here an opioid, to produce the same effect. Herein we describe three types of tolerance: central, peripheral, and differential. After repeated administration of morphine patients become tolerant to the central analgesic effects and require greater doses to maintain the same level of analgesia, a phenomenon known as central tolerance.[13] The development of peripheral tolerance (GI tract), however, does not occur as rapidly.[37] Consequently, when the dose of morphine is increased to reach a stable level of analgesia, the constipatory effect is increased. The disparity between the developmental rates of central and peripheral tolerance will be referred to as differential tolerance. Differential tolerance is a significant problem in the management of chronic pain, as the constipation experienced itself can add to the pain experienced by the patient.[38]

1.5.1   Mechanisms of Opioid Tolerance

Several theories exist regarding the mechanisms underlying the development of tolerance including the change in opioid receptors, loss of opioid receptors, and exhaustion of mediators; more specifically the classical views of receptor desensitization, receptor internalization, and adaptations in downstream signaling pathways, respectively.[13] Most currently prescribed opioids act through the μ opioid receptor, a 7-transmembrane domain GPCR. To date none of the opioid receptors (μ, κ, δ) have been structurally characterized, in fact only one GPCR crystal structure has been solved, that of rhodopsin.[39] The most thoroughly studied mechanism for μ-receptor desensitization

and internalization involves G protein-coupled receptor kinase (GRK)-mediated receptor phosphorylation that promotes the binding of β-arrestin proteins.

In order to understand the mechanisms involved with receptor desensitization and internalization it helps to understand the function of the GPCR (Figure 1.3). G-proteins consist of three subunits, α, β, and γ. When an agonist binds to the receptor it becomes activated and "attracts" the α subunit to the ligand-receptor complex. At this time GTP is exchanged for GDP at the α subunit while the β-γ complex moves toward Target 2. Once the α subunit binds GTP it then moves toward Target 1 which is then activated. Once Target 1 is activated, the GTP is hydrolyzed back to GDP and the resting/initial state is achieved.

In GPCR desensitization (phosphorylation), an agonist binds to the receptor promoting a conformational change that results in G protein activation and dissociation from the receptor. The activated receptor is then phospohorylated by GRK. The phosphorylated receptor then binds to arrestin, causing the receptor to lose ability to associate with a G-protein. At this point, the arrestin-receptor complex undergoes endocytosis, which removes the receptor from the membrane. The receptor is no longer able to recycle, and causes a decrease in available receptors for drug binding.

In receptor internalization surface receptors are removed. Internalization occurs predominately via clathrin-coated pits. Receptor phosphorylation by GRKs appears to be a critical event during internalization although other research suggests that MAPK activation is critical. Once again, a decrease in available receptors is the result.

Changes in the downstream signaling pathway also occur after agonist binding at the receptor. Briefly, the most commonly reported actions include 1) inhibition of

adenylyl cyclase, 2) activation of a potassium conductance, 3) inhibition of calcium conductance, and 4) inhibition of transmitter release.[40] More recent observations have extended the actions of opioids to include 1) the activation of protein kinase C (PKC), 2) the release of calcium from extracellular stores, 3) the activation of the mitogen-activated protein kinase (MAPK) cascade, and 4) the realization that receptor trafficking plays an important role in receptor function.[40]

Overall, the loss of surface receptors is a major mechanism involved with tolerance development. For example, when the number of receptors decreases by two, the probability of a drug molecule reaching a receptor is also decreased by two; therefore, more drug is required to produce the same effect. The ability to stop loss of surface receptors would potentially solve the tolerance problem. However, the mechanism behind receptor-mediated tolerance is complicated by the finding that not all opioids activate the arrestin-mediated downstream signaling pathway and promote opioid receptor internalization; morphine, in fact, does not activate this pathway.[40, 41]

Receptor oligomerization has been hypothesized as an alternative mechanism for opioid receptor desensitization.[42] However, receptor-mediated tolerance alone would not cause the disparity between the developmental rates of central and peripheral tolerance as similar receptor desensitization events would occur both in the brain and in the GI tract. Additional factors at the systems level, metabolism and transporters, must therefore be involved in the development of central tolerance to opioid analgesia.
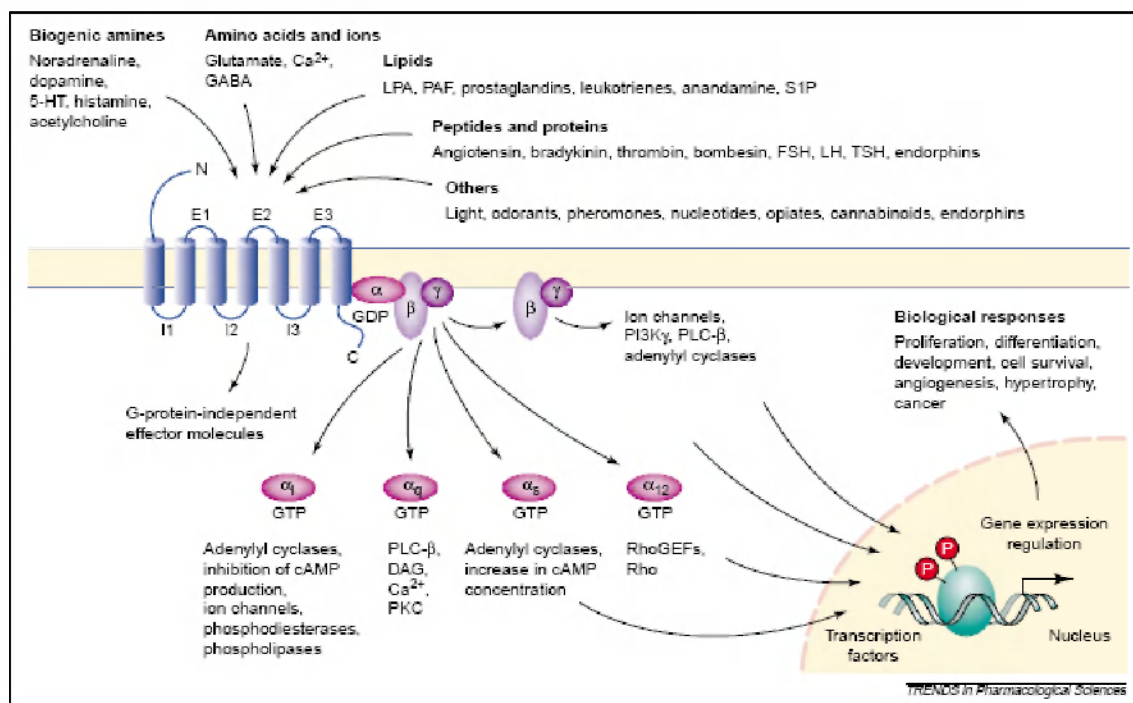
Figure 1.3. Illustration of GPCR depicting receptor orientation, α, β, γ subunits, and downstream signaling pathways which regulate key biological functions such as cell proliferation, cell survival and angiogenesis. The α, β, γ subunits located next to the GPCR are defined as Target 1, whereas the β, γ subunits away from the GPCR are defined as Target 2. Abbreviations: DAG, diacylglycerol; FSH, follicle-stimulating hormone; GEF, guanine nucleotide exchange factor; LH, leuteinizing hormone; LPA, lysophosphatidic acid; PAF, platelet-activating factor; PI3K, phosphoinositide 3-kinase; PKC, protein kinase C; PLC, phospholipase C; S1P, sphingosine-1-phosphate; TSH, thyroid-stimulating hormone. Figure reproduced from reference[43] with permission. Copyright 2001 Elsevier.

1.6 Introduction to the P-Glycoprotein (P-gp) Efflux Transporter

A significant step in understanding the development of differential tolerance is the finding that P-gp, an efflux transporter expressed in the Blood Brain Barrier (BBB), is up-regulated in morphine tolerant rats[44] and that similar up-regulation by the μ agonist oxycodone has a measurable physiological effect on the brain concentrations of P-gp substrates.[45] Morphine is a substrate for P-gp[46-48] and P-gp up-regulation at the BBB would cause relatively lower concentrations of morphine in the CNS, resulting in

relatively increased stimulation of peripheral opioid receptors and greater constipation. P-gp is also present in the GI tract, and recent studies by Eddington and co-workers have shown that P-gp is up-regulated in the BBB and the GI tract after chronic treatment with oxycodone.[45] Importantly, brain concentrations of [^{3}H]paclitaxel (a known P-gp substrate) were lower in tolerant animals compared to naïve animals, strongly suggesting that the up-regulation of P-gp contributes towards central tolerance.[45] This up-regulation results in less opioid in the general circulation, contributing to overall tolerance. Through the preparation of opioids with low P-gp substrate activity, the effects of P-gp in all tissues would be eliminated.

1.7   Project Rationale – Optimization of Meperidine

Mu opioid agonists that cause constipation to varying degrees have been identified. Among these the μ agonist meperidine (**5**) leads to a lower degree of constipation than morphine.[49] Meperidine has the lowest P-gp substrate activity of the opioids assayed,[50] although similar to morphine. Meperidine was found to have a P-gp effect (efflux:influx ratio) of 0.98 ± 0.27 while morphine had a P-gp effect of 1.24 ± 0.08.[50] We suggest that morphine-6-glucoronide (M6G) (**4**), a major active metabolite of morphine which is an excellent P-gp substrate,[4] is the species which is actively transported out of the CNS by P-gp. M6G is more lipophilic than morphine and has up to four times morphine's analgesic potency with about twice the duration of action.[51] This is consistent with the clinical findings that meperidine, which does not have such a metabolite, appears to cause low degrees of constipation.[49] This further suggests that a long-acting, non-toxic μ agonist which is neither a substrate for P-gp nor can be

metabolized to a P-gp substrate would share the desirable lower constipatory activity of meperidine. However, the use of meperidine for the treatment of chronic pain is limited. Problems with meperidine include the toxicity of its normeperidine metabolite, its short duration of action, and its low potency.[49] For these reasons we propose to optimize the clinical utility of meperidine by: 1) increasing potency, 2) increasing the duration of action, and 3) eliminating the possibility of metabolism to a toxic metabolite all while retaining or further lowering P-gp substrate activity. These μ opioid agonists with low or further reduced P-gp substrate activity will be novel analgesics of similar potency to morphine and have a reduced degree of constipation.

1.7.1 Hypothesis – The rapid central tolerance to opioid analgesia is exacerbated through increased efflux transport mediated by P-gp. Elimination of the P-gp substrate activity of opioids will therefore eliminate the development of differential tolerance and reduce the severity of constipation resulting from chronic opioid therapy.

1.7.2 Increase the Potency of Meperidine

The initial approach to increasing meperidine potency focused on N-substitutions on the meperidine piperidine ring. The most thoroughly investigated structural variation of meperidine is that of replacement of N-methyl by other groups, notably phenylalkyl. Perrine and Eddy[52] determined the relative antinociceptive activity of the meperidine analogs using the tail-flick assay in mice. The unsubstituted phenylalkyl series activity increased as the alkyl chain length between the ring nitrogen and the aryl group was lengthened from one to three carbons and declined on extension to four carbons. N-

Benzylnormeperidine is the weakest analog having activity one quarter that of meperidine, while *N*-phenylpropylnormeperidine is the strongest analog having thirteen times the activity of meperidine.[52] Additional R groups for the *N*-substituted analogs of meperidine were chosen based on previous work by McLamore *et al.*[53] to investigate the effect of chain length, unsaturation, and branching on the µ opioid potency and P-gp substrate activity of the meperidine series. *N*-alkyl chain lengths beyond four carbons were not pursued due to the dramatic decrease of cumulative brain concentration of drug.

Specific Aim 1: Increase the potency of meperidine.

The most thoroughly analyzed meperidine analogs include those of *N*-substituents other than *N*-methyl. A series of *N*-substituted meperidine analogs will be synthesized to investigate the effect of chain length, unsaturation, and branching on the µ opioid potency and P-gp substrate activity. All the while, these substitutions will provide development of the Structure Activity Relationship (SAR) between opioids and P-gp. Compounds will be tested for P-gp substrate affinity, opioid potency, duration of actions, metabolism and toxicity. (Chapter 3)

1.7.3   Increase the Duration of Action of Meperidine

Meperidine is metabolized by two different pathways; hepatic carboxylesterase metabolism to meperidinic acid, an inactive metabolite, and N-demethylation by hepatic cytochrome P450 isozyme 3A4 to normeperidine, a non-opioid active metabolite.[49] The ester of meperidine, in part, causes a shortened duration of action. In order to increase the duration of action, isosteric replacement of the ester to the corresponding amide,

ketone, and carbamate will be performed. The amide, ketone, and carbamate functionalities were chosen because they are known to be metabolized slower than esters. Studies have shown that 4-arylpiperidines with 4-position carbon substituents, such as CO_2Et and COEt, tend to show greater potency with a phenolic functionality.[54] For this reason the phenyl ring will be functionalized by the addition of a *m*-hydroxyl, which will further increase the potency and offer a site for phase-II metabolism. The glucuronide conjugated product will be excreted, therefore not producing the toxic metabolite, normeperidine. This substitution will not necessarily lead to an increased duration of action, but will further attenuate *N*-dealkylation.

Specific Aim 2: Modulate the site of action for meperidine metabolism. The ester of meperidine, in part, causes a shortened duration of action. To increase duration of action and study the Structure Activity Relationship (SAR) of the 4-position, isosteric replacement of the ester to the corresponding amide, ketone, and carbamate will be performed. The phenyl ring will also be functionalized by the addition of a *m*-hydroxyl, which will further increase potency and offer a site for phase-II metabolism. The conjugated metabolite will prevent the possibility of a toxic metabolite, since the product will be excreted as the conjugate although this modification may well decrease duration of action. The isosteric replacements and hydroxyl addition will initially be performed on the *N*-methyl to develop the synthetic process and then applied to various *N*-substituted analogs. Compounds will be tested for P-gp substrate affinity, opioid potency, duration of action, metabolism and toxicity. (Chapter 4)

1.7.4 Hinder *N*-Dealkylation of Meperidine

N-Dealkylation, which leads to the toxic metabolite normeperidine, is the clinically significant metabolic pathway of meperidine.[55-57] In order to limit *N*-dealkylation and potentially prevent formation of a toxic metabolite steric hinderance will be introduced into the piperidine ring at the 2- and 6-positions. We propose to synthesize four series of substituted meperidine analogs to include the 2-methyl-, 2,2-dimethyl-, 2,6-dimethyl-, and 2,2,6,6-tetramethyl-meperidine analogs (Figure 1.4). Limited research has been performed involving alkyl substitutions on the piperidine ring of meperidine due to stereochemical complexity, although 3-methyl meperidine analogs have been previously synthesized and show increased potency compared to meperidine.[58] Most work involving alkyl substitutions to the piperidine ring was performed on the reversed ester of meperidine due to ease of synthetic access and the fact that replacement of 4-carbethoxy (CO_2Et) by 4-propionyloxy (OCOEt) usually produces a major increase in potency (up to 20-fold regardless of the *N*-substitutent).[59] In addition, the 2-methyl and 2,6-dimethyl reversed esters of meperidine analogs have been synthesized and also show increased potency compared to meperidine.[54] These results strongly support our approach that the introduction of methyl groups will lead to potent μ opioid agonists. The work presented herein focuses solely on the synthesis of substituted meperidine analogs, since the hydrolysis of the reversed ester of meperidine even with mono substitution leads to a toxic metabolite, MPTP,[60] implicated in Parkinson's disease.
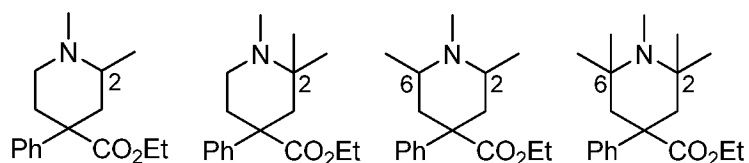
Figure 1.4. Sterically hindered meperidine analog targets, depicting the 2-methyl-, 2-2-dimethyl-, 2,6-dimethyl-, and 2,2,6,6-tetramethyl analogs, respectively.

Specific Aim 3: Eliminate the toxic metabolite of meperidine. *N*-Dealkylation of meperidine produces the toxic metabolite, normeperidine. Steric hinderance will be introduced into the piperidine ring adjacent to the nitrogen at the 2- and 6-positions, in order to favor metabolism at other positions of the molecule. In addition, when *N*-dealkylation does occur the metabolite will no longer be normeperidine, potentially eliminating toxicity. Addition of 2- and 6-methyl groups will initially be studied on *N*-methyl (meperidine) to develop the synthetic procedures and subsequently applied to various *N*-substituted analogs. Compounds will be evaluated for P-gp substrate affinity, opioid potency, duration of action, metabolism, and toxicity. (Chapter 5)

1.8   Additional Thesis Work

While most of the work in this thesis focuses on the development of novel opioids that produce less constipation, additional work was pursued simultaneously. Ongoing projects in the laboratory provided an avenue to explore and develop molecules related to both a "stimulant" and "cancer" project. The stimulant project focused on the development of selective sigma (1/2) antagonists to reverse the stimulant effects of cocaine and methamphetamine while further delineating the functions of each receptor

subtype. While the cancer project focused on the development of a dual S100β and p53 inhibitor to prevent protein-protein interactions leading to melanoma.

1.8.1 "Stimulant Project": Nitrile Analogs of Meperidine as Sigma Receptor Ligands

The *N*-substituted meperidine analog synthesis was designed to yield two different series of compounds; a nitrile series and an ester series. A representative sample of the nitrile series was sent for opioid binding analysis and the results showed that the nitrile analogs had no opioid activity as expected. Another project ongoing in the lab was the design of sigma receptor ligands. Since the nitrile series had structural similarity to previous sigma ligands, they were analyzed at the sigma receptors by our collaborator Dr. Rae Matsumoto. The nitrile analogs were found to be sigma-1 selective ligands with good binding affinity, a few even had sub-nanomolar affinity. Further pharmacological analysis is ongoing to determine the efficacy of the ligands. (Chapter 6)

1.8.2 "Cancer Project": Development of a Dual Profile S100β and p53 Inhibitor

In collaboration with the Dr. David Weber laboratory at the University of Maryland, School of Medicine a series of lead compounds were designed and synthesized in order to inhibit the protein-protein binding of S100β and p-53 which leads to melanoma development. Analysis of the compounds is still ongoing; however, the compounds provided interesting results in that the optimal chain length of the dual-site inhibitor was found using NMR perturbation experiments. (Chapter 7)

Chapter 2

Opioid Analgesics and P-Glycoprotein Efflux Transporters: A Potential

Systems-Level Contribution to Analgesic Tolerance

This chapter is currently under review for publication in *Current Topics in Medicinal Chemistry* as: Mercer, S. L.; Coop, A. Opioid Analgesics and P-Glycoprotein Efflux Transporters: A Potential Systems-Level Contribution to Analgesic Tolerance.

2.1   Introduction

A growing body of evidence suggests that efflux transporters in the Blood-Brain Barrier (BBB), specifically P-glycoprotein (P-gp) may contribute to the development of central tolerance to opioids.   P-gp is a member of the ATP-binding cassette (ABC) super-family of transport proteins, and is involved in various functions including the extrusion of xenobiotics, uptake of nutrients, transport of ions and peptides, and cell signaling.[61]   Forty-eight ABC transporters have been identified in humans and classified on the basis of phylogenetic analysis into 7 subfamilies[62] as shown in Table 2.1.   P-gp (ABCB1) is a member of the ABCB (MDR/TAP) subfamily and is one of the most characterized efflux transporters to date.   A number of excellent reviews are available which discuss the secondary and tertiary structures of P-gp as well as the substrate-binding pocket.[61, 63-65]   The exact mechanism of P-gp function has not been fully delineated to date; however, two models, the "hydrophobic vacuum cleaner" and the "flippase" are readily accepted.   A brief description of the pump function of each model follows.   In the "hydrophobic vacuum cleaner" model P-gp extracts its hydrophobic substrates from the lipid bilayer and expels them directly to the external aqueous medium,[66] whereas in the "flippase" model, substrates are flipped from the inner leaflet of the lipid bilayer to the outer leaflet of the plasma membrane or directly into the extracellular environment.[67]

Table 2.1. Phylogenetic analysis of ABC transporters

Subfamily	Number of Members	Previous Subfamily Name
ABCA	12	ABC1
ABCB	11	MDR/TAP
ABCC	12	MRP/CFTR
ABCD	4	ALD
ABCE	1	OABP
ABCF	3	GCN20
ABCG	5	White

Information derived from references [61, 62]

The substrate specificity for P-gp remains broad despite various efforts to establish a structure-activity relationship (SAR) for P-gp. In general, P-gp substrates contain a high number of hydrogen bonds, a basic nitrogen and are lipophilic with a molecular weight below 500.[61] Interestingly, a correlation between P-gp and cytochrome P450 3A4 (CYP 3A4) substrate specificity exists[68, 69] and numerous studies have demonstrated clinically relevant drug-drug interactions when a P-gp inhibitor is co-administered with a CYP 3A4 substrate. Contrary to cytochrome P450 enzymes, which are only involved in drug metabolism, P-gp participates in the absorption, distribution, and elimination phases with regard to the pharmacokinetic law (ADME: absorption, distribution, metabolism, and elimination)[70] and therefore affect the bioavailability of drugs.[71] This review briefly discusses current *in vitro* and *in vivo* P-gp analyses while focusing on reporting the P-gp substrate activity of clinically relevant mu opioid analgesics. The importance of opioid and P-gp interactions at the BBB and the GI tract will be discussed along with future research directions.

2.2   Assessment of P-gp function: *In vitro* and *in vivo* systems

Various *in vitro* and *in vivo* techniques have been developed in order to evaluate the correlation between test compounds and P-gp activity. It is understood that a combination of techniques should be employed to fully delineate the P-gp effects of a compound. A brief description of available techniques used for P-gp and opioid analysis follows along with references to current literature for a more thorough explanation of each technique including their advantages and disadvantages.

Currently, three different categories exist for *in vitro* methods which evaluate drug efflux transporter activity; a) accumulation/efflux, b) transport studies, and c) ATPase activity studies. Accumulation/efflux studies are performed using cell suspensions, cell monolayers, or membrane vesicle preparations in which the uptake of a probe, typically either a fluorescent or radiolabeled compound, is examined under controlled conditions in the presence of a P-gp inhibitor. Transfected or drug induced cells which overexpress P-gp are also used and the accumulation studies are compared to the wild-type (WT) or parental cell line.[72] P-gp transport studies are performed using confluent cell monolayers in which the test compound is applied to either the apical or basolateral side of the cell and the resulting flux of the compound across the confluent cell monolayer is measured. Examples of cell lines used in P-gp transport studies include CaCo-2,[73] LLC-PK1[74] and MDR1 transfected MDCK[75] cells. Lastly, ATPase activity studies monitor the stimulation of ATPase activity in cell membrane preparations or purified membrane proteins in order to identify compounds which increase ATPase activity over basal ATPase activity. The Promega® P-gp-GLO kit[63] is an example of an

ATPase activity study. Further details and limitations of the *in vitro* techniques can be found in the following literature.[72, 76]

In vitro assays are useful in the characterization of interactions between compounds and P-gp, however, the ultimate determination of the impact of P-gp on drug absorption, distribution, and elimination requires *in vivo* examination. Current *in vivo* P-gp techniques include the use of transgenic (genetically engineered) and mutant (naturally P-gp deficient) animal models, as well as P-gp anti-sense and inhibitors. Due to the fact that the rodent *mdr1a* and *mdr1b* genes perform the same function as the MDR1 P-gp gene in humans, a popular transgenic animal model is the P-gp knock-out (KO) animal, *mdr1a/b* (-/-), in which both rodent drug-transporting P-gp genes are deleted.[77, 78] CF-1 is a naturally occurring mutant mouse model deficient of P-gp.[79] Lastly, P-gp anti-sense[47] and inhibitors,[72] such as GF120918 and PSC833, have also been used to evaluate interactions between opioids and P-gp in WT [*mdr1a/b* (+/+)] animals by effectively blocking the protein translation or transporter action, respectively. Further details and limitations of the *in vivo* techniques can be found in the following literature.[65, 72]

2.3   Opioids and P-gp

Callahan and Riordan first discovered a correlation between synthetic and natural opioids with P-gp activity in MDR cells in 1993.[80] Since then, many opioids have been identified as P-gp substrates using *in vitro* and *in vivo* techniques as previously described. In general, for a compound to be considered a P-gp substrate it should exhibit one or more of the following characteristics:[45] a) have an efflux ratio greater than 1.5 that can be

decreased to 1 by P-gp inhibitors,[76] b) show significantly higher accumulation in brain or other tissues of mdr1a/b (-/-) mice in comparison to mdr1a/b (+/+) WT mice,[47, 81, 82] or c) results in up-regulation of P-gp upon multiple administration.[44, 83] We hypothesize that P-gp contributes to analgesic tolerance through a systems-level approach; as P-gp is located in both the BBB and the GI tract, contributing to central and peripheral tolerance, respectively. Opioids investigated within this review include morphine, methadone, loperamide, meperidine, oxycodone, and fentanyl (Figure 2.1).
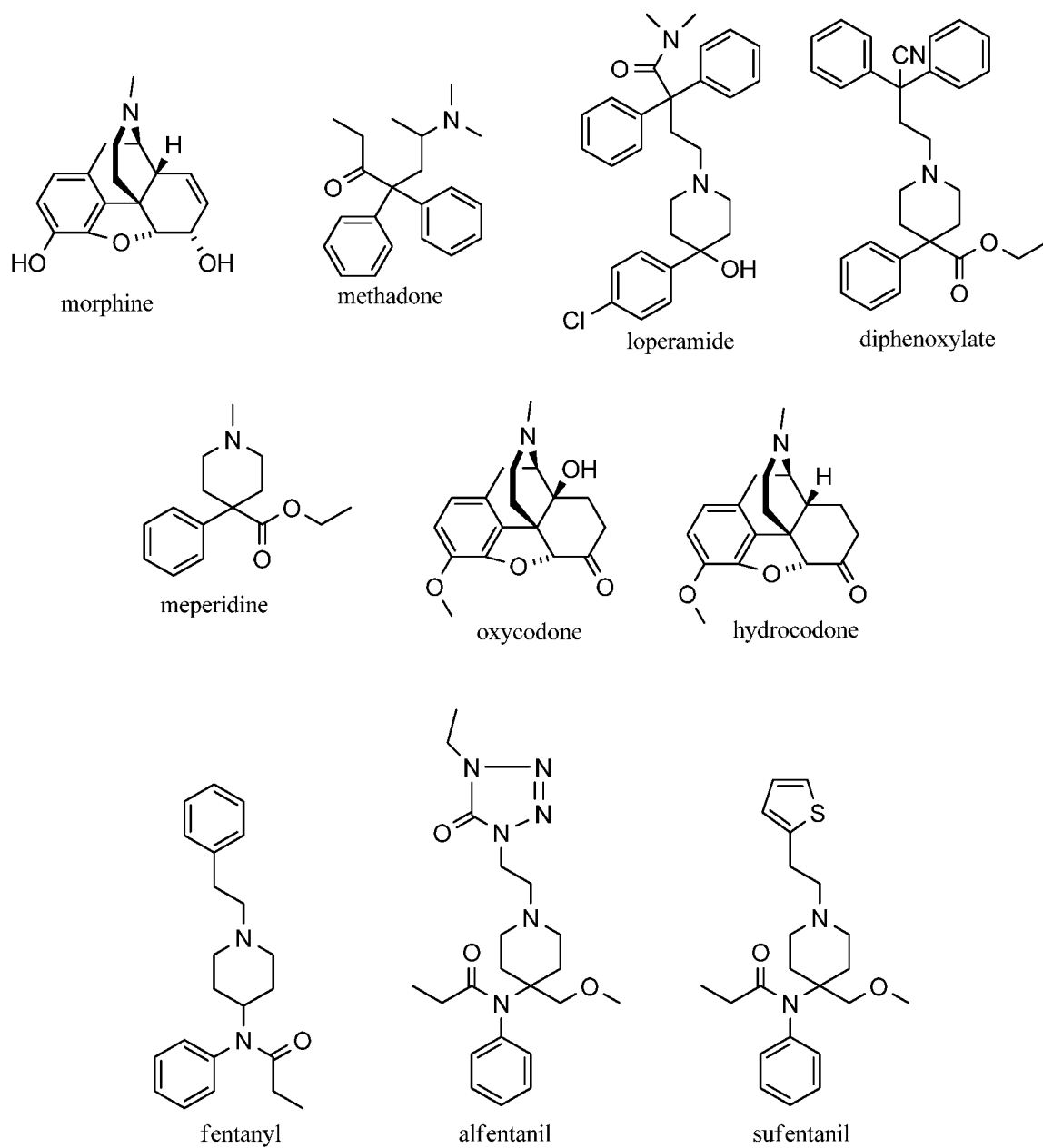
Figure 2.1 Structures of investigated opioids.

2.3.1 Morphine

The most thoroughly investigated interaction between opioids and P-gp is that involving morphine, the prototypical μ opioid analgesic. Morphine was first identified as a P-gp *in vitro* substrate in cell culture systems, through the use of radiolabeled morphine across MDR cells[80, 84] and later found to be an *in vivo* P-gp substrate, as it was the first opioid analyzed in P-gp KO mice.[85] Subsequent *in vivo* studies investigated the inhibition of P-gp in rats with GF120918 followed by morphine administration, resulting in significantly elevated antinociceptive effects.[86] Later, a microdialysis study was performed using KO and WT mice to evaluate the role of P-gp in the transport of morphine across the BBB, concluding that morphine is transported across the BBB by P-gp.[48] In 2000, Aquilante *et al.* showed that chronic administration of morphine to rats resulted in decreased antinociceptive response and a 2-fold increase of brain P-gp. They hypothesized that the P-gp up-regulation enhanced morphine efflux from the brain, reducing the pharmacological activity of morphine and ultimately purported that P-gp up-regulation may be one mechanism involved in the development of morphine tolerance.[44]

Various *in vivo* experiments with morphine and its metabolites, specifically morphine-6-glucoronide (M6G)[87, 88] have since been performed. The first dose response study with KO and WT mice by tail flick analysis showed that morphine antinociception was significantly increased in KO mice, specifically, the ED_{50} for morphine was >2-fold lower in KO mice (3.8 mg/kg) compared to WT mice (8.8 mg/kg).[81] Similarly, in the first time course study (%MPE vs. time) conducted with KO and WT mice by hot plate analysis, greater antinociceptive effects and morphine brain concentrations resulted in the KO mice.[89] Morphine was also evaluated in mice with P-gp antisense; the decreased P-

gp expression resulted in significantly enhanced systemic morphine antinociception and prevented tolerance, but diminished the antinociception of centrally administered morphine.[47]

With these new findings, studies were underway to determine the extent of morphine transport out of the brain by P-gp. Morphine was found to be a weak P-gp substrate in Caco-2[90] and L-MDR1[91] cells with a efflux:influx ratio of 1.5. Whereas, *in situ* animal studies resulted in decreased clearance uptake (Cl_{up}) of morphine[82] and confirmed that morphine is a weak P-gp substrate with a P-gp effect of 1.24 (Table 2.2).[50] Studies have also been performed in healthy human volunteer subjects, examining the CNS effects of morphine after pretreatment with quinidine, a brain and intestinal P-gp inhibitor. Human volunteers which received morphine intravenously did not experience enhanced CNS opioid effects[92] whereas, human volunteers which received morphine orally sustained increased plasma concentrations, hence a clinically relevant effect, but no influence on morphine pharmacodynamics.[93] These human results suggest that P-gp plays a role in orally administered morphine and intestinal disposition,

Most recent studies have determined the relationship between the P-gp ATPase activating effect of morphine and its P-gp dependent antinociceptive effects evaluated by dose-response and time course studies. The results between the *in vitro* and *in vivo* systems correlated well, resulting in increased ATPase activity and 2.8-fold greater antinociception in KO mice.[94, 95] Lastly, pharmacokinetic modeling has been employed and the finding show that morphine brain distribution is determined by three findings: limited passive diffusion; active efflux, reduced 42% by P-gp inhibition; and low capacity active uptake.[96]

Table 2.2. Initial brain uptake clearance of opioids during in situ perfusion in mice.

Compound	Receptor	WT Mice	KO Mice	P-gp Effect
Morphine	μ	1.04 ± 0.03	1.29 ± 0.08**	1.24 ± 0.08
Methadone	μ	41.7 ± 5.8	109 ± 17***	2.61 ± 0.55
Loperamide	μ	9.86 ± 1.73	103 ± 6***	10.4 ± 1.9
Meperidine	μ	185 ± 38	180 ± 33	0.98 ± 0.27
Fentanyl	μ	184 ± 24	228 ± 9*	1.24 ± 0.17

P-gp effect is defined by the ratio between the Cl_{up} in mdr1a (-/-) P-gp deficient (KO) and wild-type (WT) mice. Data are presented as mean $\pm$ SD of four individual experiments at a single time point or from multiple time point experiments. (N = 4 per point at three time points) * P < 0.05; ** P < 0.01; *** P < 0.001. Table modified from Dagenais *et al.* [50]

2.3.2 Methadone

Methadone is a synthetic opioid agonist used in the treatment of pain and/or opioid addiction. The racemic mixture is administered during treatment although the l-enantiomer accounts for the analgesic effects.[97] The interaction of methadone and P-gp has been studied with the use of different *in vitro* models, showing that methadone is a P-gp substrate [80, 84, 98-100] with a P-gp effect of 2.61 from *in situ* evaluation (Table 2.2).[50] *In vivo* studies performed with P-gp KO mice and rats treated with a specific P-gp inhibitor have shown that the analgesic effect of methadone was greater and its brain concentrations were markedly higher when P-gp was absent or inhibited.[89, 101, 102] Investigations of the stereoselectivity of P-gp transport are currently being investigated, and results suggest only a weak stereoselectivity for P-gp transport of methadone; the (S)-enantiomer is transported 10% more than the l-enantiomer.[103]

2.3.3   Loperamide

The synthetic opioid loperamide is commonly used as an over-the-counter anti-diarrheal drug due to its peripheral opioid-like effects on the GI tract leading to constipation, whereas CNS effects are not observed. The interaction of loperamide and P-gp has been studied with the use of different *in vitro* models, showing that loperamide is a P-gp substrate.[80, 84] Loperamide was found to a good P-gp substrate in L-MDR1 transport studies having an efflux:influx ratio of 10,[91] and by *in situ* animal studies resulting in a P-gp effect of 10.4 (Table 2.2).[50] Furthermore, Caco-2 transport studies confirm that loperamide is a good P-gp substrate, however diphenoxylate, a loperamide analog used as an anti-diarrheal agent, is not a P-gp substrate by *in vitro* transport studies.[104] Interestingly, when loperamide was administered to KO mice, they displayed opioid-mediated CNS effects and accumulated 13-fold higher levels of radioactivity in the brain and 2-fold higher levels of radioactivity in the plasma compared to WT mice.[85] These results suggest that loperamide would be a centrally active opioid without P-gp in the BBB and would therefore not be obtained as an over-the-counter drug.

2.3.4   Meperidine

Meperidine is a moderately potent, short acting μ opioid analgesic and was found to be a P-gp substrate in various *in vitro* cell culture systems.[80, 84] Interestingly, the first *in vivo* experiment with meperidine using KO mice in a time course experiment (%MPE vs. time) resulted in the finding that antinociceptive effects were not greater in KO mice compared to WT mice.[89] Further *in situ* perfusion studies in KO mice by Dagenais *et al.* confirmed the previous finding, where meperidine was determined to have a P-gp effect

of 0.98 (Table 2.2).[50] Furthermore, meperidine was found to not increase ATPase activity *in vitro* and the antinociceptive effects were the same in KO and WT mice in both time course (%MPE vs. time) and dose-response *in vivo* studies.[94] These key experiments led to the finding that meperidine is not a P-gp substrate *in vivo*, although it is a P-gp substrate *in vitro*.

2.3.5 Oxycodone

Another commonly used opioid, oxycodone, has only recently been studied for its interactions with P-gp. Initial *in vivo* studies in which rats were preadministered PSC833 and then treated with oxycodone indicated that coadministration of the inhibitor and oxycodone did not alter the plasma pharmacokinetics, brain concentrations, or the associated tail flick latency of oxycodone, suggesting that oxycodone may not be a P-gp substrate in rats.[105] Whereas, hydrocodone, an oxycodone analog was reported to be a P-gp substrate in WT animals using P-gp inhibitors.[106] However, a more recent publication reported a Caco-2 transport efflux ratio of 2.06 and that P-gp was up-regulated in oxycodone tolerant mice (5 mg/kg oxycodone, i.p., 2x daily for 8 days).[45] These studies conclude that oxycodone is a P-gp substrate *in vivo*.[45] Additionally, the oxycodone induced P-gp up-regulation had a true physiological effect as it was found to effect paclitaxel tissue distribution definitely influencing the pharmacokinetic parameters.[45]

2.3.6 Fentanyl

Fentanyl and its analogs alfentanil and sufentanil are potent short acting synthetic opioid analgesics. *In vivo* analysis of fentanyl in KO animals resulted in 2-fold

antinociceptive effects in KO versus WT mice.[89] In L-MDR1 *in vitro* cell transport studies, fentanyl, alfentanil and sufentanil did not behave as P-gp substrates.[91] However, fentanyl was shown to be a P-gp substrate by *in situ* perfusion in KO mice having a P-gp effect of 1.24 (Table 2.2)[50] and alfentanil was shown to be an *in vivo* P-gp substrate using KO animals.[107] Most recent studies have determined the relationship between the P-gp ATPase activating effect of fentanyl and its P-gp dependent antinociceptive effects evaluated by dose-response and time course studies. The results between the *in vitro* and *in vivo* systems correlated well, resulting in increased ATPase activity and 2.2-fold greater antinociception in KO versus WT animals.[94] Lastly, human studies with quinidine, an *in vivo* inhibitor for intestinal and brain P-gp, have also been performed resulting in increased oral fentanyl absorption, suggesting that P-gp plays a role in the intestinal disposition of fentanyl, whereas the role of P-gp in brain fentanyl access requires further investigation.[108]

2.4 Development of opioid analgesics lacking P-gp substrate activity

The data reported here leads to the generalized conclusion that the up-regulation of P-gp contributes to the development of opioid tolerance, specifically in morphine[44] and oxycodone[45] tolerant animals resulting in less opioid in the general circulation. Recent studies by our group have investigated the P-gp effects of various opioid analogs in order to ultimately develop a clinically useful opioid analgesic which does not exhibit P-gp substrate activity. Meperidine was primarily chosen as a lead compound due to the fact that it is not an *in vivo* P-gp substrate. Initial studies investigated the effects of *N*-substitution on meperidine and results showed that *N*-phenylbutylnormeperidine was not

a P-gp substrate *in vitro*.[109]   Additionally, this compound was previously reported as twice the potency of meperidine[110] making it a good lead compound to test our hypothesis that opioids which lack P-gp substrate activity would not induce opioid tolerance.   A series of 3- and 6-desoxymorphine analogs was also investigated, resulting in the finding that removal of the 3- and/or 6-OH group generally decreased *in vitro* P-gp substrate activity; 6-desoxymorphine was chosen as the lead compound from this series since it has about 10x the potency of morphine and it lacked *in vitro* P-gp substrate activity.[111]   The *N*-phenylbutylnormeperidine and the 6-desoxymorphine synthetic analogs were further evaluated in KO and WT animals.   Both analogs were not P-gp substrates *in vivo*, however the *N*-phenylbutylnormeperidine analog was not twice as potent as meperidine as previously reported and eventually led to toxicity issues and subsequent discontinuation of further studies.[112]   Lastly, the effects of *m*-OH addition to meperidine was investigated and the results were consistent with the morphine analog series; the *m*-OH addition dramatically increased the P-gp substrate activity.[113]

2.5   Conclusion

The development of opioids which lack P-gp substrate activity both *in vitro* and *in vivo* are necessary for the development of an opioid and P-gp structure activity relationship as well as development of a quantitative structure activity relationship (QSAR). Further investigation will lead to an optimal opioid analgesic lacking this systems-level contribution to tolerance development and allow for delineation of the mechanism responsible for opioid-related P-gp up-regulation. Analgesics lacking P-gp

substrate activity will provide further support for evidence based medicine supporting clinical opioid rotation.

Chapter 3

P-Glycoprotein Substrate Activity of *N*-Substituted Analogs of

Meperidine and 3,6-Desoxymorphine Analogs

This chapter contains material from two published manuscripts and one in press:

Hassan, H. E.; Mercer, S. L.; Cunningham, C. W.; Coop, A.; Eddington, N. D. Evaluation of the P-Glycoprotein (P-gp) Affinity Status of a Series of Novel and Currently Available Morphine Analogs: Comparative Study with Meperidine Analogs to Identify Opioids with Minimal P-gp Interactions. *Int. J. Pharmaceutics.* In press.

3.1   Introduction

The development of improved agents for the treatment of chronic pain remains an important goal in public health.[114] The vast majority of currently employed agents for the treatment of severe chronic pain are opioid analgesics, which act as agonists at mu opioid receptors in the CNS.[115] Unfortunately, clinically employed opioid analgesics suffer from the development of tolerance, necessitating escalating doses to maintain the patient in a pain-free state,[9] thereby leading to escalated side-effects such as constipation.[17, 27] Numerous mechanisms at the receptor and cellular level have been indicated in the development of tolerance to mu opioid receptor agonists,[13] but recent reports have suggested that efflux transporters at the blood-brain barrier (BBB) may also contribute towards the development of central tolerance.[116] P-glycoprotein (P-gp) is an efflux transporter which is located in numerous tissues,[64] and its function at the BBB is to actively remove xenobiotics from the CNS.[64] Two commonly employed opioid analgesics, morphine (**1**) and oxycodone (**2**) (Figure 3.1), are known substrates for this transporter and rats tolerant to both morphine[44] and oxycodone[116] show up-regulation in P-gp level at the BBB. Thus, on chronic administration, the up-regulated P-gp would be expected to result in lower brain concentrations of opioid thereby exacerbating tolerance to the central analgesic effects. P-gp knockout animals are available and offer a useful model to study the effects of P-gp on opioids,[48] but an alternative approach in wild-type animals is the development of mu opioid receptor agonists which are not substrates for P-gp. These compounds would allow a full investigation of the contribution of up-regulated P-gp to opioid tolerance, and also potentially be developed into opioid analgesics with lower degrees of tolerance.
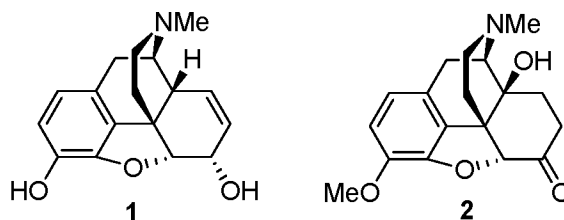
Figure 3.1. Morphine (**1**) and oxycodone (**2**).

The development of opioids with diminished P-gp substrate activity involves combining structure-activity relationships (SAR) of opioid agonists with SAR of P-gp substrates. Modifications affecting opioid antinociceptive potency have been well characterized,[51] however, P-gp SAR is less defined. Therefore, synthetic analogs of two readily used opioid analgesics, meperidine and morphine, were analyzed for their opioid pharmacology and P-gp substrate activity. The best lead compound from each series was selected for further P-gp *in vivo* analysis.

The mu opioid analgesic meperidine (**3**) has been shown to possess low activity as a P-gp substrate,[50] but only moderate antinociceptive activity *in vivo*.[58, 110] Thus, initial investigations described herein are focused on delineating the SAR of the *N*-substituent in this class for low P-gp substrate activity, while increasing opioid potency. Additionally, a morphine series of analogs was synthesized by Christopher W. Cunningham in order to investigate the effect of hydrogen bonding on P-gp SAR while maintaining opioid potency comparable to morphine.[117] The dissertation candidate has performed the P-gp *in vitro* and *in vivo* (partial) analysis of the morphine series which will be presented herein.

3.2   Results and Discussion

3.2.1   Chemistry

A range of previously reported and novel N-substituted analogs of meperidine were prepared from nitrile **4**, via alkylation with alkyl halides in DMF in the presence of K_2CO_3, followed by hydrolysis of the nitrile to the ethyl esters (**5-14**) through treatment with H_2SO_4 and EtOH[118] (Scheme 3.1). The alkyl substituents were chosen based on known active meperidine analogs and also following a series as previously described for other classes of opioids,[53] and include arylalky, alkyl, and branched alkyl groups (Table 3.1). All esters were converted to oxalate salts.
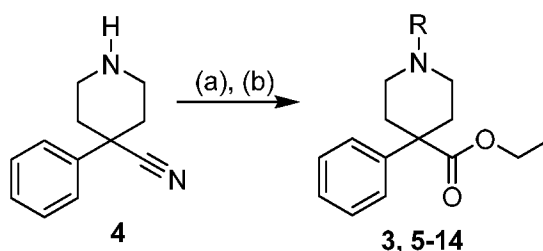
Scheme 3.1. Reagents and conditions: (a) RX, K_2CO_3, DMF; (b) H_2SO_4, EtOH, reflux.

Table 3.1. Compounds prepared, salt form, yield, and melting points. Citations reference previously known compounds. Table reproduced from reference[109] and republished with permission.

R	Ester	Salt, Yield, mp
CH_3	**3**[118]	Oxalate, 7%, 190-192°C
$(CH_2)_2(C_6H_5)$	**5**[52]	Oxalate, 33%, 205-20°C
$(CH_2)_3(C_6H_5)$	**6**[119]	Oxalate, 14%, 225°C
$(CH_2)_4(C_6H_5)$	**7**[119]	Oxalate, 25%, 170°C
$CH_2(C_6H_5)$	**8**[118]	Oxalate, 46%, 204-205°C
$CH_2CH=CH_2$	**9**[120]	Oxalate, 40%, 213-214°C
$(CH_2)_2CH_3$	**10**[121]	Oxalate, 57%, 215-216°C
$CH_2CH=CHCH_3$	**11**	Oxalate, 67%, 173-177°C
$(CH_2)_3CH_3$	**12**[121]	Oxalate, 24%, 190-192°C
$CH_2C(CH_3)=CH_2$	**13**	Oxalate, 35%, 180-181°C
$CH_2CH(CH_3)_2$	**14**	Oxalate, 55%, 165-167°C

3.2.2 Opioid Receptor Binding Studies

Most of the N-substituted meperidine analogs have been previously synthesized; however, binding studies were repeated to ensure data accuracy since new methodology has evolved for binding analysis. Binding studies were conducted as previously described.[122] As shown in Table 3.2, we are currently awaiting pharmacology for five meperidine analogs, specifically, **5 – 8**, and **11**. However, we are able to determine that all other analogs are selective for the μ opioid receptor, although the binding affinities are relatively weak. Meperidine (**3**) has a K_i of 231 nM whereas the N-butyl analog (**12**) has the most similar binding affinity of 270 nM. Compounds **9** and **10** have similar binding affinities of 527 and 505 nM, respectively; whereas compounds **13** and **14** have the lowest binding affinity of 752 and 704 nM, respectively of the series. These data overall suggest that binding affinity for meperidine analogs can be significantly improved.

Table 3.2. Opioid receptor binding affinity to cloned opioid receptors

R	Ester	Ki^a (nM) $\pm$ SEM		
		μ	κ	δ
H	normeperidine[123]	>10000	>10000	>10000
CH$_3$	**3**	231 ± 37	8780 ± 2060	3410 ± 1580
(CH$_2$)$_2$(C$_6$H$_5$)	**5**	AP	AP	AP
(CH$_2$)$_3$(C$_6$H$_5$)	**6**	AP	AP	AP
(CH$_2$)$_4$(C$_6$H$_5$)	**7**	AP	AP	AP
CH$_2$(C$_6$H$_5$)	**8**	AP	AP	AP
CH$_2$CH=CH$_2$	**9**	527 ± 175	$> 10,000$	$> 10,000$
(CH$_2$)$_2$CH$_3$	**10**	505 ± 215	5060 ± 320	4800 ± 680
CH$_2$CH=CHCH$_3$	**11**	AP	AP	AP
(CH$_2$)$_3$CH$_3$	**12**	270 ± 45	5640 ± 340	4320 ± 990
CH$_2$C(CH$_3$)=CH$_2$	**13**	752 ± 315	3780 ± 1650	$> 10,000$
CH$_2$CH(CH$_3$)$_2$	**14**	704 ± 146	5310 ± 700	5490 ± 1030
morphine[117]		1.70 ± 0.50	65.5 ± 22.6	104.57 ± 27.18

Analysis performed in cloned opioid receptors transfected into C$_6$ rat glioma cells (μ, δ) and Chinese hamster ovary (CHO) cells (κ) by the Drug Evaluation Committee. ^{a} K$_i$ values for standard compounds: DAMGO (μ, 7.6 nM), SNC80 (δ, 0.8 nM), U69593 (κ, 0.3 nM). Mean $\pm$ SEM for displacement of [^{3}H]diprenorphine from three experiments, performed in duplicate. AP = awaiting pharmacology.

3.2.3 Antinociception Studies

Analogs were also sent for *in vivo* antinociception studies; results are shown in Table 3.3 for all analogs with the exception of compounds **9** and **11**. All compounds analyzed are weak agonists possessing PPQ activity, with compounds 5 and 6 resulting as the most potent. Most compounds were considered inactive based on the definition of ED$_{50}$, however certain test compounds showed some activity which is more fully described in the caption. A more complete analysis would be to test all compounds at 30 mg/kg.

Table 3.3. In vivo potency of N-substituted meperidine analogs in mice[a]

	ED$_{50}$ ($s.c.$, mg/kg)[b]		
Ester	TF	PPQ	HP
3	Inactive[c]	6.03 (3.49 – 10.43)	Inactive[c]
5	8.15 (5.34 – 12.43)	2.18 (1.36 – 3.51)	5.5 (2.6 – 11.6)
6	12.3 (7.0 – 21.6)	4.5 (2.4 – 8.5)	Inactive[d]
7	Inactive	6.76 (3.15 – 14.49)	Inactive[e]
8	Inactive[f]	3.26 (0.83 – 12.82)	Inactive[f]
9	AP	AP	AP
10	Inactive	0.063 (0.012 – 33.3)	Inactive[g]
11	AP	AP	AP
12	Inactive[h]	8.7 (4.4 – 17.3)	Inactive[h]
13	Inactive[i]	9.53 (4.37 – 20.74)	Inactive[i]
14	Inactive[j]	5.5 (1.3 – 24.0)	Inactive[j]

[a] TF = tail-flick assay; PPQ = p-phenylquinone writhing assay; HP = hot plate assay. [b] Effective dose 50% (95% C.L.); subcutaneous ($s.c.$) administration. AP = awaiting pharmacology. Test compounds considered inactive according to ED$_{50}$ definition, however some activity was seen at the following doses during specified analysis: [c] 22% at 10 mg/kg (TF), 33% at 10 mg/kg (HP); [d] 65% at 10 mg/kg (HP); [e] 39% at 10 mg/kg (HP); [f] 23% at 30 mg/kg (TF), 36% at 10 mg/kg (HP); [g] 40% at 10 mg/kg (HP); [h] 68% at 30 mg/kg (TF), 15% at 10 mg/kg (HP); [i] 22% at 30 mg/kg (TF), 24% at 10 mg/kg (HP); [j] 7% at 30 mg/kg (TF), 10% at 10 mg/kg (HP). Analysis performed by the Drug Evaluation Committee.

3.2.4 Drug Stimulated P-gp ATPase Activity

Drug stimulated P-gp ATPase activity was estimated by Pgp-Glo assay system[63] (Promega, Madison, WI) and the results are shown in Figure 3.2. This method relies on the ATP dependence of the light-generating reaction of firefly luciferase where ATP consumption is detected as a decrease in luminescence. P-gp dependent decreases in luminescence reflect ATP consumption by P-gp; thus the greater the decrease in signal the higher the P-gp activity. Vanadate, a selective P-gp inhibitor, was used as a negative

control, whereas verapamil was used as a positive control. Test compounds (all tested at 200 μM) which are significantly lower than the control (NT) are P-gp substrates, whereas test compounds significantly higher than NT are P-gp inhibitors. Compounds which are significantly equal to the NT are neither P-gp substrates nor inhibitors. Three distinct P-gp binding classes exist; therefore, a mid-range concentration of 200 uM is used for all test compound analyses. A full range concentration dependent study on oxymorphone has been completed in order to justify using the 200 uM concentration for our experiments (Supplemental Material).
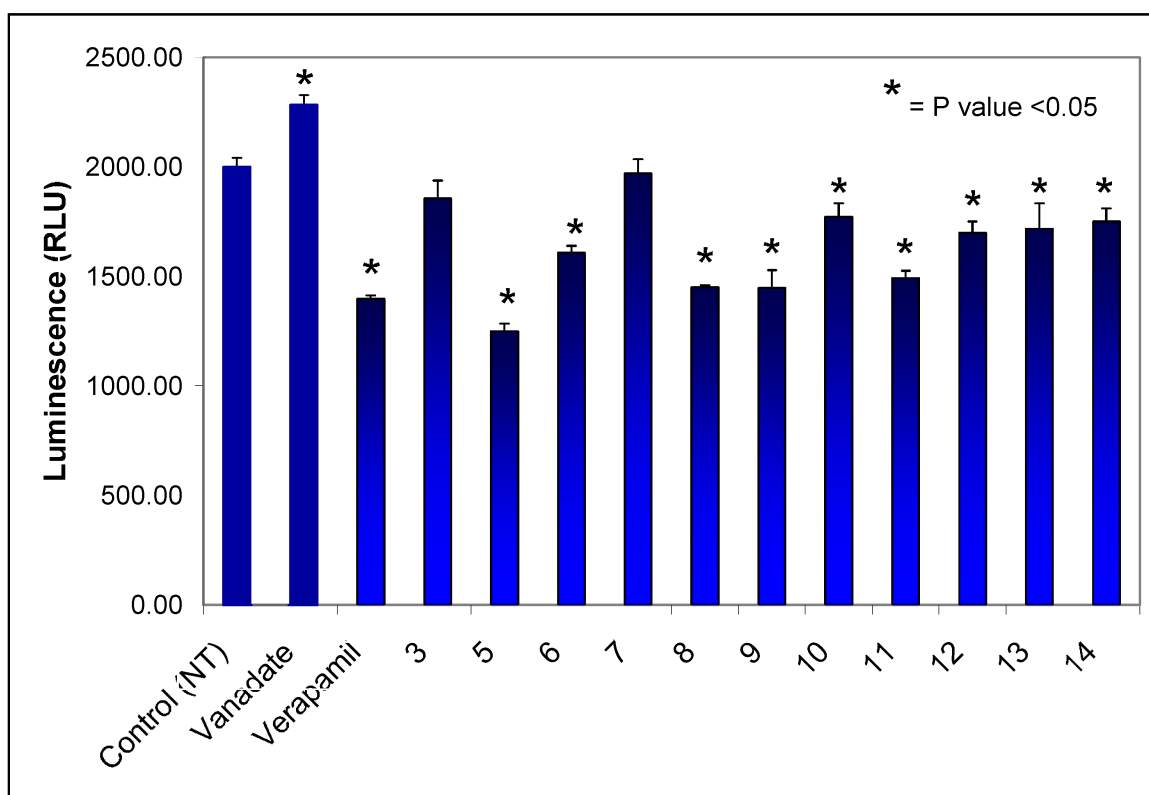
Figure 3.2. Results of compounds and standards in the P-gp-Glo assay system; all compounds assayed at 200 μM. Data are represented as mean $\pm$ SEM ($n = 4$). * Indicates significant difference from the control at $p < 0.05$ as indicated by t-test. Figure reproduced from reference[109] and republished with permission.

The P-gp substrate activity of the esters showed differences depending on the nature of the *N*-substituent. Most analogs were substrates for P-gp, with the exception of meperidine itself and *N*-phenylbutyl normeperidine (**7**). These results show a distinct SAR for P-gp substrate activity in this series as *N*-phenylalkyl analogs of shorter length (phenethyl (**5**), phenylpropyl (**6**)) were substrates.

Previous studies have shown that **7** has twice the antinociceptive activity as meperidine,[110] and thus has the profile required of low P-gp substrate activity and greater potency than meperidine for use as a tool to study the influence of P-gp on the development of opioid tolerance.

3.2.5   Assessment of the Antinociceptive Effects of Meperidine and *N*-phenylbutyl normeperidine (7) in *mdr1a/b* (-/-) and *mdr1a/b* (+/+) Mice

N-Phenylbutyl normeperidine (**7**) (ED_{50}) was pursued for further P-gp analysis, due to its increased potency compared to meperidine (ED_{50}) and also its lack of P-gp substrate activity. The antinociceptive effects of meperidine (50 mg/kg) and *N*-phenylbutyl normeperidine (3 and 60 mg/kg) were monitored for 150 minutes post dose in both P-gp knockout (KO) and P-gp competent mice (WT) using the tail flick test (Figures 3.3 and 3.4). Opioid administration to P-gp WT mice will cause antinociception as expected; however we are interested as to the level of antinociception the same dose of opioid will cause in P-gp KO mice. When a P-gp substrate is administered to KO mice, an increased level of antinociception is achieved, due to the fact that more of the drug is able to reach the brain and cause central opioid effects. However, when a non P-gp substrate is administered to KO mice, the same level of antinociception should be reached

when compared to WT animals administered the same dose. Both meperidine and **7** were found to be non-P-gp substrates through the *in vitro* P-gp ATPase assay; therefore, no difference in antinociception between KO and WT animals was expected. Our results support the hypothesis, showing that the genetic disruption of P-gp caused no significant increase in the antinociceptive activity of either meperidine or the *N*-phenylbutyl analog. High doses of meperidine can lead to the accumulation of the neurotoxic metabolite,[124] normeperidine; therefore, care was taken to avoid unnecessary high doses during this experiment. No toxicity was seen with meperidine, however toxicity was experienced with the highest dose of *N*-phenylbutyl normeperidine (**7**) (60 mg/kg). Mice in both groups (WT and KO) experienced episodes of convulsion that lasted for 1-2 minutes, 35 minutes post dose, which lead to eventual death ($n = 4$). Although both *in vitro* and *in vivo* evaluation of *N*-phenylbutyl normeperidine (**7**) indicates that it is not a P-gp substrate, it is not a suitable lead compound due to its dose dependent toxicity and low potency (Figure 3.4).
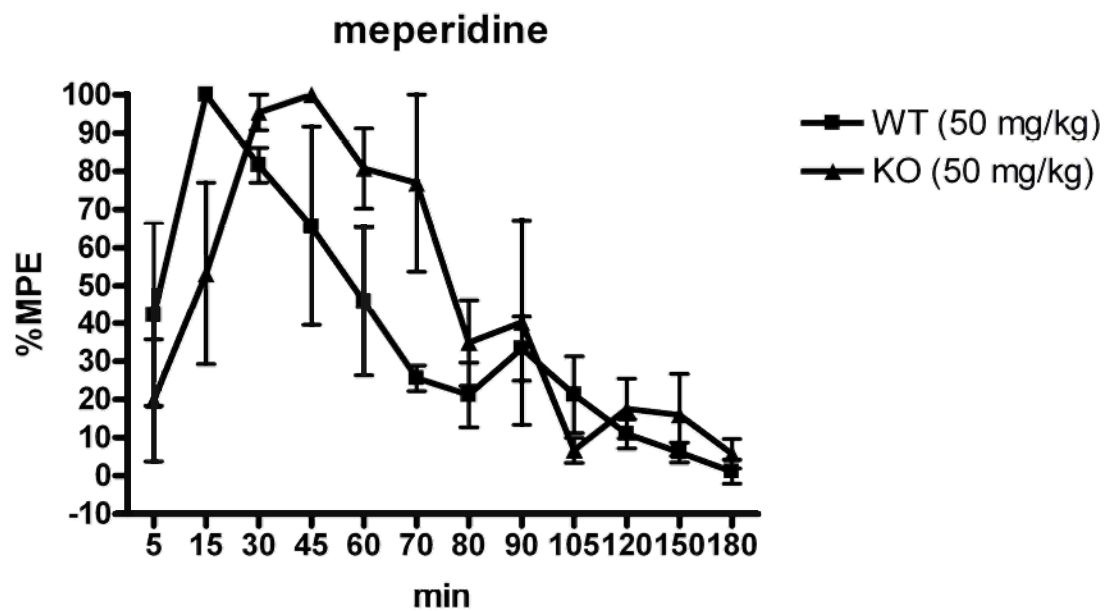
Figure 3.3. Tail flick latencies expressed as %MPE versus time for *mdr1a/b* (+/+) mice (WT) and *mdr1a/b* (-/-) mice (KO) that received single *i.p.* dose of 50 mg/kg meperidine. Data are expressed as the mean ± SEM (*n* = 5). Figure adopted from reference[112]
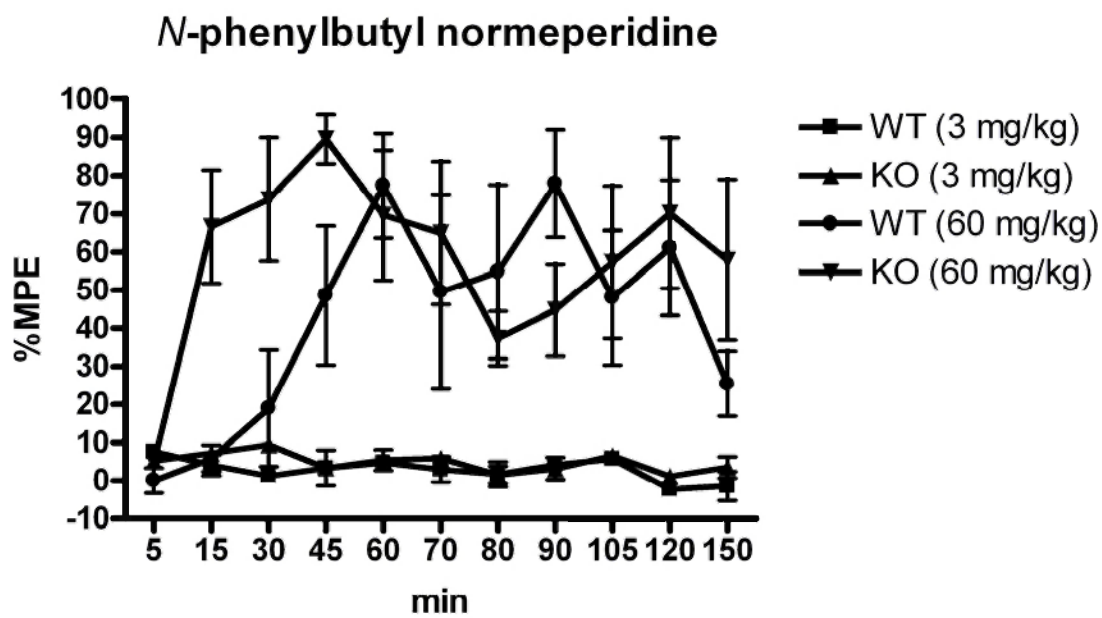
Figure 3.4. Tail flick latencies expressed as %MPE versus time for *mdr1a/b* (+/+) mice (WT) and *mdr1a/b* (-/-) mice (KO) that received single *i.p.* dose of 3 mg/kg or 60 mg/kg *N*-phenylbutyl normeperidine. Data are expressed as the mean ± SEM (*n* = 5). Figure adopted from reference[112]

3.2.6 Morphine Series

While the work on the meperidine series was being completed, my colleague, Christopher W. Cunningham, had synthesized a series of morphine analogs to investigate the SAR effect of hydrogen bonding, opioid potency and P-gp. The dissertation candidate has performed the P-gp *in vitro* and partial *in vivo* analysis of the morphine series. Morphine (**1**) and codeine (**15**) (Figure 5) are the parent compounds for this series and were analyzed as controls along with the synthesized compounds in the Promega P-gp-Glo assay system as previously explained in section 3.2.4. The drug stimulated P-gp ATPase activity results for this series is found in Figure 3.6. Both parent compounds, morphine and codeine, where confirmed as P-gp substrates as well as heterocodeine, 6-desoxycodeine and 3,6-didesoxymorphine. The following test compounds were neither P-gp substrates nor inhibitors: 3-desoxymorphine, codeine-6-methylether, 3-desoxyheterocodeine, and 6-desoxymorphine.
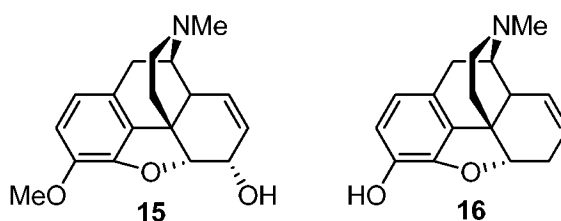
Figure 3.5. Codeine (**15**) and 6-desoxymorphine (**16**)

6-Desoxymorphine (**16**) was selected for further analysis, as it exhibited the greatest binding affinity of the non P-gp substrates and would not be prone to demethoxylation *in vivo*. Antinociception studies were subsequently performed for compound **16.** As shown in Table 3.4, compound **16** produces potent antinociception,

exhibiting greater potency compared to morphine in all assays performed. 6-Desoxymorphine (**16**) is approximately 10 times more potent than morphine in the tail flick (0.2 vs. 1.92 mg/kg) and phenylquinone (0.03 vs. 0.4 mg/kg) assays.
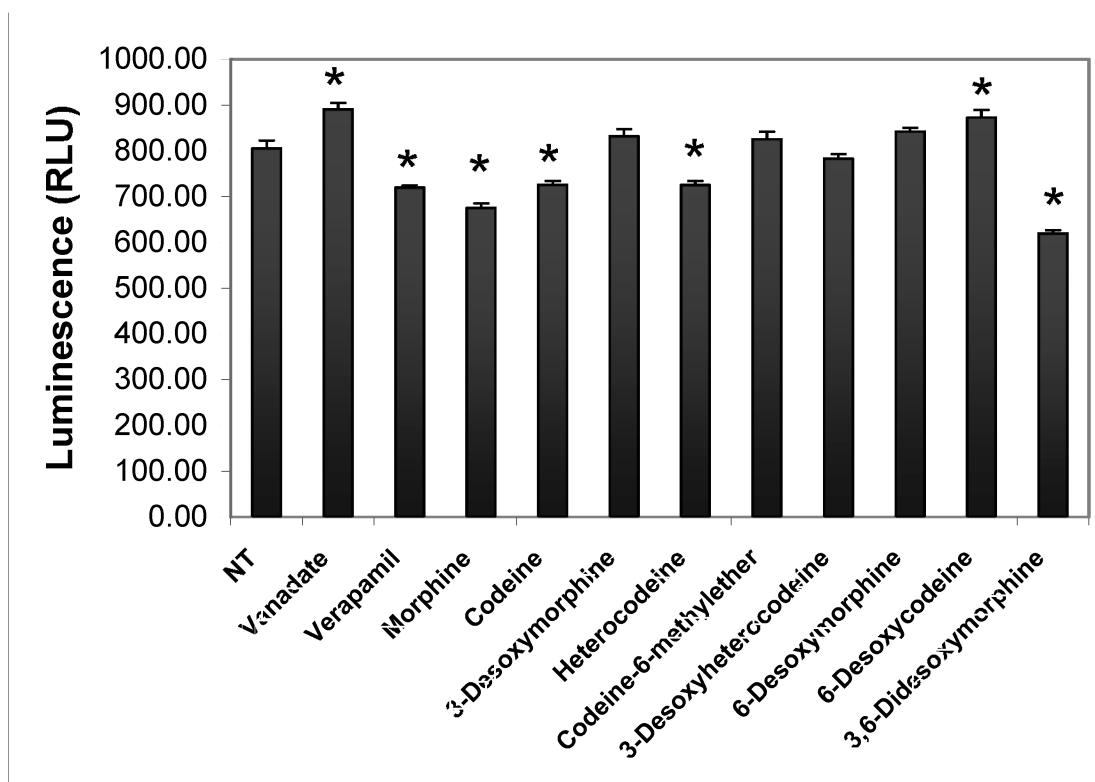
Figure 3.6. Results of compounds and standards in the P-gp-Glo assay system; all compounds assayed at 200 μM. Data are represented as mean ± SEM ($n = 4$). * Indicates significant difference from the control at $p < 0.05$ as indicated by t-test. Figure reproduced from reference[117] and republished with permission.

Table 3.4. In vivo potency of 6-desoxymorphine in mice[a]

	ED50 ($s.c.$, mg/kg)[b]		
Compound	TF	PPQ	HP
morphine[c]	1.92 (0.89-4.14)	0.4 (0.2-0.8)	0.85 (0.39-1.86)
6-desoxymorphine	0.2 (0.1-0.3)	0.03 (0.018-0.055)	0.33 (0.15-0.72)

[a] TF = tail-flick assay; PPQ = p-phenylquinone writhing assay; HP = hot plate assay. [b] Effective dose 50% (95% C.L.); subcutaneous ($s.c.$) administration. [c] Data from reference[125]. Figure reproduced from reference[117] and republished with permission.

Since 6-desoxymorphine (**16**) has the desired profile of a potent opioid lacking P-gp substrate activity, it then underwent *in vivo* evaluation in P-gp KO and WT mice (see Section 3.2.5). Testing low (0.2 mg/kg) and high (2 mg/kg) doses of 6-desoxymorphine (**16**) in both P-gp KO and WT mice showed that lack of P-gp had no significant influence on the antinociceptive activity of **16** (Figure 3.7). This suggests that it is not a P-gp substrate *in vivo* which is consistent with the P-gp ATPase assay findings (Figure 3.6). Notably, after administration of high dose (2 mg/kg) of 6-desoxymorphine (**16**), the %MPE reached its maximum (100%) for 45 minutes in both P-gp KO and WT mice, indicating the dose was too high for the time course study. For this reason, further investigation of the drug effect at 5-45 minutes post dose was explored.
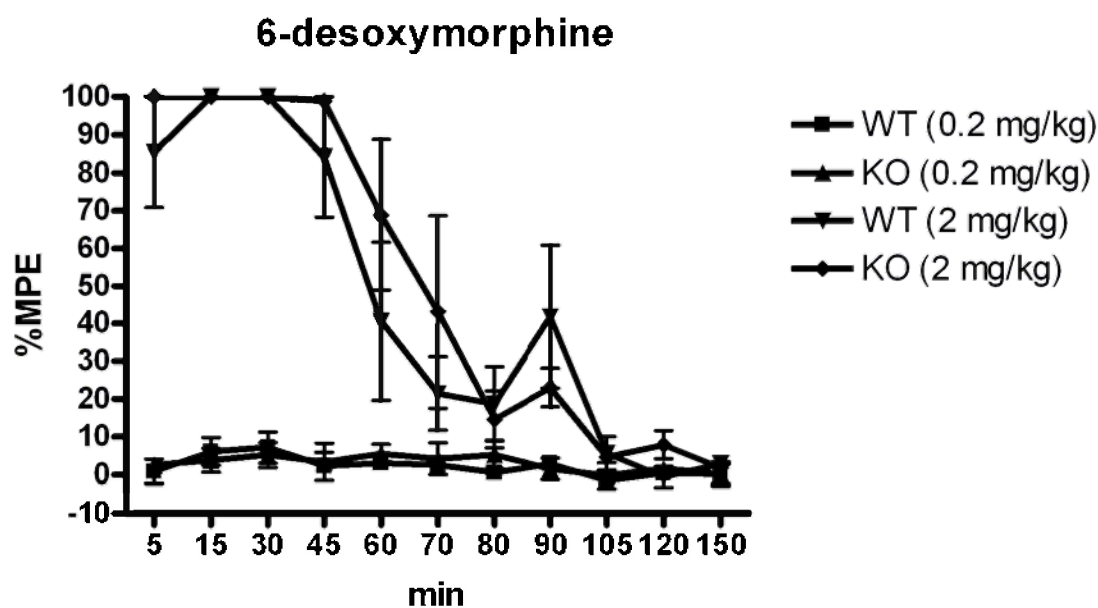
Figure 3.7. Tail flick latencies expressed as %MPE versus time for *mdr1a/b* (+/+) mice (WT) and *mdr1a/b* (-/-) mice (KO) that received single *i.p.* dose of 0.2 mg/kg or 2 mg/kg 6-desoxymorphine. Data are expressed as the mean ± SEM (n = 5). Figure adopted from reference[112]

In order to more fully investigate the drug effect between the 0.2 and 2.0 mg/kg doses initially studied during the time course experiment, a dose response study was designed. Three doses to include 0.5, 1.0, and 1.5 mg/kg of 6-desoxymorphine (**16**) were chosen for administration to both P-gp KO and WT mice. The antinociceptive effect of each dose was monitored at 15 and 30 minutes post dose using the tail flick test (Figure 3.8). Results show two distinct dose response curves for the P-gp KO and WT mice. The P-gp competent animals experienced 12.6, 36.1, and 81.8 %MPE at doses 0.5, 1.0, and 1.5 mg/kg, respectively, whereas the P-gp deficient animals experienced 54.5, 91.0, and 99.2 %MPE at doses 0.5, 1.0, and 1.5 mg/kg, respectively. Overall, a greater antinociceptive effect was achieved in the KO mice, indicating that 6-desoxymorphine (**16**) is a P-gp substrate at lower doses. These results are inconsistent with previous studies and suggest that further studies should be conducted with a larger set of animals with an increased range of doses to fully delineate the P-gp substrate activity of 6-desoxymorphine.
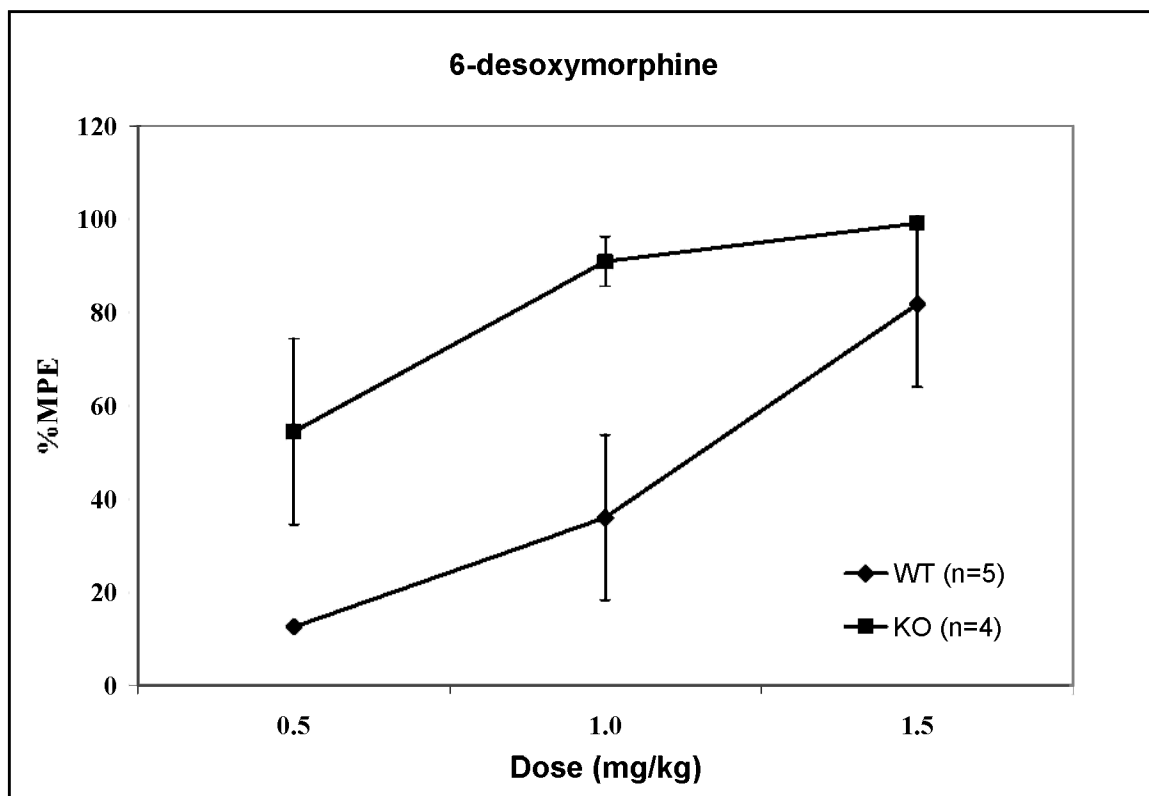
Figure 3.8. Tail flick latencies expressed as %MPE versus dose (mg/kg) for *mdr1a/b*
(+/+) mice (WT) and *mdr1a/b* (-/-) mice (KO) that received single *i.p.* dose of 0.5, 1.0
and 1.5 mg/kg of 6-desoxymorphine. Data are expressed as the mean ± S.E.M (*n* = as
noted).

3.3   Conclusion

A series of *N*-substituted meperidine analogs were synthesized in order to increase opioid potency while also investigate their SAR at P-gp.   All analogs were substrates for P-gp in the P-gp ATPase assay with the exception of meperidine itself and the *N*-phenylbutyl normeperidine analog (**7**).   Since compound **7** was reportedly twice as potent as meperidine and it lacked P-gp substrate activity it was chosen as a lead compound for further investigation.   Meperidine (50 mg/kg) and *N*-phenylbutyl normeperidine (**7**) (3 and 60 mg/kg) underwent *in vivo* P-gp analysis in P-gp KO and WT mice.   Although neither compound was a P-gp substrate *in vivo*, it was determined that *N*-phenylbutyl normeperidine (**7**) was not twice as meperidine, as it required a higher dose to achieve an antinociceptive effect.   The 60 mg/kg dose of *N*-phenylbutyl normeperidine (**7**) caused toxicity in the mice, exhibited as episodes of convulsions eventually resulting in the death of four mice.   This toxicity was hypothesized to be the result of normeperidine, the toxic metabolite of meperidine which causes neurotoxic effects when accumulated in the brain.   As a direct result, *N*-phenylbutyl normeperidine (**7**) was discontinued as a lead compound and no further analysis was performed.

A morphine series was also developed in order to investigate the effects of hydrogen bonding, opioid potency, and P-gp substrate activity.   Four compounds in the series: 3-desoxymorphine, codeine-6-methylether, 3-desoxyheterocodeine, and 6-desoxymorphine (**16**) were non P-gp substrates in the P-gp ATPase assay.   6-Desoxymorphine (**16**) was chosen for further analysis due to its high opioid potency and lack of P-gp substrate activity.   *In vivo* results of a time course study performed in P-gp KO and WT animals indicated that 6-desoxymorphine (**16**) was not a P-gp substrate *in*

vivo; however, the dose used in the study (2 mg/kg) was too high and caused 100 %MPE during the first 45 minutes of the analysis. To analyze this result further, a dose response study was designed to investigate the antinociceptive effect of **16** at 0.5, 1.0, and 1.5 mg/kg in both P-gp WT and KO mice. Results showed two distinct curves between the WT and KO mice. The KO mice experienced an increased antinociceptive effect compared to the WT mice, suggesting that 6-desoxymorphine (**16**) is a P-gp substrate at lower doses. Further studies are needed to clarify these results.

3.4 Experimental Section

3.4.1 Chemistry

All reactions were performed under an atmosphere of nitrogen, and all solvents were removed on a rotary evaporator under reduced pressure. TLC was performed on plates coated with silica gel GHLF-0.25 mm plates (60 F_{254}) (Analtech). Mass spectra were obtained on a ThermoFinnigan LCQ Classic. ^{1}H NMR spectra were obtained using a 500 MHz Varian NMR. Melting points were determined in open capillary tubes using a Mel-Temp melting point apparatus; melting points are uncorrected. Combustion analysis was performed by Atlantic Microlab, Inc. (Norcross, GA).

General Procedure for the Synthesis of *N*-substituted Ester Meperidine Analogs (3-14): The corresponding nitriles were suspended in a 1:1 H_2SO_4-dH_2O solution (15 mL/g) and refluxed at 170°C for 4 h. Upon cooling, absolute EtOH (30 mL/g) was added to the flask and was subsequently removed under reduced pressure (4x). The resulting oil was redissolved in absolute EtOH and refluxed overnight. After cooling, the solvent was

removed under reduced pressure. The resulting acidic residue was cooled in an ice bath and neutralized with aqueous $NaHCO_3$ until pH 10 was obtained. The resulting mixture was extracted into $CHCl_3$ and dried (Na_2SO_4). Removal of the solvent under reduced pressure yielded the crude compound. Recrystallization from acetone and oxalic acid yielded the pure oxalate salts.

Ethyl 1-methyl-4-phenylpiperidine-4-carboxylate oxalate (3): RX = methyl iodide (Sigma-Aldrich); purified from acetone and oxalic acid to produce oxalate salt; yield 7%; mp 190-192°C; ^{1}H NMR ($CDCl_3$) δ 7.38 (d, 7.56 Hz, 2H), 7.32 (t, 7.78 Hz, 2H), 7.23 (t, 7.56 Hz, 1H), 4.13 (q, 7.10 Hz, 2H), 2.79 (t, 13.52 Hz, 2H), 2.57 (t, 13.78 Hz, 2H), 2.27 (s, 3H), 2.15 (t, 11.77 Hz, 2H), 1.98 (t, 11.60 Hz, 2H), 1.18 (t, 7.42 Hz, 3H); MS (ESI) m/z = 248.17 (M + H$^+$); Anal. ($C_{17}H_{23}NO_6$•0.25H_2O) C, H, N.

Ethyl 1-phenylethyl-4-phenylpiperidine-4-carboxylate oxalate (5): RX = 2-bromoethyl benzene (Sigma-Aldrich); yield 33%; mp 205-207°C; ^{1}H NMR ($CDCl_3$) δ 7.39 (d, 7.93 Hz, 4H), 7.33 (t, 7.56 Hz, 4H), 7.20 (t, 7.18 Hz, 2H), 4.14 (q, 7.21 Hz, 2H), 2.98 (t, 8.52 Hz, 2H), 2.83 (t, 7.21 Hz, 2H), 2.61 (t, 13.10 Hz, 2H), 2.27 (t, 11.14 Hz, 2H), 2.03 (t, 10.48 Hz, 2H), 1.60 (t, 7.81 Hz, 2H), 1.18 (t, 7.07 Hz, 3H); MS (ESI) m/z = 338.21 (M + H$^+$); Anal. ($C_{24}H_{29}NO_6$•H_2O) C, H, N.

Ethyl 1-phenylpropyl-4-phenylpiperidine-4-carboxylate oxalate (6): RX = 1-bromo-3-phenylpropane (Sigma-Aldrich); yield 18%; mp 225°C; ^{1}H NMR ($CDCl_3$) δ 7.70 (d, 7.76 Hz, 4H), 7.53 (t, 6.54 Hz, 4H), 7.32 (t, 8.17 Hz, 2H), 4.17 (q, 7.25 Hz, 2H),

3.17 (d, 12.38 Hz, 2H), 2.87 (t, 11.25 Hz, 2H), 2.62 (t, 7.88 Hz, 2H), 2.56 (t, 12.37 Hz, 2H), 2.37 (t, 10.13 Hz, 2H), 2.17 (t, 7.15 Hz, 2H), 1.99 (m, 2H), 1.18 (t, 7.10 Hz, 3H); MS (ESI) m/z = 352.22 (M + H$^+$); Anal. ($C_{25}H_{31}NO_6 \cdot 2HO_2CCO_2H \cdot 2H_2O$) C, H, N.

Ethyl 1-phenylbutyl-4-phenylpiperidine-4-carboxylate oxalate (7): RX = 1-chloro-4-phenylbutane (Sigma-Aldrich); yield 25%; mp 170°C; ^{1}H NMR (CDCl$_3$) δ 7.34 (m, 8H), 7.24 (t, 7.46 Hz, 2H), 4.14 (q, 7.46 Hz, 2H), 3.15 (d, 13.06 Hz, 2H), 2.85 (t, 12.13 Hz, 2H), 2.57 (d, 13.37 Hz, 2H), 2.34 (m, 2H), 2.16 (m, 2H), 1.92 (t, 11.51 Hz, 2H), 1.56 (m, 4H), 1.18 (t, 7.15 Hz, 3H); MS (ESI) m/z = 366.24 (M + H$^+$); Anal. ($C_{26}H_{33}NO_6 \cdot 1.25C_2H_2O_4$) C, H, N.

Ethyl 1-benzyl-4-phenylpiperidine-4-carboxylate oxalate (8): RX = benzyl bromide (Sigma-Aldrich); yield 46%; mp 204-205°C; ^{1}H NMR (CDCl$_3$) δ 7.38 (d, 7.93 Hz, 4H), 7.31 (t, 7.14 Hz, 4H), 7.23 (t, 7.34 Hz, 2H), 4.11 (q, 7.14 Hz, 2H), 3.48 (s, 2H), 2.83 (d, 9.12 Hz, 2H), 2.56 (d, 12.50 Hz, 2H), 2.19 (t, 11.50 Hz, 2H), 1.97 (t, 11.11 Hz, 2H), 1.17 (t, 6.94 Hz, 3H); MS (ESI) m/z = 324.19 (M + H$^+$); Anal. ($C_{23}H_{27}NO_6 \cdot 1.5H_2O$) C, H, N.

Ethyl 1-allyl-4-phenylpiperidine-4-carboxylate oxalate (9): RX = allyl bromide (Sigma-Aldrich); yield 40%; mp 225-226°C; ^{1}H NMR (CDCl$_3$) δ 7.38 (d, 7.84 Hz, 2H), 7.32 (t, 8.18 Hz, 2H), 7.23 (t, 7.16 Hz, 1H), 5.88 (m, 1H), 5.18 (m, 2H), 4.13 (q, 7.28 Hz, 2H), 3.50 (s, 2H), 2.97 (m, 2H), 2.61 (d, 12.69 Hz, 2H), 2.11 (m, 2H), 1.66 (m, 2H), 1.18 (t, 7.03 Hz, 3H); MS (ESI) m/z = 274.18 (M + H$^+$); Anal. ($C_{19}H_{25}NO_6$) C, H, N.

Ethyl 1-propyl-4-phenylpiperidine-4-carboxylate oxalate (10): RX = allyl bromide (Sigma-Aldrich); yield 57%; mp 215-216°C; ^{1}H NMR (CDCl$_3$) δ 7.34 (m, 5H), 4.14 (m, 2H), 2.93 (t, 11.93 Hz, 2H), 2.6 (t, 11.27 Hz, 2H), 2.35 (t, 7.95 Hz, 2H), 2.22 (t, 10.27 Hz, 2H), 2.04 (t, 11.60 Hz, 2H), 1.56 (m, 2H), 1.18 (t, 6.96 Hz, 3H), 0.90 (t, 7.95 Hz, 3H); MS (ESI) m/z = 276.19 (M + H$^+$); Anal. (C$_{19}$H$_{27}$NO$_6$•H$_2$O) C, H, N.

Ethyl 1-crotyl-4-phenylpiperidine-4-carboxylate oxalate (11): RX = crotyl bromide (Sigma-Aldrich); yield 67%; mp 173-177°C; ^{1}H NMR (CDCl$_3$) δ 7.33 (m, 5H), 5.60 (m, 1H), 5.52   (m, 1H), 4.12 (m, 2H), 2.93 (m, 2H), 2.58 (m, 6H), 1.96 (m, 3H), 1.63 (m, 2H), 1.16 (m, 3H); MS (ESI) m/z = 288.19 (M + H$^+$); Anal. (C$_{20}$H$_{27}$NO$_6$•2H$_2$O) C, H, N.

Ethyl 1-butyl-4-phenylpiperidine-4-carboxylate oxalate (12): RX = crotyl bromide (Sigma-Aldrich); yield 54%; mp 190-192°C; ^{1}H NMR (CDCl$_3$) δ 7.39 (d, 7.70 Hz, 2H), 7.32 (t, 7.13 Hz, 2H), 7.13 (t, 7.42 Hz, 1H), 4.13 (q, 6.84 Hz, 2H), 2.86 (m, 2H), 2.57 (d, 12.55 Hz, 2H), 2.30 (t, 7.70 Hz, 2H), 2.13 (t, 10.84 Hz, 2H), 1.98 (t, 11.69 Hz, 2H), 1.48 (m, 2H), 1.32 (m, 2H), 1.18 (t, 7.13 Hz, 3H), 0.92 (t, 7.45 Hz, 3H); MS (ESI) m/z = 290.21 (M + H$^+$); Anal. (C$_{20}$H$_{29}$NO$_6$•H$_2$O) C, H, N.

Ethyl 1-(2-methylallyl)-4-phenylpiperidine-4-carboxylate oxalate (13): RX = 3-bromo-2-methyl-propene (Sigma-Aldrich); yield 35%; mp 180-181°C; ^{1}H NMR (CDCl$_3$) δ 7.39 (d, 8.32 Hz, 2H), 7.33 (t, 7.40 Hz, 2H), 7.24 (t, 7.86 Hz, 1H), 5.25 (m, 1H), 5.14 (m, 1H), 4.14 (q, 7.16 Hz, 2H), 3.10 (s, 2H), 3.06 (d, 12.99 Hz, 2H), 2.80 (t,

11.99 Hz, 2H), 2.55 (d, 12.83 Hz, 2H), 1.83 (t, 11.49 Hz, 2H), 1.61 (s, 3H), 1.19 (t, 7.00

Hz, 3H); MS (ESI) m/z = 288.19 (M + H$^+$); Anal. (C$_{20}$H$_{27}$NO$_6$•0.5C$_2$H$_2$O$_4$) C, H, N.

Ethyl 1-isobutyl-4-phenylpiperidine-4-carboxylate oxalate (14): RX = 3-
bromo-2-methyl-propene (Sigma-Aldrich); yield 55%; mp 165-167°C; ^{1}H NMR (CDCl$_3$)

δ 7.39 (d, 8.32 Hz, 2H), 7.33 (t, 7.55 Hz, 2H), 7.22 (t, 7.35 Hz, 1H), 4.12 (m, 2H), 2.80 (t,

11.80 Hz, 2H) 2.55 (d, 12.56 Hz, 2H), 2.05 (d, 7.35 Hz, 2H), 1.96 (t, 11.45 Hz, 2H), 1.83

(t, 11.22 Hz, 2H), 1.61 (s, 1H), 1.18 (m, 3H), 0.88 (d, 6.58 Hz, 6H); MS (ESI) m/z =

290.21 (M + H$^+$); Anal. (C$_{20}$H$_{29}$NO$_6$•0.5C$_2$H$_2$O$_4$) C, H, N.

Table 3.5. Analytical Data for Compounds **3-14**

Compound Number	Calculated (%)			Found (%)		
	C	H	N	C	H	N
3 • 0.25 H$_2$O	59.72	6.92	4.10	59.80	6.88	4.05
5 • 1 H$_2$O	64.70	7.01	3.14	64.62	6.77	3.14
6 • 2 C$_2$H$_2$O$_4$ • 2 H$_2$O	52.97	5.98	2.13	52.52	5.98	2.13
7 • 1.25 C$_2$H$_2$O$_4$	60.06	6.30	4.47	59.62	6.54	4.34
8 • 1.5 H$_2$O	62.71	6.86	3.18	63.08	6.41	3.08
9	62.80	6.93	3.85	62.42	6.93	3.80
10 • 1 H$_2$O	59.52	7.62	3.65	59.56	7.04	3.73
11 • 2 H$_2$O	58.10	7.56	3.39	58.60	7.05	3.40
12 • 1 H$_2$O	60.44	7.86	3.52	60.12	7.12	3.55
13 • 0.5 C$_2$H$_2$O$_4$	59.71	6.68	3.32	59.51	6.66	4.28
14 • 0.5 C$_2$H$_2$O$_4$	59.42	7.12	3.30	58.97	6.92	3.70

3.4.2 Pharmacological Assays

3.4.2.1 Opioid Binding

Binding assays were performed as previously described[122] using [^{3}H]diprenorphine in membranes from C_6 rat glioma cells expressing recombinant μ or δ receptors and CHO cells expressing the recombinant κ receptors.

3.4.2.2 Opioid Antinociception Studies

Antinociception was determined using the tail flick (TF), p-phenylquinone (PPQ), and hot plate (HP) assays in mice as previously described by the Drug Evaluation Committee (DEC) of the College on Problems of Drug Dependence (CPDD).[126]

3.4.2.3 Drug Stimulated P-gp ATPase Activity

Drug stimulated P-gp ATPase activity was estimated by Pgp-Glo assay system[1] (Promega, Madison, WI). This method relies on the ATP dependence of the light-generating reaction of firefly luciferase where ATP consumption is detected as a decrease in luminescence. In a 96 well plate, recombinant human P-gp (25 μg) was incubated with P-gp-Glo assay buffer™ (20 μl) (control, n = 4), verapamil (200 μM) (n = 4), sodium orthovanadate (100 μM) (n = 4), and test compounds (200 μM) (n = 4). Each compound was loaded in four individual wells. Verapamil served as a positive control while sodium orthovanadate (vanadate) was used as a P-gp ATPase inhibitor. The reaction was initiated by addition of MgATP (10 mM), then stopped 40 minutes later by addition of 50 μL of firefly luciferase reaction mixture (ATP detection reagent) that initiated an ATP-dependent luminescence reaction. Signals were measured 60 minutes later and integrated

for 10 seconds by Lmax® luminometer (Molecular Devices Corporation, Sunnyvale, CA).

3.4.2.4   Experimental Animals

Male *mdr1a/b (-/-)* and male FVB *mdr1a/b (+/+)* mice weighing 28 ± 5 g (20-24 weeks of age) were purchased from Taconic Laboratories (Germantown, NY). The mice were housed individually and allowed to acclimate at least one week prior to the experiment. Animals were fed chow and water *"ad libitum"* and maintained on a 12-hour light/dark cycle. The protocol for the animal studies was approved by the School of Pharmacy, University of Maryland IUCUC.

3.4.2.5   Assessment of the Antinociceptive Effects of Opioids in mdr1a/b (-/-) and mdr1a/b (+/+) Mice for the Time Course Study

The tail flick test was used to determine the antinociceptive effects of meperidine, *N*-phenylbutyl normeperidine, and 6-desoxymorphine. These three opioids were selected because they showed no significant ($p < 0.05$) stimulation of P-gp ATPase activity. Each opioid was administered *i.p.* to two groups of mice [*mdr1a/b* (-/-) and *mdr1a/b* (+/+)] (*n* = 5-6/group). No mouse in any group received more than one single *i.p.* dose of any opioid. The doses of the tested opioids were as follow: 50 mg/kg meperidine, 3 and 60 mg/kg *N*-phenylbutyl normeperidine, and 0.2 and 2 mg/kg 6-desoxymorphine. Antinociceptive effect was monitored at 5, 15, 30, 45, 60, 90, 120, and 150 minutes post dosing using the tail flick analgesia meter (Pamotor, Burlingame, CA).[127] The test was carried out using a modified tail flick test (radiant heat method). Briefly, each mouse was

placed on the surface of the tail flick analgesia meter and radiant heat was applied from a halogen lamp focused on the dorsal surface of its tail (2-3 cm from the base of the tail). The intensity of the radiant heat was adjusted so that baseline tail flick occurred within 1-2 seconds. Tail flick latency responses were measured in duplicate. A cut-off time of 9 seconds was used to prevent tail damage. Mice that failed to respond within the respective cut-off time were defined as "analgesic". The percentages of the maximum possible effect (%MPE) were calculated using Equation 3.1. The tail flick latency values were converted to %MPE and plotted against time.[128, 129] All data were presented as mean $\pm$ SEM. ANOVA with repeated measures (SigmaStat™ 2.03 statistical package) was used to determine the statistical significance between groups. The 0.05 level of probability was used as the criterion of significance.

Equation 3.1 $\%MPE = \dfrac{post\ drug\ latency - pre\ drug\ latency}{cutoff - pre\ drug\ latency} \times 100$

3.4.2.6 Assessment of the Antinociceptive Effects of 6-Desoxymorphine in *mdr1a/b* (-/-) and *mdr1a/b* (+/+) Mice for the Dose Response Study

The tail flick test was used to determine the antinociceptive effects of 6-desoxymorphine. This opioid was selected for further investigation since the 2 mg/kg curve "topped-out" in the time course study. 6-Desoxymorphine was administered *i.p.* to two groups of mice [*mdr1a/b* (-/-) and *mdr1a/b* (+/+)] (n = 6/group). Each animal received 3 doses of 6-desoxymorphine total, one of each dose to include 0.5, 1.0, and 1.5 mg/kg. A three day wash out period was observed in between doses. Antinociceptive effect was monitored at 15 and 30 minutes post dosing using the tail flick analgesia meter

(Pamotor, Burlingame, CA).[127] The test was carried out using a modified tail flick test (radiant heat method). Briefly, each mouse was placed on the surface of the tail flick analgesia meter and radiant heat was applied from a halogen lamp focused on the dorsal surface of its tail (2-3 cm from the base of the tail). The intensity of the radiant heat was adjusted so that baseline tail flick occurred within 1-2 seconds. Tail flick latency responses were measured in duplicate. A cut-off time of 9 seconds was used to prevent tail damage. Mice that failed to respond within the respective cut-off time were defined as "analgesic". The percentages of the maximum possible effect (%MPE) were calculated using Equation 3.1. The tail flick latency values were converted to %MPE and plotted against dose. All data were presented as mean $\pm$ SEM. The 0.05 level of probability was used as the criterion of significance between the test dose and baseline.

Chapter 4

P-Glycoprotein Substrate Activity of 3-Hydroxyl Addition to

Meperidine Analogs

This chapter contains material from the following in press manuscript:

Mercer, S. L.; Cunningham, C. W.; Eddington, N. D.; Coop, A. Opioids and Efflux Transporters. Part 3: P-Glycoprotein Substrate Activity of 3-Hydroxyl Addition to Meperidine Analogs. *Bioorg. Med. Chem. Lett.* **2008**, *18*, 3638-3640. Copyright 2008 Elsevier.

4.1   Introduction

There is a growing body of evidence that suggests efflux transporters, specifically P-glycoprotein (P-gp), may play a role in the development of opioid related central tolerance and constipation.[44, 45, 64, 109, 111, 112] Recent studies have shown that opioids are substrates for P-gp, although to differing extents,[50] and P-gp is up-regulated at the blood-brain barrier (BBB) of morphine[64] (**1**) and oxycodone[45] (**2**) (Figure 4.1) tolerant rats. Upon chronic administration, the up-regulated P-gp would be expected to result in lower brain concentrations of opioid, thereby exacerbating tolerance to the central analgesic effects. P-gp knockout animals[77] are available and offer a useful model to study the effects of P-gp on opioids, however an alternative approach in wild-type animals is the development of mu opioid receptor agonists which are not P-gp substrates. These compounds would allow a full investigation of the contribution of up-regulated P-gp to opioid tolerance, as full cross-tolerance between morphine and the opioid lacking P-gp substrate activity would not be anticipated to occur. Additionally, opioids lacking P-gp substrate activity may potentially be developed into analgesics with lower degrees of tolerance.

Meperidine (**3**), a moderately potent mu opioid analgesic,[58, 110] possesses low P-gp substrate activity.[50]   Therefore, our investigations are focused on delineating the structure-activity relationship (SAR) for the addition of a *m*-OH, while increasing mu opioid potency based on known SAR for this series.[110]
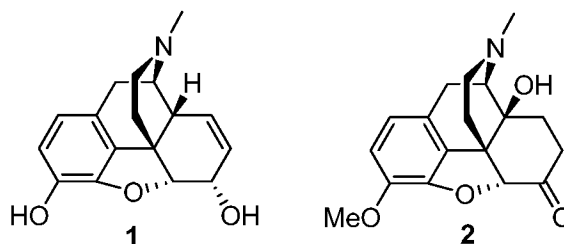
Figure 4.1. Morphine (**1**) and oxycodone (**2**).

4.2   Results and Discussion

4.2.1   Chemistry

The compounds synthesized are readily known in the literature as mu opioid analgesics;[110] however, the syntheses described here are novel approaches. Meperidine (**3**) was prepared from nitrile **4** (obtained from Sigma-Aldrich, Inc.), via alkylation with MeI in DMF in the presence of K_2CO_3, followed by aqueous NH_4Cl hydrolysis of the N-methyl nitrile **5** to the ethyl ester through treatment with H_2SO_4 and EtOH. Treatment of **5** with EtMgBr, via a Grignard reaction,[130] produced the ketone meperidine analog **6** (Scheme 4.1). Compounds **3** and **6** were converted to their respective salts (Table 4.1).
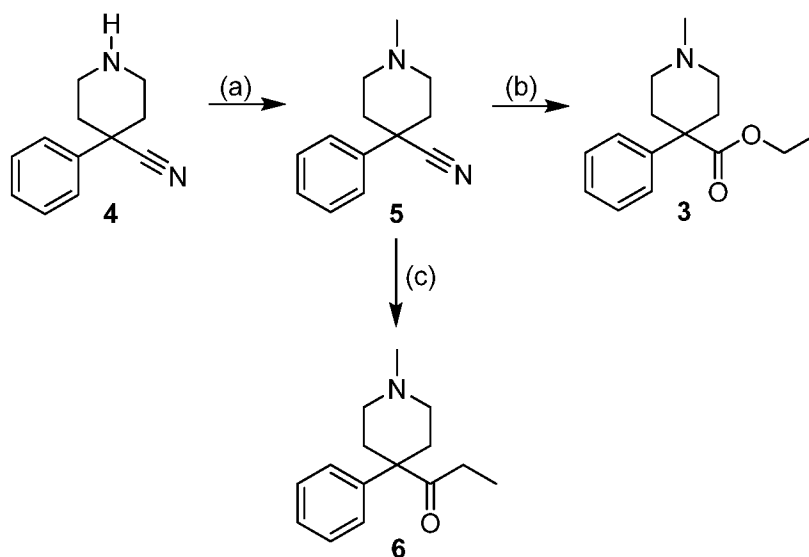
Scheme 4.1. Reagents and conditions: (a) MeI, K$_2$CO$_3$, DMF; (b) H$_2$SO$_4$, EtOH, reflux; (c) EtMgBr, NH$_4$Cl hydrolysis.

Bemidone **9** was prepared from the condensation of mechloroethamine hydrochloride and 3-methoxyphenyl-acetonitrile (both reagents obtained from Sigma-Aldrich, Inc.) with NaH and NaOH to yield **7**. *O*-dealkylation of **7** was performed with BBr$_3$ and NH$_4$OH,[131] converting the methoxy group to a phenol **8**, followed by nitrile hydrolysis to give the *m*-OH ethyl ester as previously described.[109] Treatment of **7** with an EtMgBr Grignard reagent,[130] followed by aqueous NH$_4$Cl hydrolysis produced **10**, which then underwent treatment with BBr$_3$ to produce ketobemidone (**11**) (Scheme 4.2). Compounds **9** and **11** were converted to oxalate salts (Table 4.1).
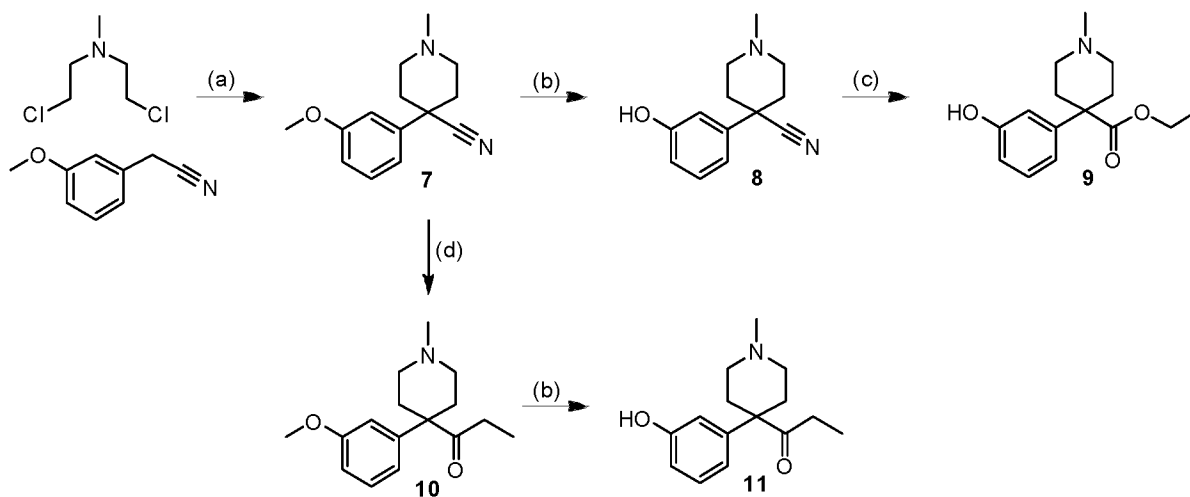
Scheme 4.2. Reagents and conditions: (a) NaH, NaOH; (b) BBr$_3$, NH$_4$OH; (c) H$_2$SO$_4$, EtOH; (d) EtMgBr, NH$_4$Cl hydrolysis.

4.2.2 Drug Stimulated P-gp ATPase Activity

Drug stimulated P-gp ATPase activity was estimated using the Pgp-Glo assay system[63] (Promega, Madison, WI) and the results are shown in Table 4.1. Briefly, this method relies on the ATP dependence of the light-generating reaction of firefly luciferase where ATP consumption is detected as a decrease in luminescence; the greater the decrease in signal the higher the P-gp activity. Sodium orthovanadate was used as a P-gp ATPase inhibitor, whereas verapamil was used as a positive control. All test compounds were analyzed at 200 µM and fold stimulation values were calculated using Equation 4.1. Fold stimulation values greater than 2.0 indicate a P-gp substrate.[76]

Table 4.1. Fold stimulation values of test compounds prepared, salt form, yield, and melting points.

Cmpd	Name	Salt	Yield (%)	m.p. (°C)	Fold Stimulation ± SEM
	Non Treated (control)				1.00
3	Meperidine	oxalate	7	190-192	1.78 ± 0.39*
6	Ketone analog	citrate	56	170-171	1.37 ± 0.19*
9	Bemidone	oxalate	36	200-202	2.64 ± 0.82*
11	Ketobemidone	oxalate	51	233-235	4.89 ± 1.94*

All compounds assayed at 200 µM. Data are represented as fold stimulation ± SEM ($n =$ 3). * Indicates significant difference ($p<0.05$) from control (non-treated) as determined from t-test. All compounds gave satisfactory CHN (± 0.4%) and spectral analysis.

Equation 4.1.
Fold stimulation by a test compound = $\dfrac{\textit{Test compound stimulated P-gp activity}}{\textit{Basal P-gp activity}}$

The addition of a *m*-OH into the phenyl ring significantly increased the P-gp fold stimulation of meperidine analogs. Meperidine itself had a P-gp fold stimulation value of 1.78 and increased to 2.64 with the *m*-OH addition (bemidone, **9**). Whereas the ketone analog **6**, with a P-gp fold stimulation value of 1.37, increased to 4.89 with the *m*-OH

addition (ketobemidone, **11**). Thus, the addition of a *m*-OH increases the P-gp substrate activity of these meperidine analogs, which are members of the 4-phenylpiperidine class of opioids.

4.3 Conclusion

The hydroxylated meperidine analogs were initially pursued to investigate the relationship between P-gp and increased opioid potency. Interestingly, these results are consistent with previous studies in our laboratory which showed that removal of the 3- and 6-OH from morphine resulted in decreased P-gp substrate activity,[111] as morphine is a P-gp substrate.[50] These studies attest that the *m*-OH substituent increases P-gp substrate activity across the phenylpiperidine and morphinan classes of opioids. Furthermore, the development of opioids lacking P-gp substrate activity should not posses a *m*-OH substituent. The interaction between opioids and P-gp is currently under investigation and these results will aid in further SAR development. The ultimate goal is development of a potent opioid with low P-gp substrate activity for use as a tool to study the contribution of P-gp up-regulation to the development of opioid tolerance and cross-tolerance between opioids with P-gp substrate activity and those without.

4.4 Experimental Section

4.4.1 Chemistry

All reactions were performed under an atmosphere of nitrogen, and all solvents were removed on a rotary evaporator under reduced pressure. TLC was performed on plates coated with silica gel GHLF-0.25 mm plates (60 F_{254}) (Analtech). Mass spectra

were obtained on a ThermoFinnigan LCQ Classic. ^{1}H NMR spectra were obtained using a 500 MHz Varian NMR. Melting points were determined in open capillary tubes using a Mel-Temp melting point apparatus; melting points are uncorrected. Combustion analysis was performed by Atlantic Microlabs, Inc. (Norcross, GA).

Ethyl 1-methyl-4-phenylpiperidine-4-carboxylate oxalate (3): Purified from acetone and oxalic acid to produce oxalate salt; yield 7%; mp 190-192°C; ^{1}H NMR (CDCl$_3$) δ 7.38 (d, 7.56 Hz, 2H), 7.32 (t, 7.78 Hz, 2H), 7.23 (t, 7.56 Hz, 1H), 4.13 (q, 7.10 Hz, 2H), 2.79 (t, 13.52 Hz, 2H), 2.57 (t, 13.78 Hz, 2H), 2.27 (s, 3H), 2.15 (t, 11.77 Hz, 2H), 1.98 (t, 11.60 Hz, 2H), 1.18 (t, 7.42 Hz, 3H); MS (ESI) m/z = 247.17 (M + H$^+$); Anal. (C$_{17}$H$_{23}$NO$_6$•0.25H$_2$O) C, H, N.

1-(1-methyl-4-phenylpiperidin-4-yl)propan-1-one citrate (6): Purified by flash chromatography (SiO$_2$/1:20 MeOH-CHCl$_3$); converted to citrate salt from acetone and citric acid; yield 56%; mp 170-171°C; ^{1}H NMR (CDCl$_3$) δ 7.53 (d, 8.16 Hz, 2H), 7.47 (t, 7.91 Hz, 2H), 7.41 (t, 7.16 Hz, 1H), 3.71 (t, 13.58 Hz, 2H), 3.40 (t, 13.58 Hz, 2H), 2.95 (s, 3H), 2.68 (q, 7.51 Hz, 2H), 2.55 (t, 14.62 Hz, 2H), 2.33 (t, 14.19 Hz, 2H), 0.78 (t, 7.10 Hz, 3H); MS (ESI) m/z = 231.33 (M + H$^+$); Anal. (C$_{21}$H$_{29}$NO$_8$) C, H, N.

Ethyl 4-(3-hydroxyphenyl)-1-methylpiperidine-4-carboxylate oxalate (9): Purified from acetone and oxalic acid to produce oxalate salt; yield 36%; mp 200-202°C; ^{1}H NMR (CD$_3$OD) δ 7.52 (d, 8.36 Hz, 1H), 7.25 (d, 7.44 Hz, 1H), 7.01 (s, 1H), 6.85 (d, 8.09 Hz, 1H), 5.55 (s, 1H), 4.25 (q, 7.21 Hz, 2H), 2.92 (m, 4H), 2.22 (s, 3H), 2.05 (m,

4H), 1.26 (t, 7.10 Hz, 3H); MS (ESI) m/z = 263.33 (M + H$^+$); Anal. ($C_{15}H_{21}NO_3 \cdot 3C_2H_2O_4$) C, H, N.

1-(4-(3-hydroxyphenyl)-1-methylpiperidin-4-yl)propan-1-one oxalate (11):

Purified from MeOH and oxalic acid to produce oxalate salt; yield 51%; mp 235-236°C; ^{1}H NMR (CD$_3$OD) δ 7.32 (t, 7.97 Hz, 1H), 6.98 (d, 7.67 Hz, 1H), 6.89 (s, 1H), 6.82 (d, 7.91 Hz, 1H), 5.55 (s, 1H), 3.88 (t, 13.60 Hz, 2H), 3.55 (d, 13.35 Hz, 2H), 3.39 (m, 2H), 3.18 (s, 3H), 2.73 (d, 16.02 Hz, 2H), 2.42 (q, 8.01 Hz, 2H), 0.91 (t, 7.12 Hz, 3H); MS (ESI) m/z = 247.33 (M + H$^+$); Anal. ($C_{17}H_{23}NO_6$) C, H, N.

Table 4.2. Analytical Data for Compounds **3**, **6**, **9**, **11**.

Compound Number	Calculated (%)			Found (%)		
	C	H	N	C	H	N
3 • 0.25 H$_2$O	59.72	6.92	4.10	59.80	6.88	4.05
6	59.56	6.90	3.31	59.36	6.84	3.18
9 • 3C$_2$H$_2$O$_4$	47.27	5.06	2.62	47.16	5.15	3.08
11	60.52	6.87	4.15	60.35	6.57	3.90

4.4.2   Drug Stimulated P-gp ATPase Activity

Drug stimulated P-gp ATPase activity was estimated by Pgp-Glo assay system[63] (Promega, Madison, WI). This method relies on the ATP dependence of the light-generating reaction of firefly luciferase where ATP consumption is detected as a decrease in luminescence. In a 96 well plate, recombinant human P-gp (25 μg) was incubated with P-gp-Glo assay buffer™ (20 μl) (control, n = 4), verapamil (200 μM) (n = 4), sodium orthovanadate (100 μM) (n = 4), and test compounds (200 μM) (n = 3). Each compound was loaded in three individual wells. Verapamil served as a positive control while

sodium orthovanadate (vanadate) was used as a P-gp ATPase inhibitor. The reaction was initiated by addition of MgATP (10 mM), then stopped 40 minutes later by addition of 50 µL of firefly luciferase reaction mixture (ATP detection reagent) that initiated an ATP-dependent luminescence reaction. Signals were measured 60 minutes later and integrated for 10 seconds by Lmax® luminometer (Molecular Devices Corporation, Sunnyvale, CA). Drug stimulated P-gp ATPase activity was reported as fold stimulation relative to the basal P-gp ATPase activity in the absence of drug (control) (Equation 4.1). Student's t-test was used to determine the statistical significance of the difference between groups. The 0.05 level of probability was used as the criterion of significant.

Chapter 5

Meperidine Piperidine Ring Substitutions

5.1   Introduction

Meperidine, a synthetic opioid, is one of the most widely prescribed analgesics in the United States, especially for child birth.   More than 60% of physicians prescribe meperidine for acute painful conditions and over 20% of physicians prescribe it for chronic pain.[56, 132] Meperidine is most often administered by the *i.m.* or *i.v.* routes due to its poor oral bioavailability and extensive liver metabolism.[56, 133]   Peak plasma concentrations vary according to route of administration and occur 1.2 minutes post dose (*i.v.*), 15-60 minutes post dose (*i.m.*), and 2 hours post dose (*p.o.*).[56]

The biotransformation of meperidine occurs in the body by two different pathways (Figure 5.1). The predominant pathway is hepatic carboxylesterase metabolism to meperidinic acid, an inactive metabolite. However, the most clinically significant pathway is *N*-demethylation by the hepatic cytochrome P450 isozyme 3A4 to normeperidine, a non-opioid active metabolite. Normeperidine can be further metabolized to normeperidinic acid by carboxylesterase. All metabolites eventually undergo renal elimination.[49, 56, 134] The half life ($t_{1/2}$) of meperidine is 2.5-4 hours after therapeutic dosing, but rises to 4-5 hours with doses greater than 100-150 mg/kg, and over 10 hours in individuals with cirrhosis.[56, 135, 136] The $t_{1/2}$ of normeperidine ranges from 14-21 hours,[137] but in patients with renal failure the $t_{1/2}$ can increase up to 34 hours.[138, 139]

Repeated large doses of meperidine at short intervals can produce tremors, mydriasis, and eventual convulsions.[140-142] Normeperidine, a neurotoxic metabolite, has half the analgesic potency of meperidine, but 2-3 times the potency as a CNS excitatory agent.[143-146] Accumulation of normeperidine results in marked CNS stimulatory effects

consisting of anxiety, agitation, hyperreflexia, myoclonus, tremors, mood changes and seizures.[137, 142, 147, 148] Patients with such adverse drug reactions (ADRs) are generally older individuals with longer hospital stays and have diseases such as sickle cell crisis, renal failure, pancreatitis, or cancer.[56, 57, 137, 142, 148] ADRs are especially predominate in patients who receive high, repeated, or frequent doses of meperidine either by injection or through use of patient-controlled analgesia devices.

Seizures resulting from normeperidine toxicity are extremely dangerous as they could lead to death. The mechanism by which normeperidine causes seizures is not fully understood. Normeperidine may produce CNS toxicity by an opioid-related mechanism; however, its seizure-inducing effects are not reversed by naloxone, an opioid antagonist. In fact, naloxone treatment exacerbates the convulsant activity.[149, 150] Additional research showed clinical evidence that normeperidine convulsant activity was reversed by physostigmine, strongly suggesting normeperidine-related anticholinergic activity as an etiological factor.[151]
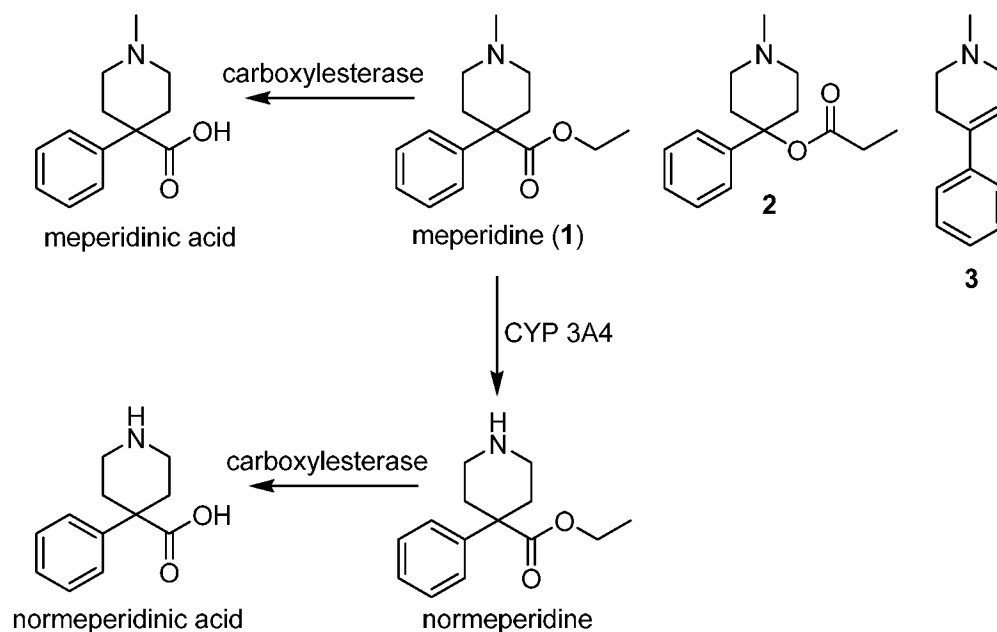
Figure 5.1. Major pathways of meperidine (**1**) biotransformation and structures of the reversed ester of meperidine (**2**) and MPTP (**3**).

Since *N*-dealkylation is the clinically significant metabolic pathway of meperidine, leading to the toxic metabolite normeperidine,[55, 57, 152] we proposed to limit *N*-dealkylation and potentially prevent formation of a toxic metabolite by introducing steric hinderance in the piperidine ring at the 2- and 6-positions. We proposed to synthesize four series of substituted meperidine analogs to include 2-methyl-, 2,2-dimethyl-, 2,6-dimethyl-, and 2,2,6,6-tetramethyl-meperidine analogs (Fig 5.2). Limited research has been performed involving alkyl substitutions on the piperidine ring of meperidine due to stereochemical complexity, although 3-methyl meperidine analogs have been previously synthesized[58] and show increased potency compared to meperidine. Most work involving alkyl substitutions to the piperidine ring was performed on the reversed ester of meperidine (**2**), due to ease of synthetic access and the fact that

replacement of the 4-carbethoxy (CO_2Et) by 4-propionyloxy (OCOEt) usually produces a major increase in potency, up to 20-fold regardless of the N-substituent.[59] In addition, the 2-methyl and 2,6-dimethyl reversed ester of meperidine analogs have been synthesized and also show increased potency compared to meperidine.[54] These results strongly support our approach that the introduction of methyl groups will lead to potent μ opioid agonists. The work presented herein will focus solely on the synthesis of substituted meperidine analogs, since the hydrolysis of the reversed ester of meperidine even with mono-substitution leads to a toxic metabolite, MPTP (3),[60] implicated in Parkinson's disease. Structural changes to the tetrahydropyridine ring of 3 markedly decreased neurotoxicity further supporting our hypothesis.[153]
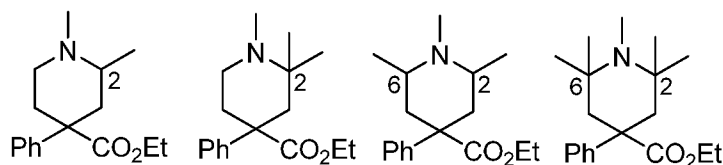
Figure 5.2. Synthetic targets for sterically hindered meperidine analogs: 2-methyl, 2,2-dimethyl, 2,6-dimethyl, and 2,2,6,6-tetramethyl, respectively. Stereochemistry not shown for clarity.

5.2   Results and Discussion

The following descriptions are the original proposed reaction schematics for the synthesis of the 2-methyl, 2,2-dimethyl, 2,6-dimethyl, and 2,2,6,6-tetramethyl meperidine analogs. Immediately following are detailed reaction descriptions, synthetic progress, and future synthetic considerations to complete the target compounds.

5.2.1 Original Proposed Synthesis

The 2-methyl meperidine analogs will be prepared as outlined in Scheme 5.1. The nitrile of meperidine will be treated with *m*-chloroperbenzoic acid to yield an *N*-oxide, **5**, which will then be treated with trifluoroacetic anhydride and aqueous potassium cyanide[60] of pH 4 to produce **6**. Extreme care will be taken for the preceding reaction due to its toxicity and vigorous nature. The nitrile intermediate will then be converted to the corresponding ethyl ester, **7**, by the addition of sulfuric acid and absolute ethanol.[118] L-Selectride[154] at reduced temperature will be used to selectively reduce the 2-position ester, since the 4-position ester is sterically hindered. The alcohol of **8** will be protected by treatment with *p*-toluenesulfonyl chloride. Lithium aluminum hydride[155] will be used to reduce both the tosylate and 4-ester of **9**, yielding a 2-methyl substitution. The alcohol of **10** will then be reoxidized using Jones reagent[156] to yield the acid, **11**. The acid will then be converted to the corresponding ethyl ester by the addition of sulfuric acid and absolute ethanol.[157]
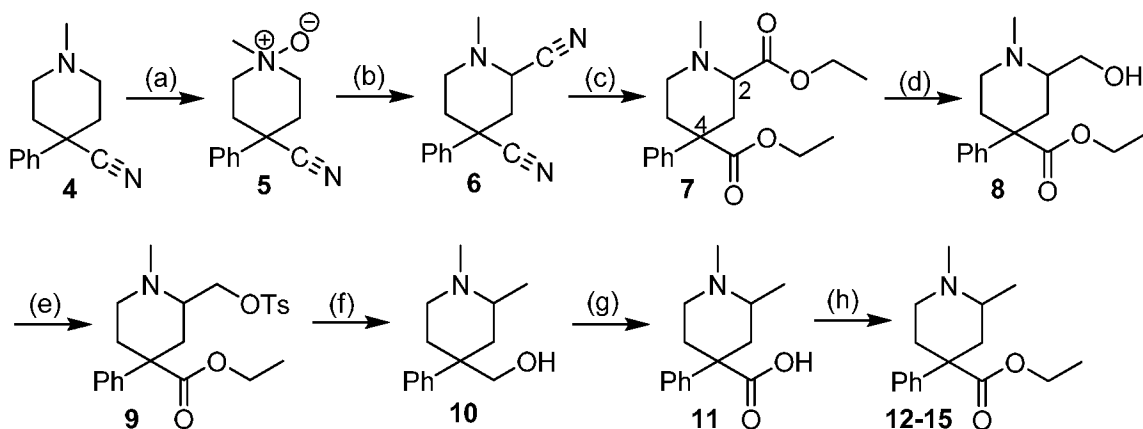
Scheme 5.1. Reagents and conditions: (a) *m*-CPBA; (b) TFAA, aq. KCN, pH 4; (c) H_2SO_4, EtOH, reflux; (d) L-selectride, -78 °C; (e) TsCl; (f) LiAlH$_4$; (g) Jones reagent; (h) H_2SO_4, EtOH, reflux.

79

Two diastereoisomers result due to the presence of two chiral centers. One diastereoisomer (**12**, **15**) has methyl/phenyl in *cis* orientation, the other diastereoisomer (**13**, **14**) has methyl/phenyl in *trans* orientation. Column chromatography will be used to separate diastereoisomers. Chiral salts and/or chiral HPLC will be used to isolate enantiomers for a total of four compounds (Figure 5.3).
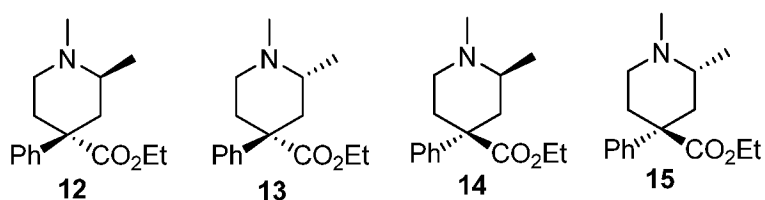
Figure 5.3. Proposed 2-methyl substituted meperidine analogs.

The 2,2-dimethyl meperidine analogs will be prepared as shown in Scheme 5.2. The 2,4-dinitrile compound, **6**, will have an acidic proton at the 2-position. We will take advantage of the acidic proton and treat **6** with sodamide and methyl iodide,[157] adding a 2-methyl group, **16**. Synthetic steps b-g follow Scheme 5.1.
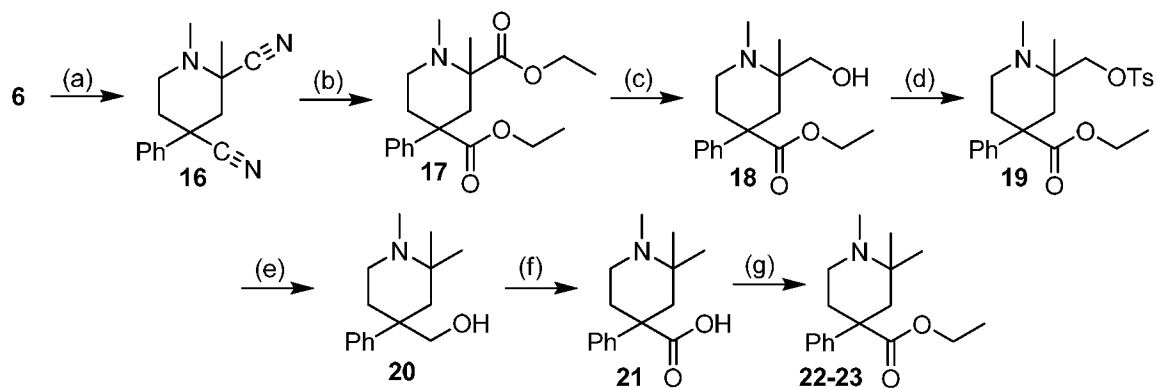
Scheme 5.2. Reagents and conditions: (a) NaNH₂, MeI; (b) H₂SO₄, EtOH, reflux; (c) L-Selectride, -78°C; (d) TsCl; (e) LiAlH₄; (f) Jones reagent; (g) H₂SO₄, EtOH, reflux.

Only two products, **22** and **23** (Figure 5.4), are possible from the 2,2-dimethyl meperidine analog synthesis since there is only one chiral center present. **22** and **23** are enantiomers and will be separated via chiral salts and/or chiral HPLC.
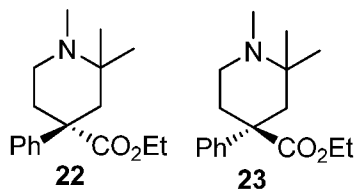
Figure 5.4. Proposed 2,2-dimethyl substituted meperidine analogs.

The 2,6-dimethyl meperidine analogs will be prepared as shown in Scheme 5.3. 2-Bromopropanoic acid will be purchased from Sigma-Aldrich and reduced[158, 159] to its corresponding alcohol, 2-bromopropanol; borane will reduce the acid to the alcohol without reducing the bromine. Methylamine will be added to two equivalents of 2-bromopropanol and the reaction will be allowed to proceed until **24** is synthesized. Both alcohols will be protected with p-toluenesulfonyl chloride to yield **25**. Benzyl cyanide will be treated with two equivalents of sodamide, and the resultant dianion will be condensed with **25** which is now a reactive mustard-type agent. The nitrile intermediate **26** will be converted to the corresponding ethyl ester by the addition of sulfuric acid and absolute ethanol, similar to the original meperidine synthesis.[118]
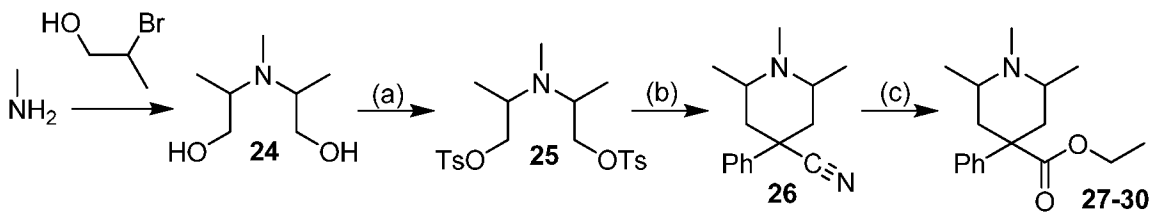
Scheme 5.3. Reagents and conditions: (a) TsCl; (b) Ph(CH₂)CN, NaNH₂; (c) H₂SO₄, EtOH, reflux.

This synthetic scheme potentially produces eight products (Figure 5.5), due to the presence of three chiral centers (2^3), but only four products (**27-30**) will exist due to the symmetry of the molecule. All possible products are drawn out in Figure 5.5, where the symmetry due to rotation is shown. Two diastereoisomers will be produced; one diastereoisomer (**27**, **30**) will have the methyls in cis orientation, the other diastereoisomer (**28**, **29**) will have the methyl in trans orientation. Column chromatography will be used to separate diastereoisomers. Chiral salts and/or chiral HPLC will be used to isolate enantiomers, for a total of four compounds.
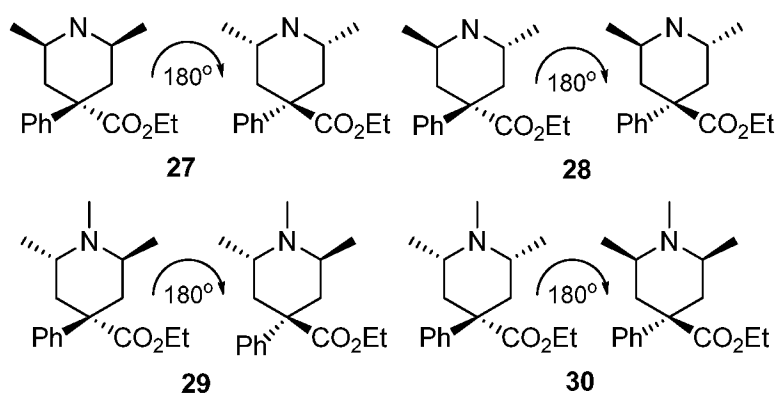
Figure 5.5. Proposed 2,6-dimethyl substituted meperidine analogs.

Lastly, the 2,2,6,6-tetramethyl meperidine analogs will be prepared as shown in Scheme 5.4. 2,2,6,6-Tetramethyl piperidine hydrochloride will be purchased from Sigma-Aldrich and methylated to yield **31**. A Grignard reaction with phenylmagnesium bromide (PhMgBr) will be performed, introducing the 4-phenyl and 4-hydroxyl, **32**. The 4-hydroxyl will then be converted to a nitrile using trimethylsilylchoride[160] (TMS-Cl), sodium cyanide (NaCN), and a catalytic amount of sodium iodide (NaI) producing **33**,

which will then undergo hydrolysis to the ethyl ester, **34**, as previously described. Only one compound will be produced from this synthesis due to the symmetry of the molecule.
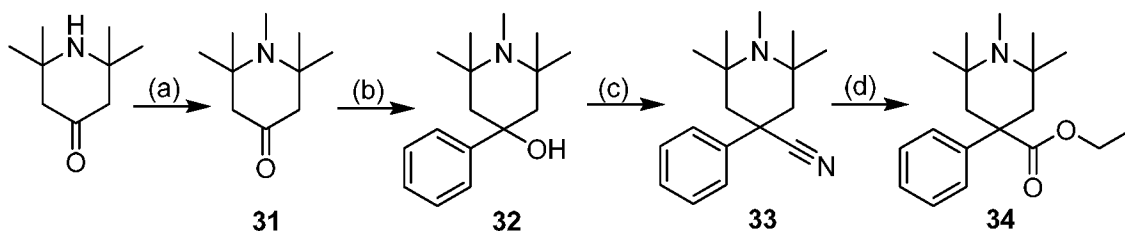
Scheme 5.4. Reagents and conditions: (a) MeI, K_2CO_3, DMF; (b) PhMgBr, THF; (c) Me_3SiCl, NaCN, cat. NaI, 1:1 CH_3CN:DMF; (d) H_2SO_4, EtOH, reflux.

Chiral compounds will initially be prepared and evaluated as racemates, and compounds showing good binding affinity to μ opioid receptors ($K_i < 50$ nM), and low P-gp substrate activity (similar efflux:influx ratio to meperidine) will be prepared in chiral form either through resolution of the racemate as a chiral salt, or through stereospecific synthesis. An enantiomeric excess (e.e.) of >99% is required for the compound to be considered optically pure, and will be measured using chiral HPLC. Optical rotations will be performed to assign (+)- or (-)-isomers, but this does not assign absolute stereochemistry. For the determination of absolute stereochemistry, salts with known chiral acids (e.g. (+)-tartaric) will be prepared and evaluated through X-ray crystallography.

5.2.2   Synthetic Progress to Date

5.2.2.1   2-Methyl Meperidine Analog Synthesis

Compound **4** was dissolved in CH_2Cl_2 followed by slow addition of *m*-CPBA (1.1 eq.) at -10°C. Stirring continued for 1.5 hours at -10°C, the reaction was allowed to come to room temperature and stirred for an additional 15 minutes. Excess K_2CO_3 was added to the reaction and stirred for 15 minutes at room temperature. The resulting mixture was filtered through Celite and washed with CH_2Cl_2; the resulting filtrate was evaporated under reduced pressure producing **5** in 95% yield, product was not further purified.

Compound **5** was immediately re-dissolved in CH_2Cl_2 and treated with TFAA (2 eq.) at 0°C and stirred for 1 hour. The reaction was allowed to come to room temperature and was stirred for an additional 15 minutes. Slow addition of aqueous KCN (1.5 eq.) of pH 4 followed; stirring continued for another 15 minutes at room temperature. The bi-phasic mixture was treated with 10% Na_2CO_3, followed by extraction into CH_2Cl_2 and evaporated under reduced pressure producing **6** in 90% yield; product was used without further purification.

Compound **6**, was subsequently dissolved in a 1:1 $H_2O:H_2SO_4$ (12 eq.) mixture and heated at 180°C for 2 hours. After cooling, absolute EtOH was used to azeotrop the water off (3-4x). The resulting mixture was re-dissolved in absolute EtOH and refluxed overnight. After cooling to room temperature, the solvent was removed under reduced pressure and the residue was treated with supersaturated $NaHCO_3$ to pH 10, followed by extraction into $CHCl_3$ and solvent removal. Compound **7** had a crude yield of 51%. The desired mass was present by MS; therefore, column chromatography was performed

using a $CHCl_3$, 5% MeOH gradient. Separation of the resulting product proved difficult; neither column chromatography, preparative thin-layer chromatography, nor salt formation allowed for isolation of pure material. Further purification work must be performed in order to continue with this synthetic scheme.

5.2.2.2   2,2-Dimethyl Meperidine Analog Synthesis

No further work was pursued on these proposed analogs, as the synthetic methodology from Scheme 5.1 was not developed and applied to Scheme 5.2.

5.2.2.3   2,6-Dimethyl Meperidine Analog Synthesis

$NaBH_4$ was slowly added to 2-bromopropanoic acid (Sigma-Aldrich) in THF, followed by slow addition of $BF_3 \cdot Et_2O$[159] (dissolved in THF) at room temperature. After gas formation subsided, the reaction mixture was refluxed for 2 hours. Upon completion, the reaction mixture was cooled to 0°C, quenched with H_2O and the THF removed under pressure. Stirring continued for 1 hour in CH_2Cl_2. The organic layer was collected and evaporated under reduced pressure producing 2-bromopropanol in 90% yield.

Aqueous $MeNH_2$ (40%) was added to 2-bromopropanol (2 eq.) in EtOH and stirred at room temperature until **24** was synthesized, generally 2-3 days. The alcohols of **24** were then protected with TsCl after refluxing for 5 hours in acetone with K_2CO_3.[161] The tosylated compound **25** was not visible by MS; therefore, identification was proven by NMR.

Condensation of the piperidine ring to produce **26** proved difficult even with various reaction conditions (Table 5.1). Our starting point for this particular synthesis

was based on the original meperidine synthesis[118] wherein a mustard salt was condensed

with benzyl cyanide using NaOH and NaNH$_2$ in toluene. A few alterations made include

the use of NaH in place of NaNH$_2$ for convenience, and the lack of NaOH in some

reaction conditions. Since **25** is not a salt, we did not believe the NaOH was necessary

for free base purposes. We also explored DMF and benzyl cyanide as solvents, thinking

that solvent effects may be prohibiting ring closure. Despite all these attempts, the ring

closure was unsuccessful.

Table 5.1. Reaction conditions for **25 → 26**.

Reaction	Cmpd.**25** (eq.)	NaH (eq.)	NaOH (eq.)	Ph(CH$_2$)CN (eq.)	Solvent	Conditions	M/S (m/z)
SLM 99	1	10	0	1	DMF	24h RT	360.1
SLM 126	1	10	2	1	toluene	24h Δ	mix
SLM 127	1	10	2	1	toluene	1h Δ	mix
SLM 128	1	10	2	1	toluene	24h Δ	mix
SLM 129	1	10	0	1	DMF	24h Δ	mix
SLM 140	1	10	2	solvent	x	1h RT	234.8
SLM 147	1	10	0	1	toluene	24h Δ	mix 242.2
SLM 148	1	10	0	1	toluene	24h Δ	248.3
SLM 149	1	10	2	solvent	x	24h Δ	234.2
SLM 150	1	10	0	solvent	x	24h Δ	234.2

Desired molecular weight of **26** is 228.33; Δ – refers to temperature; specifically reflux conditions.

5.2.2.4   2,2,6,6-Tetramethyl Meperidine Analog Synthesis

Free based 2,2,6,6-tetramethylpiperidone•HCl starting material (Sigma-Aldrich)

was methylated using MeI and K$_2$CO$_3$ in DMF at room temperature to yield **31** in 98%.

Without further purification, **31** was dissolved in THF and underwent a Grignard reaction

with PhMgBr (2.5 eq.). Upon reaction completion, hydrolysis was performed with

aqueous NH$_4$Cl, followed by extraction into Et$_2$O and solvent removal under reduced pressure producing **32** in 86% yield.

Conversion of the 4-alcohol (**32**) to the 4-nitrile (**33**) proved difficult even with various reaction conditions and fresh reagents (Table 5.2). The starting point for this reaction is based on the Davis et al. manuscript[160] which provides a mechanism for a direct one-step conversion of alcohols into nitriles. Briefly, the reaction protocol was performed as follows: Me$_3$SiCl (2 eq.) was slowly added to a mixture of NaCN (2 eq.), NaI (cat.), and **32** in 1:1 CH$_3$CN:DMF at room temperature. The reaction was then placed in a pre-heated oil bath at 65°C for 5 hours. Upon reaction completion, the mixture was poured into H$_2$O, extracted into Et$_2$O, washed with H$_2$O, and dried (Na$_2$SO$_4$) before removal of solvent under reduced pressure. The paper indicates the mechanism results in inversion of configuration, implying the mechanism is S$_N$2-like; however, the inversion is not an immediate concern at this time.

Initial reactions, using various reaction conditions gave the demethylated 4-nitrile product; SLM 92.3 was proof that heat was not needed to allow the reaction to proceed. In order to save a synthetic step, this reaction was also performed on nor-**32**, in hopes of alkylating at a later time; surprisingly, the reaction did not proceed. Subsequent reactions to methylate the demethylated products via the MeI/K$_2$CO$_3$ method were unsuccessful. It is hypothesized that the methylation reaction did not work with the 2,6-dimethyl 4-phenyl-4-nitrile compound due to the increased steric hinderance now present in the analog. Lastly, the equivalents of TMS-Cl and NaCN were increased from 2 to 3 to see if an unusual mechanism was occurring, but no desired product was found by MS.

Table 5.2. Reaction conditions for **32** → **33**.

Reaction	Cmpd. **32** (eq.)	TMS-Cl (eq.)	NaCN (eq.)	Conditions	M/S (m/z)	Comments
SLM 92.1	1	2	2	5h Δ 65°C	243.3	demethylated pdt.
SLM 92.2	1	2	2	24h Δ 70°C	243.3	demethylated pdt.
SLM 92.3	1	2	2	24h RT	243.3	demethylated pdt. No Δ needed
SLM 110	1-nor	2	2	24h RT	mix	
SLM 132	1-nor	2	2	5h Δ 65°C	mix	
SLM 112	1	2	2	24h RT	243.3	demethylated pdt.
SLM 137	1	2	2	24h RT	mix	
SLM 138	1	2	2	5h Δ 65°C, 18h RT	mix	
SLM 139	1	2	2	24h RT	248.2	starting material
SLM 141	1	3	3	24h Δ 65°C	mix	

Desired molecular weight of **33** is 256.33; Δ – refers to temperature, specifically that of the oil bath. All reactions were performed with a catalytic amount of NaI in a 1:1 mixture of $CH_3CN:DMF$.

Alkylation on the resulting demethylated nitrile product from the SLM 112 reaction was attempted, however it did not appear to work, giving a mix by MS. The ester hydrolysis reaction was performed regardless with interesting results. The crude product of **34** gave 260.3 at 100% RA and 304.3 at 25% RA (the desired product) by MS. Column chromatography was performed using a $CHCl_3$, 10% MeOH gradient and multiple fractions were collected containing the desired mass, but they were not pure by TLC and MS. Subsequent purification attempts by salt formation were not successful. These results were not reproduced.

5.3 Conclusion

Synthetic difficulties were experienced with each meperidine analog schematic. Discussion on the progress of each analog and future consideration will be provided herein. The 2-methyl substituted meperidine synthesis was halted due to purification issues with **7**. It has been determined from previous synthetic work (Chapter 3) that the

4-position (nitrile) is very hindered and requires a lot of energy in order for the esterification reaction to proceed. We could use this information to selectively esterify the 2-nitrile at lower temperatures. If possible, this reaction would essentially eliminate the need to "protect" the 4-ester while subsequent reactions convert the 2-ester to the 2-methyl. Additionally, we have found that the 4-ester was more stable than expected (Chapter 4) and that proposed treatment with LiAlH₄ (synthetic step f in Scheme 5.1) would selectively reduce the 2-position and not reduce the 4-ester, saving multiple synthetic steps.

Initial problems with the 2,6-dimethyl analog synthesis were solved and allowed for characterization of compounds **24** and **25**; however the ring condensation to form compound **26** was difficult and has not been finalized. The 2,2,6,6-tetramethyl meperidine analog synthesis proved difficult during the TMS-Cl reaction; converting the 4-hydroxyl (**32**) to a 4-nitrile (**33**), as the N was demethylated. The ring closure (Scheme 5.3) and re-methylation (Scheme 5.4) may not have worked due to the increased steric hinderance located in the piperidine ring. Although this provides synthetic difficulties, it potentially supports our hypothesis that *N*-dealkylation can be prevented or hindered by adding steric hinderance into the piperidine ring.

5.4   Experimental Section

5.4.1   Chemistry

All reactions were performed under an atmosphere of nitrogen, and all solvents were removed on a rotary evaporator under reduced pressure. TLC was performed on plates coated with silica gel GHLF-0.25 mm plates (60 F_{254}) (Analtech). Mass spectra

were obtained on a ThermoFinnigan LCQ Classic. ^{1}H NMR spectra were obtained using a 500 MHz Varian NMR.

4-Cyano-1-methyl-4-phenylpiperidine 1-oxide (5): No purification required; yield 84%; ^{1}H NMR (CDCl$_3$) δ 7.59 (d, 7.88 Hz, 2H), 7.45 (t, 7.88 Hz, 2H), 7.38 (t, 7.63 Hz, 1H), 3.67 (t, 12.50 Hz, 2H), 3.47 (d, 11.70 Hz, 2H), 3.16 (t, 13.99 Hz, 2H), 2.28 (s, 3H), 2.05 (d, 14.24 Hz, 2H); MS (ESI) m/z = 217.94 (M + H$^+$).

1-Methyl-4-phenylpiperidine-2,4-dicarbonitrile (6): Used without further purification; yield 90%; ^{1}H NMR (CDCl$_3$) δ 7.52 (d, 7.33 Hz, 2H), 7.43 (t, 6.29 Hz, 2H), 7.36 (t, 8.24 Hz, 1H), 3.67 (t, 13.26 Hz, 3H), 3.47 (d, 11.56 Hz, 2H), 3.34 (m, 2H), 3.09 (t, 12.74 Hz, 2H), 2.81 (d, 6.72 Hz, 2H) note: complicated NMR spectra; MS (ESI) m/z = 226.29 (M + H$^+$).

Diethyl 1-methyl-4-phenylpiperidine-2,4-dicarboxylate (7): Purification attempted by column chromatography and preparative TLC performed using a CHCl$_3$, 5% MeOH gradient and salt purification; crude yield 51%; ^{1}H NMR (CDCl$_3$) δ 7.38 (d, 7.59 Hz, 2H), 7.33 (t, 7.30 Hz, 2H), 7.24 (t, 7.45 Hz, 1H), 4.14 (q, 7.29 Hz, 4H), 3.06 (tt, 12.72 Hz, 1H), 2.80 (t, 12.31 Hz, 2H), 2.55 (d, 13.13 Hz, 2H), 2.17 (s, 3H), 1.83 (t, 11.90 Hz, 2H), 1.19 (t, 7.39 Hz, 6H); MS (ESI) m/z = 320.18 (M + H$^+$).

2,2'-(methylazanediyl)dipropan-1-ol) (24): Used without further purification; assumed 100% yield due to residual H_2O from aq. $MeNH_2$; MS (ESI) m/z = 148.13 (M + H^+).

2,2'-(methylazanediyl)bis(propane-2,1-diyl)bis(4-methylbenzenesulfonate) (25): Used without further purification; yield 95%; ^{1}H NMR ($CDCl_3$) δ 7.93 (d, 8.41 Hz, 4H), 7.41 (d, 8.16 Hz, 4H), 4.25 (m, 4H), 3.72 (m, 2H), 2.49 (s, 6H), 2.04 (s, 3H), 1.70 (d, 6.78 Hz, 6H); product not detected by MS.

1,2,6-trimethyl-4-phenylpiperidine-4-carbonitrile (26): No product isolated; desired molecular weight 228.33.

1,2,2,6,6-pentamethylpiperidin-4-one (31): Used without further purification; yield 98%; MS (ESI) m/z = 171.07 (M + H^+).

1,2,2,6,6-pentamethyl-4-phenylpiperidin-4-ol (32): Purification by column chromatography using a $CHCl_3$, 5% MeOH gradient; yield 86%; ^{1}H NMR ($CDCl_3$) δ 7.50 (d, 7.98 Hz, 2H), 7.34 (t, 7.18 Hz, 2H), 7.23 (t, 7.58 Hz, 1H), 3.49 (s, 1H), 2.17 (s, 3H), 2.04 (d, 13.16 Hz, 2H), 1.92 (d, 13.16 Hz, 2H), 1.35 (s, 6H), 1.20 (s, 6H); MS (ESI) m/z = 248.92 (M + H^+).

1,2,2,6,6-pentamethyl-4-phenylpiperidine-4-carbonitrile (33): No product isolated; desired molecular weight 256.36.

Chapter 6

"Stimulant Project"

Nitrile Analogs of Meperidine as High Affinity and Selective Sigma-1

Receptor Ligands

This chapter contains material from the following manuscript:

6.1   Introduction

σ Receptors were initially classified as subtypes of the opioid class of receptors by Martin *et al.*,[162] but his classification is no longer applied since most of the σ receptor-mediated effects are not sensitive to the opioid antagonist, naloxone.[163] σ Receptors are widely distributed throughout the body,[164] with locations in many peripheral organs,[165-167] but they are concentrated in the central nervous system, particularly in brainstem motor regions.[168, 169] Further research clarified that σ receptors were a unique class of receptors consisting of two established subtypes, σ_1 and σ_2.[170] Pharmacological effects at the σ_1 receptor include neuroprotection and motor effects, whereas effects at the σ_2 receptor include apoptosis and cell death.[171] That many of the early σ ligands interacted with numerous other biological systems complicated much of the σ receptor literature, and thus there remains an urgent need for the development of high affinity and selective ligands for both receptor subtypes to aid in the further elucidation of σ receptor mechanism(s).

We recently published a series of *N*-substituted meperidine analogs[109] during which synthesis, novel and previously reported *N*-substituted nitrile piperidine intermediates were isolated. A representative sample of the nitrile intermediates was analyzed for binding affinity at the opioid receptors, and showed no significant affinity at the mu (μ), kappa (κ), or delta (δ) opioid receptors ($K_i > 10,000$ nM). Their similarity to previously reported σ ligands including **AC927** and **UMB24** (Figure 6.1) prompted analysis for their binding affinity at the σ receptors. **AC927** (*N*-phenethylpiperidine), a selective σ receptor antagonist, has affinity at both σ_1 and σ_2 receptors[172] and has been used in the development of both σ_1[173] and σ_2[174] pharmacophores and regulates cell

proliferation pathways.[175] Preliminary studies also show that **AC927** attenuates the locomotor stimulant and neurotoxic effects of methamphetamine in mice.[176, 177] **UMB24** (1-(2-phenylethyl)-4-(2-pyridyl)piperazine) has recently been shown to be a σ_2 preferring compound[172, 178] which significantly attenuates cocaine-induced convulsions and locomotor activity.[178]

Herein we focus on the comparison of the *N*-substituted nitrile piperidine analogs (**2-10**) as well as comparison to **AC927** and **UMB24** to determine the Structure Activity Relationship (SAR) of ligand affinity at the σ_1 and σ_2 receptors. Comparative investigation will determine the relevance of: 1) unsaturation and branching two carbons away from the piperidine nitrogen; 2) the distance of a phenyl ring from the piperidine nitrogen; and 3) influence of substituents in the 4-position.

6.2 Results and Discussion

6.2.1 Chemistry

A range of novel and previously reported *N*-substituted nitrile analogs of meperidine were prepared from nitrile (**1**) (obtained from Sigma-Aldrich, Inc.), via alkylation with alkyl halides in DMF in the presence of K_2CO_3 (Scheme 6.1) to produce **2-10** (Figure 6.1).
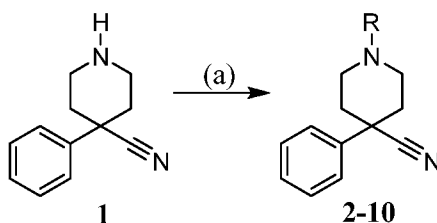
Scheme 6.1. Reagents and conditions: (a) RX, K_2CO_3, DMF.
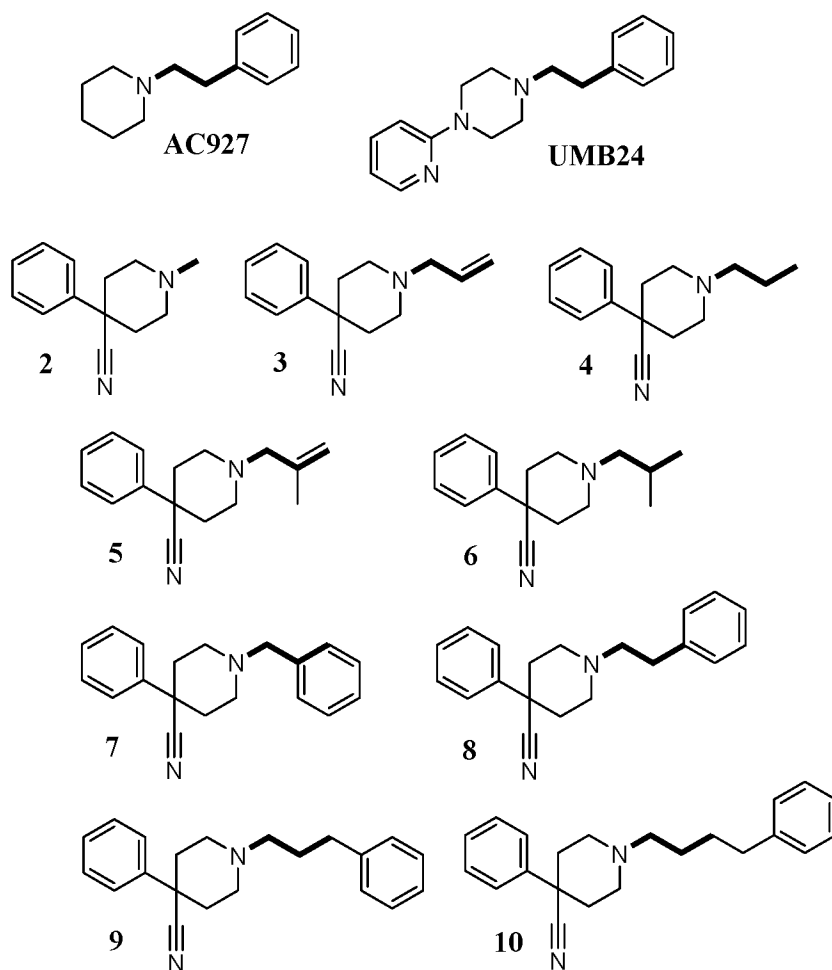
Figure 6.1. Structures of **AC927**, **UMB24**, and compounds **2-10**.

6.2.2   Opioid Receptor Binding Studies

The compounds synthesized in this manuscript are similar to meperidine, a known μ opioid analgesic and other known σ ligands. Therefore, the compounds were evaluated at the three opioid receptors (μ, κ, δ) as previously described (Table 6.1).[179] A representative sample of test compounds (**2**, **3**, **5**, **7**, **10**) was evaluated for opioid binding and was found to have no significant affinity for the opioid receptors (Table 6.1).

Table 6.1. Opioid binding affinities of test compounds **2-10**.

R	Nitrile	Opioid Binding Ki (nM) ± SEM		
		μ	κ	δ
CH_3	**2** [118]	> 10000	> 10000	> 10000
$CH_2CH{=}CH_2$	**3** [180]	> 10000	> 10000	> 10000
$(CH_2)_2CH_3$	**4**	NT	NT	NT
$CH_2C(CH_3){=}CH_2$	**5**	> 10000	> 10000	5000 ± 1300
$CH_2CH(CH_3)_2$	**6** [181]	NT	NT	NT
$CH_2(C_6H_5)$	**7** [118]	5900 ± 90	> 10000	> 10000
$(CH_2)_2(C_6H_5)$	**8**	NT	NT	NT
$(CH_2)_3(C_6H_5)$	**9**	NT	NT	NT
$(CH_2)_4(C_6H_5)$	**10** [182]	9800 ± 680	> 10000	> 10000

Citations reference previously known compounds and/or results.
NT = not tested

6.2.3 Sigma Receptor Binding Studies

The compounds synthesized herein are similar to other known σ receptor ligands. Therefore, they were evaluated at the two established σ receptor subtypes (σ_1, σ_2) as previously described (Table 6.2).[178, 183] Three test compounds exhibited subnanomolar affinity for the σ_1 receptor; compounds **6**, **9** and **7** showed K_i values of 0.35, 0.38, and 0.41 nM, respectively. Compounds **9** and **6** showed the greatest affinity at the σ_2 receptor with affinities of 46 and 63 nM, respectively. Compound **7** (*N*-benzyl) exhibited the highest selectively for the σ_1 receptor over the σ_2 receptor by a factor of 1600, whereas the *N*-Me (**2**) showed weak affinity at both σ receptors.

The series of N-alkyl substituted analogs (**2-6**) all showed high affinity for σ_1 receptors, with little if any difference in affinity with the exception of **2**. This indicates that a larger N-alkyl group leads to good σ_1 affinity, but the exact nature of the group (branching, unsaturation) is unimportant. The highest affinity for the σ_2 receptor was 63 nM by compound **6**, followed by **4**, **5**, **3**, and **2** with affinities of 143, 482, 662, and 2140 nM, respectively. Higher affinities at σ_2 were exhibited for saturated compounds **4** and **6** compared to the corresponding unsaturated compounds **3** and **5**. Overall, compound **6** has the highest affinity for both the σ_1 and σ_2 receptors with a selectivity of 180, while **3** has the highest selectivity in this series with a selectivity of 300.

Compounds **9** (*N*-phenylpropyl) and **7** (*N*-benzyl) have similar high affinity for the σ_1 receptor, with **8** (*N*-phenethyl) 10-fold lower, and **10** (*N*-phenylbutyl) 10-fold lower still. Thus, a nitrogen to phenyl ring chain length of 1-3 carbons is well tolerated at the σ_1 receptor with relatively high affinity, but extension of chain length to 4 carbons decreases affinity. Compound **9** also exhibits the highest affinity at the σ_2 receptor (46

nM), with the others in this series somewhat lower. Overall, compound **9** (*N*-phenylpropyl) exhibits the best affinity for both the σ_1 and σ_2 receptors with a selectivity of 120, while **7** (*N*-benzyl) has the highest selectivity in this series with a selectivity of 1600.

AC927, UMB 24 and **8** all contain an *N*-phenethyl substituent, but significantly vary in their 4-position substituent, allowing preliminary analysis of the 4-aryl substituent. **8** exhibits the highest affinity for σ_1 receptors (3.3 nM) followed by **AC927** and **UMB24** with affinities of 30 and 322 nM, respectively. The 4-cyano-4-phenyl substituent of **8** is superior to no 4-substituent (**AC927**) and a piperazine (**UMB24**). The 4-position substituent does not appear to significantly influence affinity at the σ_2 receptor. Compound **8** has greater selectivity than **AC927** for σ_1 over σ_2 receptors by a factor of 36 compared to 5; **UMB24** is σ_2 selective. Overall, substituents in the piperidine 4-position affect σ_1 binding affinity but do not affect σ_2 binding affinity.

Table 6.2. Sigma binding affinities of test compounds **2-10**, **AC927**, and **UMB24**.

R	Nitrile	Sigma Binding		Selectivity
		Ki (nM) $\pm$ SEM		
		$\sigma_1{}^a$	$\sigma_2{}^b$	σ_2/σ_1
CH_3	**2** [118]	113 ± 5.5	2142 ± 364	19
$CH_2CH=CH_2$	**3** [180]	2.2 ± 0.33	662 ± 78	300
$(CH_2)_2CH_3$	**4**	1.7 ± 0.22	143 ± 13	84
$CH_2C(CH_3)=CH_2$	**5**	3.7 ± 0.83	482 ± 48	130
$CH_2CH(CH_3)_2$	**6** [181]	0.35 ± 0.01	63 ± 2.7	180
$CH_2(C_6H_5)$	**7** [118]	0.41 ± 0.08	657 ± 19	1600
$(CH_2)_2(C_6H_5)$	**8**	3.3 ± 0.38	118 ± 2.6	36
$(CH_2)_3(C_6H_5)$	**9**	0.38 ± 0.04	46 ± 5.5	120
$(CH_2)_4(C_6H_5)$	**10** [182]	49 ± 3.2	1310 ± 215	27
AC927		30 ± 2	138 ± 18	5
UMB24		322 ± 32	170 ± 5	0.53

Citations reference previously known compounds and/or results.
[a]Displacement of [^{3}H](+)-pentazocine.
[b]Displacement of [^{3}H]DTG in the presence of (+)-pentazocine.

6.3   Conclusion

Analysis of the *N*-substituted nitrile piperidine analogs at σ receptors led to selective σ_1 ligands. Compounds **6**, **7**, and **9** are worth pursuing as high affinity selective ligands due to their subnanomolar affinity at the σ_1 receptor. The high affinity of the *N*-benzyl substituent is consistent with previously reported compounds.[184] Compounds **6** and **9** also have good affinity at the σ_2 receptor, whereas compound **7** with 1600 fold selectivity for σ_1 over σ_2 and no affinity at opioid receptors appears to be an ideal ligand for study of σ_1 receptor function. These σ_1 selective ligands with no opioid affinity will further aid in the investigation between the σ_1 and opioid receptors.[185]

6.4   Experimental Section

6.4.1   Chemistry

All reactions were performed under an atmosphere of nitrogen, and all solvents were removed on a rotary evaporator under reduced pressure. TLC was performed on plates coated with silica gel GHLF-0.25 mm plates (60 F_{254}) (Analtech). Mass spectra were obtained on a ThermoFinnigan LCQ Classic. ^{1}H NMR spectra were obtained using a 500 MHz Varian NMR. Melting points were determined in open capillary tubes using a Mel-Temp melting point apparatus; melting points are uncorrected. Combustion analysis was performed by Atlantic Microlab, Inc. (Norcross, GA).

General Procedure for the Synthesis of *N*-substituted Nitrile Meperidine Analogs (2, 3, 5, 7- 10):   The appropriate halogenated compound (1 eq.) and K_2CO_3 (10 eq.) were added to a solution of freebased 4-cyano-4-phenylpiperidine (Sigma Aldrich) (1 eq.) in DMF (20 mL/g). After stirring overnight at room temperature, H_2O (3x amount of DMF)

was added. The reaction mixture was extracted into Et_2O, washed with brine, and dried (Na_2SO_4). Removal of the solvent under reduced pressure gave the crude compound. All compounds were converted to salts by either recrystallization or lyophilization.

1-methyl-4-phenylpiperidine-4-carbonitrile hydrochloride (2): RX = methyl iodide (Sigma-Aldrich); Purified by flash chromatography (SiO_2/1:20 MeOH-CHCl$_3$); Lyopholized with 1M HCl to produce salt; yield 54%; mp 206-211°C; ^{1}H NMR (CDCl$_3$) δ 7.54 (d, 7.80 Hz, 2H), 7.43 (t, 7.37 Hz, 2H), 7.36 (t, 6.50, 1H), 2.99 (d, 12.14 Hz, 2H), 2.52 (t, 11.70 Hz, 2H), 2.42 (s, 3H), 2.15 (t, 11.70 Hz, 4H); MS (ESI) m/z = 201.28 (M + H$^+$); Anal. ($C_{13}H_{17}ClN_2$•0.25H$_2$O) C, H, N.

1-allyl-4-phenylpiperidine-4-carbonitrile hydrochloride (3): RX = allyl bromide (Sigma-Aldrich); Purified by flash chromatography (SiO_2/1:20 MeOH-CHCl$_3$); Lyopholized with 1M HCl to produce salt; yield 59%; mp 237-240°C; ^{1}H NMR (CDCl$_3$) δ 7.51 (d, 7.35 Hz, 2H), 7.40 (t, 7.12 Hz, 2H), 7.33 (t, 7.35 Hz, 1H), 5.88 (m, 1H), 5.25 (s, 2H), 5.20 (t, 9.64 Hz, 2H), 3.11 (d, 5.51 Hz, 2H), 3.05 (d, 11.31 Hz, 2H), 2.49 (t, 11.00 Hz, 2H), 2.12 (s, 2H); MS (ESI) m/z = 227.15 (M + H$^+$); Anal. ($C_{15}H_{19}ClN_2$) C, H, N.

1-(2-methylallyl)-4-phenylpiperidine-4-carbonitrile hydrochloride (5): RX = 3-bromo-2-methyl-propene (Sigma-Aldrich); Purified by flash chromatography (SiO_2/1:20 MeOH-CHCl$_3$); Lyopholized with 1M HCl to produce salt; yield 33%; mp 243-245°C; ^{1}H NMR (CDCl$_3$) δ 7.51 (d, 7.58 Hz, 2H), 7.40 (t, 7.58 Hz, 2H), 7.33 (t, 7.18

Hz, 1H), 4.91 (s, 1H), 4.88 (s, 1H), 2.97 (m, 4H), 2.42 (m, 2H), 2.10 (m, 4H), 1.76 (s, 3H); MS (ESI) m/z = 241.17 (M + H$^+$); Anal. (C$_{16}$H$_{21}$ClN$_2$•0.1H$_2$O) C, H, N.

1-benzyl-4-phenylpiperidine-4-carbonitrile oxalate (7): RX = benzyl bromide (Sigma-Aldrich). Purified from MeOH and oxalic acid to produce oxalate salt; yield 65%; mp 244-245°C; NMR consistent with previously reported spectra[186]; MS (ESI) m/z = 277.17 (M + H$^+$); Anal. (C$_{21}$H$_{22}$N$_2$O$_4$) C, H, N.

1-phenylethyl-4-phenylpiperidine-4-carbonitrile trifluoroacetate (8): RX = 2-bromoethyl benzene (Sigma-Aldrich); Purified by flash chromatography (SiO$_2$/1:20 MeOH-CHCl$_3$); Lyopholized with 1M TFA to produce salt; yield 30%; mp 182-187°C; ^{1}H NMR (CDCl$_3$) δ 7.60 (d, 7.27 Hz, 4H), 7.48 (m, 4H), 7.38 (m, 2H), 3.19 (d, 11.55 Hz, 2H), 3.05 (t, 7.49 Hz, 2H), 2.93 (t, 7.70 Hz, 2H), 2.81 (t, 7.49 Hz, 2H), 2.67 (t, 11.33 Hz, 2H), 2.22 (m, 2H); MS (ESI) m/z = 291.18 (M + H$^+$); Anal. (C$_{22}$H$_{23}$F$_3$N$_2$O$_2$) C, H, N.

1-phenylpropyl-4-phenylpiperidine-4-carbonitrile trifluoroacetate (9): RX = 1-bromo-3-phenylpropane (Sigma-Aldrich). Purified by flash chromatography (SiO/1:20 MeOH-CHCl$_3$). Lyopholized with 1M TFA to produce salt; yield 35%; mp 140-145°C; ^{1}H NMR (CDCl$_3$) δ 7.50-7.19 (m, 10H), 3.03 (d, 11.93 Hz, 2 H), 2.71 (t, 7.33 Hz, 2H), 2.66 (t, 7.46 Hz, 2H), 2.48 (t, 6.71 Hz, 2H), 2.11 (s, 2H), 2.00 (t, 7.33 Hz, 2H), 1.86 (t, 7.21 Hz, 2H); MS (ESI) m/z = 305.20 (M + H$^+$); Anal. (C$_{21}$H$_{24}$N$_2$•0.8C$_2$HF$_3$O$_2$) C, H, N.

1-phenylbutyl-4-phenylpiperidine-4-carbonitrile oxalate (10): RX = 1-chloro-4-phenylbutane (Sigma-Aldrich); Purified from acetone and oxalic acid to produce oxalate salt; yield 34%; mp 210-211°C; ^{1}H NMR (CDCl$_3$) δ 7.51 (d, 7.11 Hz, 4H), 7.41 (t, 7.44 Hz, 4H), 7.33 (t, 7.28 Hz, 2H), 3.18 (m, 4H), 2.10 (d, 12.61 Hz, 2H), 2.00 (m, 2H), 1.56 (m, 8H); MS (ESI) m/z = 319.21 (M + H$^+$).

General Hydrogenation Procedure (4, 6) derived from Maeda et al.[187]: A suspension of 10% Pd/C in EtOH (1 mL) was added to a solution of alkene (1 eq.) and NH$_4$HCO$_2$ (10 eq.) in EtOH (20 mL/g). After refluxing overnight and cooling, the solution was filtered through Celite and the solvent removed under reduced pressure. The resulting residue was redissolved in EtOAc, washed with brine, and dried (Na$_2$SO$_4$). Removal of the solvent under reduced pressure yielded the crude compound. Compounds were purified using flash chromatography (SiO/1:20 MeOH-CHCl$_3$) and converted to salts.

1-propyl-4-phenylpiperidine-4-carbonitrile oxalate (4): Recrystallized from acetone and oxalic acid to produce oxalate salt; yield 27%; mp 170°C; ^{1}H NMR (CDCl$_3$) δ 7.59 (d, 7.75 Hz, 2H), 7.45 (m, 3H), 4.12 (q, 6.97 Hz, 2H), 3.80 (d, 13.75, 1H), 3.65 (m, 1H), 3.49 (s, 1H), 3.13 (d, 9.71 Hz, 1H), 2.98 (t, 7.77 Hz, 1H), 2.22 (d, 10.68 Hz, 1H), 2.05 (s, 2H), 1.26 (t, 7.21 Hz, 3H), 1.06 (t, 7.31, 1H), 0.91 (m, 1H); MS (ESI) m/z = 229.40 (M + H$^+$); Anal. (C$_{17}$H$_{22}$N$_2$O$_4$•H$_2$O) C, H, N.

1-isobutyl-4-phenylpiperidine-4-carbonitrile trifluoroacetate (6): Lyopholized with 1M TFA to produce salt; yield 21%; mp 144-147°C; ^{1}H NMR (CDCl$_3$) δ 7.45 (m,

4H), 7.37 (t, 6.94 Hz, 1H), 4.64 (m, 1H), 4.22 (m, 1H), 3.80 (m, 1H), 3.62 (m, 1H), 3.12

(m, 1H), 2.20 (m, 4H), 1.97 (m, 2H), 1.62 (m, 3H), 0.92 (m, 2H); MS (ESI) m/z = 243.18

(M + H$^+$); Anal. (C$_{18}$H$_{23}$F$_3$N$_2$O$_2$) C, H, N.

Table 6.3. Analytical Data for Compounds **2-10**.

Compound Number	Calculated (%)			Found (%)		
	C	H	N	C	H	N
2 • 0.25 H$_2$O	64.72	7.31	11.61	64.94	7.08	11.36
3	68.56	7.29	10.66	68.21	7.15	10.55
4 • 1 H$_2$O	60.70	7.19	8.33	60.55	6.89	8.11
5 • 0.1 H$_2$O	68.98	7.67	10.05	68.87	7.35	9.73
6	60.66	6.50	7.86	60.68	6.47	7.95
7	68.84	6.05	7.65	68.94	6.11	7.61
8	65.34	5.73	6.93	65.84	5.97	7.12
9 (1 fb • 0.8 TFA)	68.61	6.32	7.08	68.47	6.27	6.98
10	CHN not possible, see attached document (Cmpd 10 NMR)					

6.4.2 Opioid Binding

Binding assays were performed as previously described[122] using [^{3}H]diprenorphine in membranes from C$_6$ rat glioma cells expressing recombinant μ or δ receptors and CHO cells expressing the recombinant κ receptors.

6.4.3 Sigma Binding

Competition binding assays were performed in homogenates from rat brain minus cerebellum (450-500 μg protein/tube) using procedures previously described in detail.[178, 183, 188] The assays were conducted in 50 mM Tris-HCl, pH 8.0 using a total volume of 500 μL/tube. σ$_1$ Receptors were labeled using 5 nM [^{3}H](+)-pentazocine; σ$_2$ receptors were labeled with 3 nM [^{3}H]di-o-tolylguanidine in the presence of 300 nM (+)-

pentazocine to mask σ_1 receptors. Non-specific binding was determined in the presence of 10 μM haloperidol. Twelve concentrations of test ligand were used in each assay. After incubation for 120 min at 25°C, the assays were terminated with the addition of ice-cold 10 mM Tris-HCl, pH 8.0 and vacuum filtration through glass fiber filters. K_i values were calculated from the data using Graph Pad Prism and previously determined K_d values.

Chapter 7

"Cancer Project"

Dual Profile Inhibitors of S100β and p53

The following project was performed as an interdisciplinary collaborative effort between Dr. David Weber (Principle Investigator - University of Maryland, School of Medicine) and Drs. Andrew Coop and Alexander MacKerell (Co-Investigators – University of Maryland, School of Pharmacy). The Weber group has completed the preliminary experiments described in this chapter leading to the binding and NMR perturbation results.

7.1   Introduction

The S100 protein family consists of over 20 proteins originally named due to their solubility in 100% saturated ammonium sulfate.[189] EF-hand containing S100 proteins typically function as a calcium-activated switch that bind and regulate the biological function of numerous protein targets.[190-193] Members of the S100 protein family are distributed in a cell-specific manner,[190, 191, 194] including a large number of human cancers.[195-197] One member, S100β, is 21.5 kDa symmetric homodimer that is highly conserved among mammals (>95%).[189, 194] In general, low S100β levels cause trophic effects, while higher levels are toxic, resulting in uncontrolled cell growth. S100β protein levels are elevated in malignant melanoma,[195] anaplastic astrocytomas,[198, 199] and glioblastomas.[200] In malignant melanoma, high concentrations of S100β correlate directly with poor patient prognosis;[201-203] therefore, it is used as a clinical marker for this and other cancers.

Recent mechanistic studies have shown that S100β binds directly to the p53 tumor suppressor protein in primary human malignant melanoma cells causing reduced p53 protein levels and inhibition of wild-type p53 functions.[204-209] p53 is a transcription activator that signals for cell cycle arrest and apoptosis, playing a pivotal role in the maintenance and regulation of normal cellular functions.[210, 211] Elevated levels of S100β therefore contribute to cancer progression by down-regulating the wild-type p53 protein.[209] However, p53 protein levels and its associated activities were restored in malignant melanoma when S100β protein expression was inhibited by siRNA.[206] With these siRNA results in hand, a rational drug design approach was initiated to develop small molecule inhibitors that bind to Ca^{2+}-S100β, prevent the S100β-p53 complex

formation, and restore p53-dependent tumor suppression in cancers with wild-type p53 such as malignant melanoma.[212-214]

Atomic structures of S100β in the Ca^{2+} and p53 peptide bound states together with computer aided drug design (CADD) and high throughput screening (HTS) approaches were used to identify small molecules which bound to S100β.[212-214] A resulting lead compound, pentamidine (Figure 7.1), was characterized by NMR and found to interact with aromatic residues in helix 4 and the C-terminal loop of Ca^{2+}-S100β.[212] In the calcium-bound state, S100β was found to bind two pentamidine molecules per S100β subunit at two distinct binding pockets. One pentamidine molecule bound near the p53 peptide binding site (referred to as *Site 1* and/or the pentamidine site) and the second molecule bound at the dimer interface of Ca^{2+}-S100β in which a 12-mer peptide, TRTKIDWNKILS (TRTK), also binds (referred to as *Site 2* and/or the TRTK site).
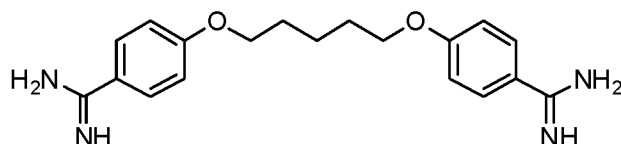
Figure 7.1. Structure of pentamidine.

As S100β and p53 interact at two specific binding sites, leading to downregulation of p53 and causing eventual cancer cell proliferation, a rational drug design approach was implored to develop a dual profile ligand to prevent the S100β-p53 complexation. The ultimate design goal was to join a half pentamidine molecule (to bind at *Site 1*) and the TRTK-12 peptide (to bind at *Site 2*) while varying the chain linker

length, all the while improving binding affinity through allosteric modulation. The results contained herein are preliminary as additional experiments are ongoing.

7.2 Results and Discussion

7.2.1 Chemistry

A series of half-pentamidine derivatives with various chain lengths was synthesized according to Hisashi *et al.* with minor variations as described in the experimental (Scheme 7.1).[215] Briefly, 4-cyanophenol was alkylated with the appropriate brominated ester to give compounds **1a-1d**. Treatment of the nitrile with HCl and EtOH produced compounds **2a-2d**; subsequent treatment with NH_4Cl, NH_3, and EtOH under reflux conditions introduced the amidine group into compounds **3a-3d**. Amidine protection (**4a-4d**) followed by ester hydrolysis gave compounds **5a-5d** which were ready for peptide linkage to the TRTK-12 peptide. Only one compound, **5b**, was actually linked to TRTK-12 by the Biopolymer/Genomics Core Facility at the University of Maryland, School of Medicine; however, the mass of the **5b+TRTK** conjugate was M-18 possibly correlating to a dehydrated and cyclized peptide, which may have negatively affected further results. All intermediates were isolated, purified, and analyzed for binding affinity and NMR perturbations at $S100\beta$.
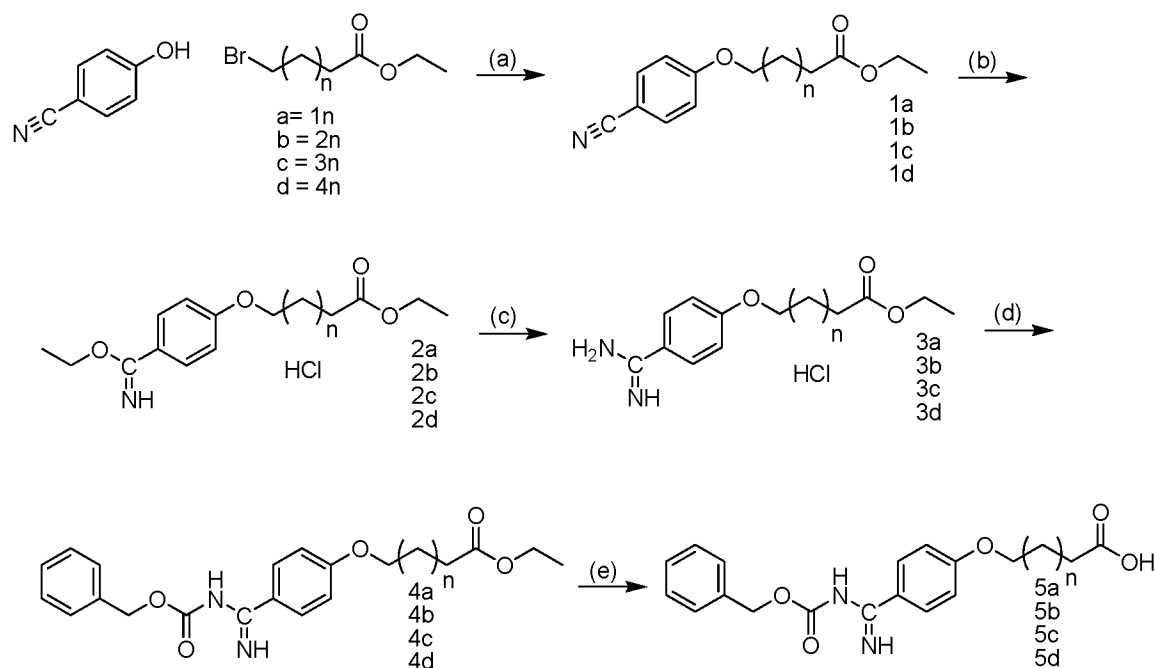
Scheme 7.1. Reagents and conditions: (a) K_2CO_3; (b) HCl, EtOH; (c) NH_4Cl, NH_3, EtOH, reflux; (d) $ClCO_2CH_2C_6H_5$, NaOH; (e) NaOH

7.2.2   S100β Binding Studies

A representative set of test compounds was analyzed for their binding affinity to S100β using a direct fluorescence assay monitoring binding at *Site 1*; pentamidine was included for comparative and control purposes. The **b** series with a 5 carbon chain length was the first series synthesized and therefore has the most data compiled. Of particular interest was **3b**, which contains the desired amidine moiety. Compound **3b** was analyzed under normal assay conditions and also in Ca^{2+} deficient conditions; producing K_d values of 210 and 190 uM, respectively. These results are interesting in that **3b** binding to S100β is not Ca^{2+} dependent, whereas pentamidine binding is Ca^{2+} dependent. Hydrolysis of the **3b** ester to the acid was also analyzed to determine the intracellular effect of the compound, however the K_d increased to 1140 uM. Only one compound, **5b**,

was linked to TRTK and its K_d of 6.7 uM was similar to that of TRTK alone; the hypothetical allosteric binding increase was not seen, potentially due to peptide dehydration or cyclization causing a decrease in binding affinity. Lastly, the six carbon chain length of compound 3c was determined superior to the five carbon chain length as its K_d of 90 uM was increased.

Controversy exists as to whether this assay was applicable to these test compounds, as they were thought to possibly bind at *Site 2*, for which the assay is not valid. In order to further investigate where the test compounds were binding NMR perturbation studies were carried out.

Table 7.1. Preliminary binding affinities of selected compounds determined by direct fluorescence.

Compound	n	Kd (uM)	SD (+)
Pentamidine	3	44	4
1b	2	280	60
2b	2	250	40
3b	3	210	20
3b (no Ca^{2+})	1	190	70
3b (acid)	2	1140	700
4b	2	205	3
5b + TRTK	2	6.7	0.4
4a	2	380	30
3c	1	90	20

7.2.3 NMR Perturbation Studies

The availability of the ^{15}N labeled S100β protein has allowed for full characterization by NMR. Figure 7.2 shows the HSQC spectra of ^{15}N S100β, in which each spot correlates to the chemical shift for each amino acid residue in the protein backbone as labeled. Figure 7.3 is an example of a NMR perturbation study in which

ligands or test compounds are titrated into the NMR tube and the change of chemical shift is monitored.

Figure 7.2. HSQC spectra of ^{15}N labeled S100β. Courtesy of Tom Charpentier (Weber Laboratory).
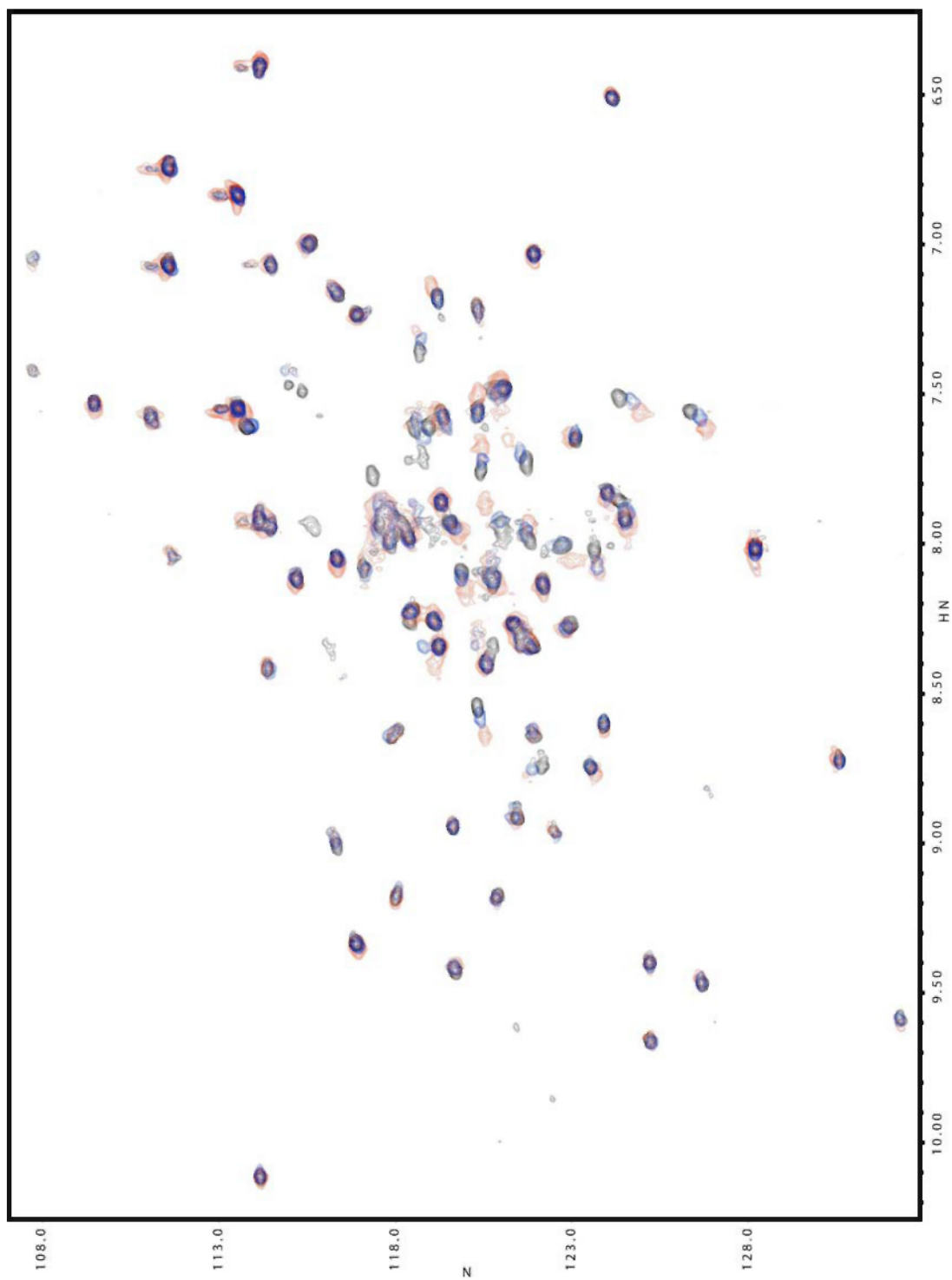
Figure 7.3. HSQC overlay spectra of pentamidine (red), test compound **3c** (blue) and control (black, no ligand) interactions with S100β. Courtesy of Tom Charpentier (Weber Laboratory).

The chemical shift movements are qualitatively measured by examining the change in Hz (ΔHz) between the two HSQC spectra of ^{15}N S100β alone and with ligand or test compound. Figures 7.4-7.11 represent the qualitative change of ΔHz with the respective ligand or test compound; the X-axis correlates to the amino acid residues, while the Y-axis correlates to ΔHz. The four helixes (H1-H4) of the protein are crudely marked in Figure 7.4, along with the "hinge region" of the protein located in between helixes 2 and 3.

[H1   I   H2   I   H3   I   H4   ]
[hinge region   ]
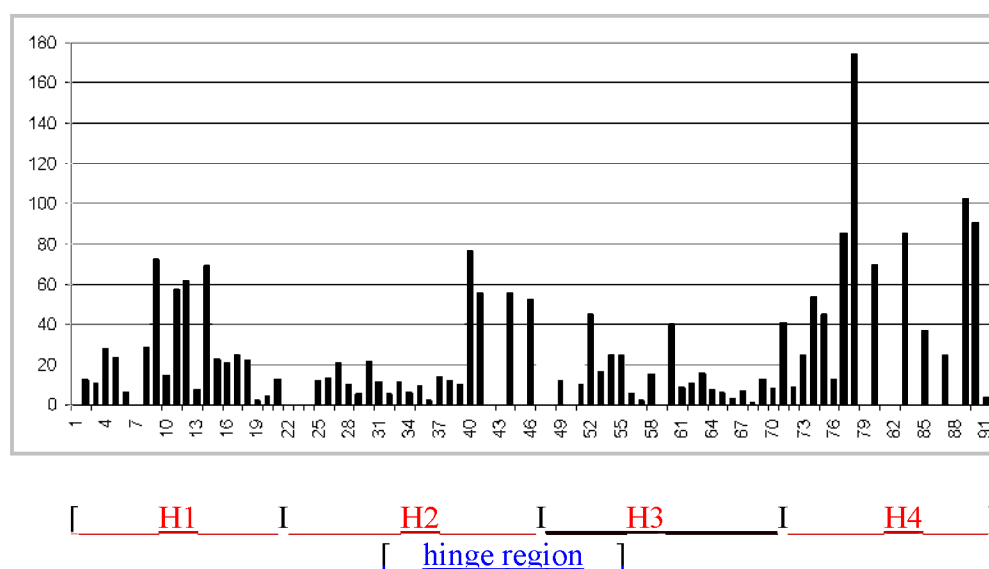
Figure 7.4. NMR perturbation of pentamidine.

Figures 7.5-7.10 show that the individual test compounds analyzed have increased ΔHz or perturbations in helix 4 which correlate to the pentamidine perturbations. These NMR studies suggest that the test compounds are binding in a similar region as pentamidine; however, since these interactions are not Ca^{2+} dependent, they may be binding on the other side of the protein or at a novel binding site.
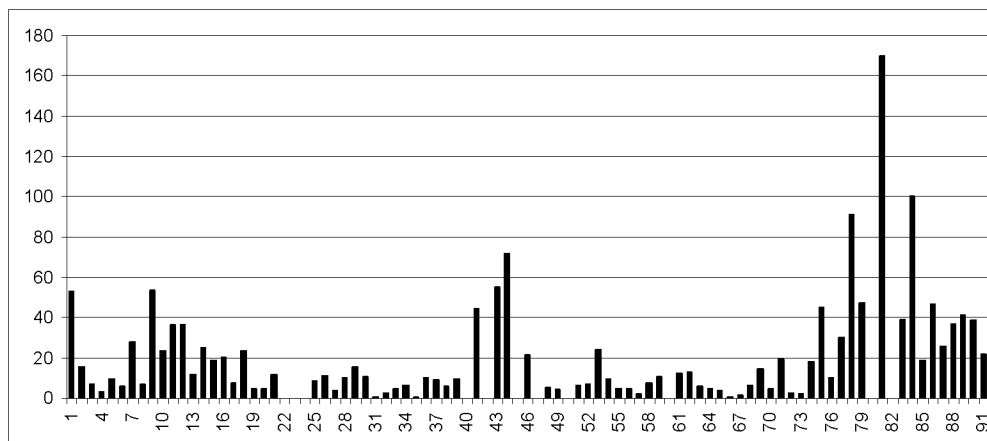
Figure 7.5. NMR perturbation of **2c.**
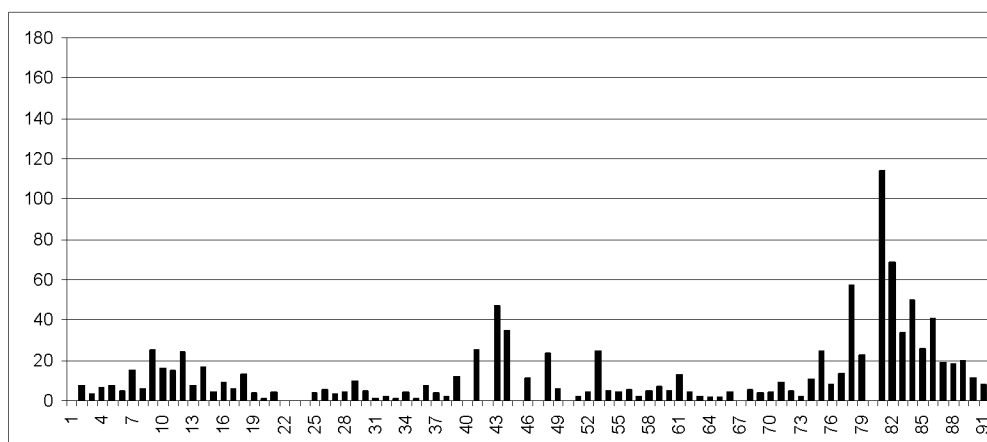
Figure 7.6. NMR perturbation of **3a.**
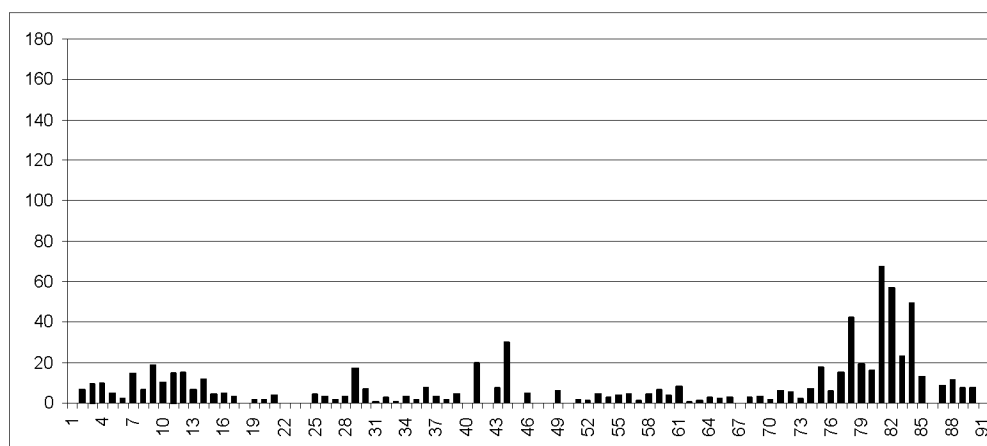
Figure 7.7. NMR perturbation of **3b.**
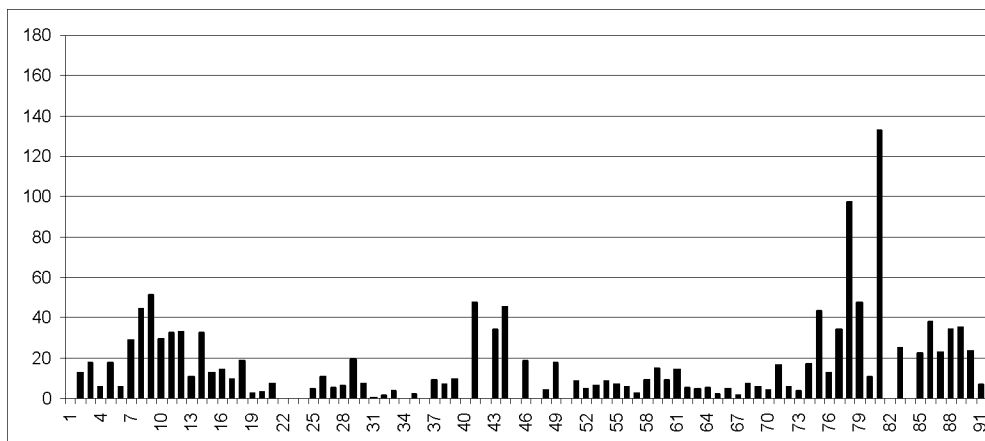
Figure 7.8. NMR perturbation of **3c.**
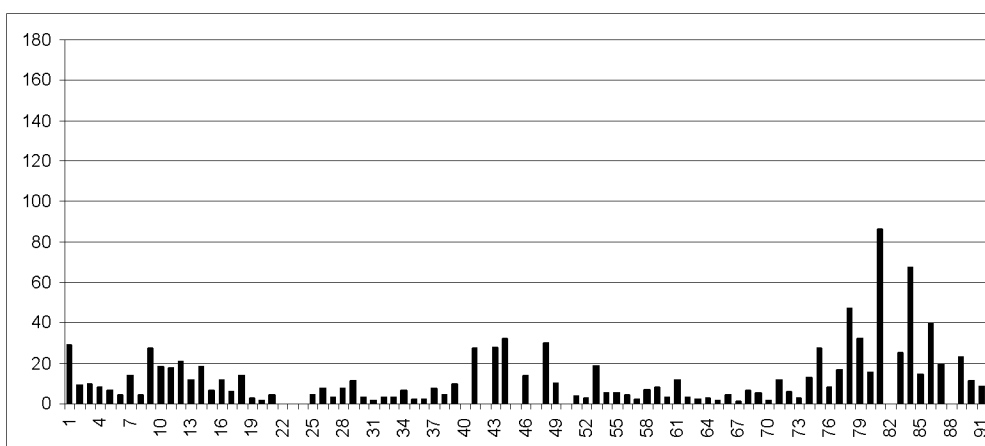
Figure 7.9. NMR perturbation of **3d.**
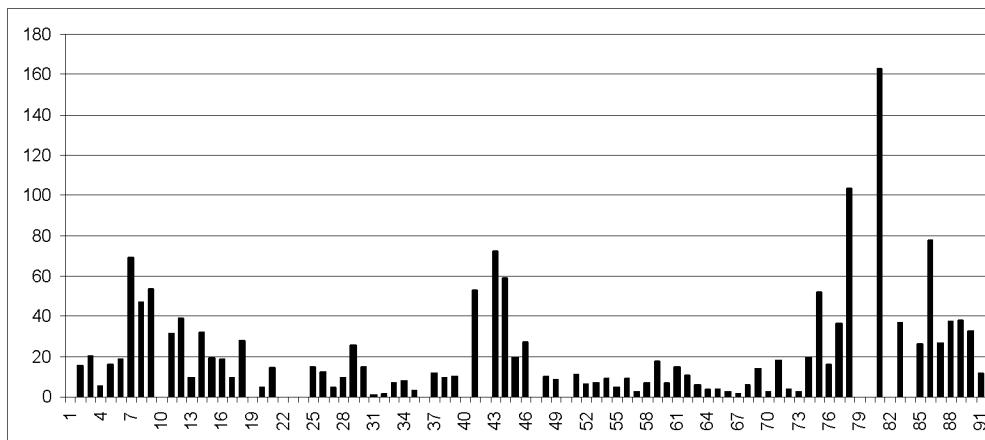
Figure 7.10. NMR perturbation of **4c.**

A different pattern of perturbations result in Figure 7.11, which investigates the NMR perturbation effects of the **5b+TRTK** conjugate on S100β. ΔHz are less marked in helix 4 compared to pentamidine, whereas ΔHz are more pronounced in the hinge region suggesting that the test compound does not solely bind at *Site 1*, but also interacts with *Site 2* as expected.
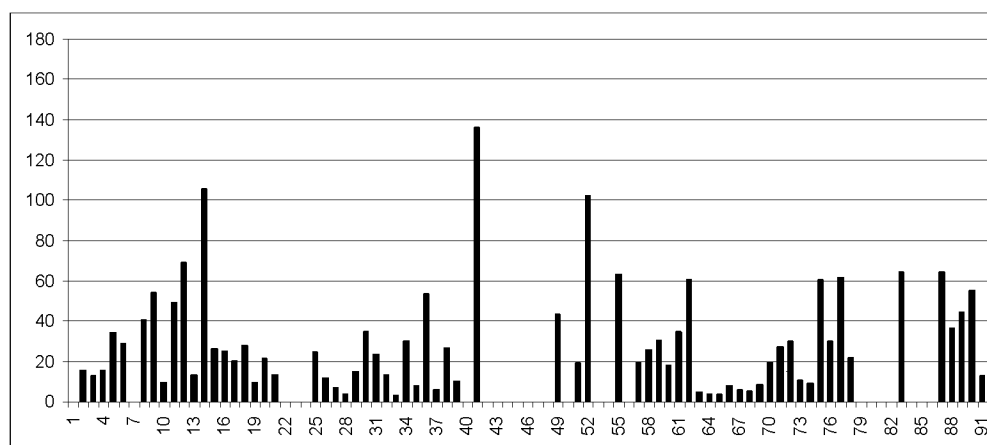
Figure 7.11. NMR perturbation of **5b+TRTK.**

7.3 Conclusion

While further studies are required to fully delineate the functions of these test compounds at S100β, broad conclusions can be drawn from this data. The binding of pentamidine at *Site 1* is Ca^{2+} dependent, requiring Ca^{2+} to open the binding pocket allowing for pentamidine insertion. Test compound **3b** has the same K_d in the presence or absence of Ca^{2+}, suggesting this and the other test compounds may bind at a different site than pentamidine. NMR perturbation studies showed that all test compounds interacted with S100β in a similar region (helix 4) as pentamidine; however, due to the lack of Ca^{2+} dependence this data further supports the idea that the compounds may bind

on the other side of the pentamidine binding site or a novel binding site all together. Investigation of the amidine containing series of intermediate compounds **3a-3d** proved valuable in determinating the optimal chain linker length, as compound **3c** with a six carbon carbon chain length created the highest perturbations in the helix 4 region. Lastly, the **5b+TRTK** conjugate had increased perturbations in both the hinge and helix 4 regions, suggesting that it interacts at both *Site 1* and *Site 2*, providing further evidence to the hypothesis that dual inhibitors can be synthetized to interace at both the pentamidine and TRTK binding sites. Further binding and NMR perturbation studies need to be completed in order to investigate the remaining test compounds, specifically for binding at *Site 2*; however, a novel systematic assay and/or probe for the TRTK site must first be developed.

7.4   Experimental Section

7.4.1   Chemistry

All reactions were performed under an atmosphere of nitrogen, and all solvents were removed on a rotary evaporator under reduced pressure. TLC was performed on plates coated with silica gel GHLF-0.25 mm plates (60 F_{254}) (Analtech). Mass spectra were obtained on a ThermoFinnigan LCQ Classic. ^{1}H NMR spectra were obtained using a 500 MHz Varian NMR. Melting points were determined in open capillary tubes using a Mel-Temp melting point apparatus; melting points are uncorrected. Combustion analysis was performed by Atlantic Microlab, Inc. (Norcross, GA). Synthesis follows that of Hisashi et al.[215]

General Procedure for the Synthesis of (1): 4-Cyanophenol obtained from Sigma-Aldrich (1 eq.) was dissolved in DMF (10 mL/g) and followed by the addition of K_2CO_3 (1.5 eq.) and the appropriate brominated ester (1 eq.). After stirring overnight at room temperature, the reaction mixture was poured into H_2O (3x amount of DMF). The reaction mixture was extracted into EtOAc, washed with sodium bicarbonate, washed with brine, and dried (Na_2SO_4). After removal of the solvent under reduced pressure the resulting solid was washed with anhydrous Et_2O for purification.

Ethyl 4-(4-cyanophenoxy)butanoate (1a): Ester = ethyl-4-bromobutyrate (Sigma-Aldrich); yield 64%; mp 58-60°C; ^1H NMR (CD_3OD) δ 7.70 (d, 8.52 Hz, 2H), 7.12 (d, 7.74 Hz, 2H), 4.18 (m, 4H), 2.57 (t, 6.77 Hz, 2H), 2.16 (m, 2H), 1.30 (t, 7.13 Hz, 3H); MS (ESI) m/z = 234.2 (M + H^+); Anal. ($C_{13}H_{15}NO_3$); C, H, N.

Ethyl 5-(4-cyanophenoxy)pentanoate (1b): Ester = ethyl-5-bromovalerate (Sigma-Aldrich); yield 69%; mp 55-57°C; ^1H NMR (CD_3OD) δ 7.70 (d, 8.24 Hz, 2H), 7.11 (d, 8.67 Hz, 2H), 4.15 (m, 4H), 2.46 (t, 6.94 Hz, 2H), 1.87 (m, 4H), 1.30 (t, 7.37 Hz, 3H); MS (ESI) m/z = 248.3 (M + H^+); Anal. ($C_{14}H_{17}NO_3$); C, H, N.

Ethyl 6-(4-cyanophenoxy)hexanoate (1c): Ester = ethyl-6-bromohexanoate (Sigma-Aldrich); yield 56%; mp 41-42°C; ^1H NMR (CD_3OD) δ 7.69 (d, 8.67 Hz, 2H), 7.10 (d, 8.67 Hz, 2H), 4.17 (q, 6.94 Hz, 2H), 4.11 (t, 5.63 Hz, 2H), 2.40 (t, 7.37 Hz, 2H), 1.87 (t, 6.94 Hz, 2H), 1.74 (t, 6.94 Hz, 2H), 1.56 (t, 6.94 Hz, 2H), 1.30 (t, 7.37 Hz, 3H); MS (ESI) m/z = 262.1 (M + H^+); Anal. ($C_{15}H_{19}NO_3$); C, H, N.

Ethyl 7-(4-cyanophenoxy)heptanoate (1d): Ester = ethyl-7-bromoheptanoate (Sigma-Aldrich); yield 55%; mp 42-45°C; ^{1}H NMR (CD$_3$OD) δ 7.69 (d, 8.62 Hz, 2H), 7.10 (d, 8.62 Hz, 2H), 4.17 (q, 7.39 Hz, 2H), 4.11 (t, 6.57 Hz, 2H), 2.38 (t, 7.39 Hz, 2H), 1.86 (t, 6.98 Hz, 2H), 1.70 (t, 6.98 Hz, 2H), 1.56 (t, 7.78 Hz, 2H), 1.47 (t, 6.98 Hz, 2H), 1.30 (t, 6.98 Hz, 3H); MS (ESI) m/z = 276.3 (M + H$^+$); Anal. (C$_{16}$H$_{21}$NO$_3$); C, H, N.

General Procedure for the Synthesis of (2): Purified **1** was dissolved in EtOH (25 mL/g) and HCl gas was bubbled into the reaction vessel at 0°C for 4 hours. Reaction completeness was monitored by TLC of the free base. When reaction was complete, N$_2$ was bubbled into the reaction vessel at room temperature for 30 minutes. After removal of the solvent under reduced pressure the resulting solid was washed with absolute anhydrous Et$_2$O.

Ethyl 4-(4-(ethoxy(imino)methyl)phenoxy)butanoate hydrochloride (2a): Yield 57%; mp 58-60°C; ^{1}H NMR (CD$_3$OD) δ 7.70 (d, 8.33 Hz, 2H), 7.12 (d, 8.33 Hz, 2H), 4.18 (m, 4H), 2.57 (t, 8.93 Hz, 2H), 2.16 (m, 2H), 1.30 (t, 7.14 Hz, 3H); MS (ESI) m/z = 280.3 (M + H$^+$); Anal. (C$_{13}$H$_{15}$NO$_3$); C, H, N. Missing ethyl group by NMR and CHN which correlates to starting material; however, MS correlates to desired product.

Ethyl 5-(4-(ethoxy(imino)methyl)phenoxy)pentanoate hydrochloride (2b): Yield 50%; mp 50°C; (CDCl$_3$) δ 7.57 (d, 9.19 Hz, 2H), 6.92 (d, 9.19 Hz, 2H), 4.13 (q, 7.96 Hz, 2H), 4.02 (t, 4.90 Hz, 2H), 2.39 (t, 6.74 Hz, 2H), 1.84 (m, 4H), 1.26 (t, 8.58 Hz, 3H); MS (ESI) m/z = 294.4 (M + H$^+$); Anal. (C$_{14}$H$_{17}$NO$_3$); C, H, N. Missing ethyl group

by NMR and CHN which correlates to starting material; however, MS correlates to desired product.

Ethyl 6-(4-(ethoxy(imino)methyl)phenoxy)hexanoate hydrochloride (2c):
Yield 16%; mp 42-43°C; ^{1}H NMR (CD$_3$OD) δ 7.69 (d, 8.60 Hz, 2H), 7.10 (d, 8.60 Hz, 2H), 4.18 (q, 6.99 Hz, 2H), 4.12 (t, 6.45 Hz, 2H), 3.55 (q, 7.52 Hz, 2H), 2.41 (t, 7.52 Hz, 2H), 1.87 (quintet, 7.52 Hz, 2H), 1.75 (quintet, 7.52 Hz, 2H), 1.57 (quintet, 6.99 Hz, 2H), 1.30 (t, 6.99 Hz, 3H), 1.24 (t, 7.52 Hz, 3H); MS (ESI) m/z = 308.4 (M + H$^+$); Anal. (C$_{15}$H$_{19}$NO$_3$); C, H, N. Missing ethyl group by NMR and CHN which correlates to starting material; however, MS correlates to desired product.

Ethyl 7-(4-(ethoxy(imino)methyl)phenoxy)heptanoate hydrochloride (2d):
Yield 38%; mp 44-45°C; ^{1}H NMR (CD$_3$OD) δ 7.69 (d, 8.98 Hz, 2H), 7.11 (d, 8.98 Hz, 2H), 4.17 (q, 7.06 Hz, 2H), 4.11 (t, 6.42 Hz, 2H), 3.67 (q, 7.70 Hz, 2H), 2.38 (t, 7.06 Hz, 2H), 1.86 (quintet, 7.06 Hz, 2H), 1.70 (quintet, 7.70 Hz, 2H), 1.56 (quintet, 8.34 Hz, 2H), 1.46 (quintet, 7.70 Hz, 2H), 1.30 (t, 7.70 Hz, 3H), 1.24 (t, 7.70 Hz, 3H); MS (ESI) m/z = 322.4 (M + H$^+$); Anal. (C$_{16}$H$_{21}$NO$_3$); C, H, N. Missing ethyl group by NMR and CHN which correlates to starting material; however, MS correlates to desired product.

General Procedure for the Synthesis of (3): Purified **2** (1 eq.) was dissolved in EtOH (10 mL/g) followed by the addition of NH$_4$Cl (1.1 eq.), and EtOH solution of NH$_3$ (22.5 eq.) and stirred overnight at reflux. Upon reaction completeness the mixture was cooled

to room temperature. After removal of the solvent under reduced pressure the resulting solid was washed with absolute anhydrous Et_2O.

Ethyl 4-(4-carbamimidoylphenoxy)butanoate hydrochloride (3a): Yield 80%; mp 58-60°C; ^1H NMR (CD_3OD) δ 7.70 (d, 8.69 Hz, 2H), 7.12 (d, 8.69 Hz, 2H), 4.18 (m, 4H), 2.57 (t, 7.61 Hz, 2H), 2.16 (quintet, 7.61 Hz, 2H), 1.30 (t, 7.61 Hz, 3H); MS (ESI) m/z = 251.2 (M + H^+); CHN not possible.

Ethyl 5-(4-carbamimidoylphenoxy)pentanoate hydrochloride (3b): Yield 71%; mp 50°C; ^1H NMR ($CDCl_3$) δ 7.57 (d, 8.94 Hz, 2H), 6.93 (d, 8.25 Hz, 2H), 4.14 (q, 6.88 Hz, 2H), 4.02 (t, 6.19 Hz, 2H), 2.39 (t, 6.88 Hz, 2H), 1.84 (m, 4H), 1.26 (t, 6.88 Hz, 3H); MS (ESI) m/z = 265.4 (M + H^+); CHN not possible.

Ethyl 6-(4-carbamimidoylphenoxy)hexanoate hydrochloride (3c): Yield 35%; mp 42-44°C; ^1H NMR (D_2O) δ 7.70 (d, 9.06 Hz, 2H), 7.12 (d, 9.06 Hz, 2H), 4.18 (q, 6.80 Hz, 2H), 4.12 (t, 6.19 Hz, 2H), 2.41 (t, 7.26 Hz, 2H), 1.88 (quintet, 7.52 Hz, 2H), 1.75 (quintet, 7.94 Hz, 2H), 1.57 (quintet, 7.53 Hz, 2H), 1.30 (t, 7.00 Hz, 3H); MS (ESI) m/z = 279.3 (M + H^+); CHN not possible.

Ethyl 7-(4-carbamimidoylphenoxy)butanoate hydrochloride (3d): Yield 41%; mp 45-47°C; ^1H NMR (CD_3OD) δ 7.69 (d, 8.94 Hz, 2H), 7.11 (d, 8.87 Hz, 2H), 4.17 (q, 7.21 Hz, 2H), 4.11 (t, 6.24 Hz, 2H), 2.38 (t, 7.44 Hz, 2H), 1.87 (quintet, 7.74 Hz, 2H),

124

1.70 (quintet, 7.59 Hz, 2H), 1.56 (quintet, 7.81 Hz, 2H), 1.47 (quintet, 7.21 Hz, 2H), 1.30 (t, 7.21 Hz, 3H); MS (ESI) m/z = 293.2 (M + H$^+$); CHN not possible.

General Procedure for the Synthesis of (4): Purified **3** was dissolved in THF (10 mL/g) and placed in an ice bath. NaOH (1N) was added as needed to maintain the reaction pH = 10. Benzyl chloroformate (1.5 eq.) was slowly added at 0°C and the reaction stirred for 2 hours at 10°C. Upon reaction completeness, the reaction mixture was poured into EtOAc (20 mL/g). The organic layer was collected, washed with brine, and dried (Na$_2$SO$_4$). After removal of the solvent under reduced pressure the resulting solid was washed with absolute anhydrous Et$_2$O for purification.

Ethyl 4-(4-(N-benzyloxycarbonyl)carbamimidoyl)phenoxy)butanoate (4a): Yield 22%; mp 52-54°C; ^{1}H NMR (CD$_3$OD) δ 7.70 (d, 9.36 Hz, 2H), 7.41 (m, 5H), 7.11 (d, 9.36 Hz, 2H), 5.11 (s, 2H), 4.17 (m, 4H), 2.57 (t, 7.80 Hz, 2H), 2.15 (m, 2H), 1.30 (t, 7.02 Hz, 3H); MS (ESI) m/z = 385.3 (M + H$^+$); Anal. (C$_{21}$H$_{24}$N$_2$O$_5$); C, H, N.

Ethyl 5-(4-(N-benzyloxycarbonyl)carbamimidoyl)phenoxy)pentanoate (4b): Yield 17%; mp 50°C; ^{1}H NMR (CDCl$_3$) δ 7.58 (d, 8.79 Hz, 2H), 7.37 (m, 5H), 6.93 (d, 8.72 Hz, 2H), 5.11 (s, 2H), 4.13 (q, 7.11 Hz, 2H), 4.01 (t, 5.64 Hz, 2H), 2.38 (t, 7.40 Hz, 2H), 1.83 (m, 4H), 1.26 (t, 7.42 Hz, 3H); MS (ESI) m/z = 399.3 (M + H$^+$); Anal. (C$_{22}$H$_{26}$N$_2$O$_5$); C, H, N.

Ethyl 6-(4-(*N*-benzyloxycarbonyl)carbamimidoyl)phenoxy)hexanoate (4c):

Yield 29%; mp 38-39°C; ^{1}H NMR (CD$_3$OD) δ 7.69 (d, 9.14 Hz, 2H), 7.41 (m, 5H), 7.10 (d, 8.49 Hz, 2H), 5.11 (s, 2H), 4.18 (q, 7.84 Hz, 2H), 4.11 (t, 6.53 Hz, 2H), 2.41 (t, 7.84 Hz, 2H), 1.87 (quintet, 7.11 Hz, 2H), 1.75 (quintet, 7.59 Hz, 2H), 1.57 (quintet, 7.11 Hz, 2H), 1.30 (t, 7.11 Hz, 3H); MS (ESI) m/z = 413.4 (M + H$^+$); Anal. (C$_{23}$H$_{28}$N$_2$O$_5$); C, H, N.

Ethyl 7-(4-(*N*-benzyloxycarbonyl)carbamimidoyl)phenoxy)heptanoate (4d):

Yield 32%; mp 38-40°C; ^{1}H NMR (CD$_3$OD) δ 7.69 (d, 9.14 Hz, 2H), 7.41 (m, 5H), 7.11 (d, 9.14 Hz, 2H), 5.11 (s, 2H), 4.17 (q, 7.52 Hz, 2H), 4.11 (t, 6.99 Hz, 2H), 2.38 (t, 7.52 Hz, 2H), 1.86 (quintet, 6.98 Hz, 2H), 1.70 (quintet, 7.52 Hz, 2H), 1.56 (quintet, 8.06 Hz, 2H), 1.46 (quintet, 7.52 Hz, 2H), 1.30 (t, 6.99 Hz, 3H); MS (ESI) m/z = 427.3 (M + H$^+$); Anal. (C$_{24}$H$_{30}$N$_2$O$_5$); C, H, N.

General Procedure for the Synthesis of (5): Purified **4** was dissolved in EtOH (10 mL/g) followed by the addition of 1N NaOH (2 eq.). The reaction was stirred overnight at room temperature. Removal of the solvent under reduced pressure gave the Na salt.

This protocol is different from the patent. The patent stated hydrolysis under acidic conditions, but it removed both the ester and the benzyl group. This reaction was performed under basic and acidic conditions; basic conditions only hydrolyzed the ester, while the acidic conditions (HCl) (basification to pH=4 with bicarb instead of NaOH) still took off both the ester and the benzyl group.

Sodium 4-(4-(*N*-(benzyloxycarbonyl)carbamimidoyl)phenoxy)butanoate (5a):

Yield 86%; mp 250°C; ^{1}H NMR (D$_2$O) δ 7.74 (d, 9.77 Hz, 2H), 7.44 (m, 5H), 7.11 (d, 9.26 Hz, 2H), 4.66 (s, 2H), 4.15 (t, 6.69 Hz, 2H), 2.36 (t, 7.72 Hz, 2H), 2.06 (quintet, 7.20 Hz, 2H); Anal. (C$_{19}$H$_{19}$N$_2$NaO$_5$•1.5Na•1H$_2$O); C, H, N.

Sodium 5-(4-(*N*-(benzyloxycarbonyl)carbamimidoyl)phenoxy)pentanoate (5b): Yield 98%; mp 235-240°C; ^{1}H NMR (CD$_3$OD) δ 7.68 (d, 8.60 Hz, 2H), 7.39 (m, 5H), 7.11 (d, 9.15 Hz, 2H), 4.66 (s, 2H), 4.13 (t, 6.10 Hz, 2H), 2.29 (t, 7.21 Hz, 2H), 1.86 (m, 4H); Anal. (C$_{20}$H$_{21}$N$_2$NaO$_5$•1.1Na•0.9H$_2$O); C, H, N.

Sodium 6-(4-(*N*-(benzyloxycarbonyl)carbamimidoyl)phenoxy)hexanoate (5c):

Yield 79%; mp 250°C; ^{1}H NMR (D$_2$O) δ 7.72 (d, 8.78 Hz, 2H), 7.44 (m, 5H), 7.09 (d, 8.78 Hz, 2H), 4.66 (s, 2H), 4.14 (t, 6.59 Hz, 2H), 2.26 (t, 7.03 Hz, 2H), 1.82 (quintet, 7.47 Hz, 2H), 1.64 (quintet, 7.91 Hz, 2H), 1.47 (quintet, 8.34 Hz, 2H); Anal. (C$_{21}$H$_{23}$N$_2$NaO$_5$•1Na•2H$_2$O); C, H, N.

Sodium 7-(4-(*N*-(benzyloxycarbonyl)carbamimidoyl)phenoxy)heptanoate (5d): Yield 92%; mp 250°C; ^{1}H NMR (D$_2$O) δ 7.74 (d, 9.24 Hz, 2H), 7.44 (m, 5H), 7.11 (d, 9.24 Hz, 2H), 4.66 (s, 2H), 2.20 (t, 7.61 Hz, 2H), 1.82 (quintet, 8.15 Hz, 2H), 1.60 (quintet, 7.61 Hz, 2H), 1.49 (quintet, 8.15 Hz, 2H), 1.38 (quintet, 8.15 Hz, 2H); Anal. (C$_{22}$H$_{25}$N$_2$NaO$_5$•2Na•2.5H$_2$O); C, H, N.

Table 7.2. Analytical Data for Compounds **1a-5d**.

Compound Number	Calculated (%)			Found (%)		
	C	H	N	C	H	N
1a	66.94	6.48	6.00	66.83	6.48	5.98
1b	68.00	6.93	5.66	67.76	6.97	5.66
1c	68.94	7.33	5.36	68.70	7.13	5.36
1d	69.79	7.69	5.09	69.95	7.67	5.08
2a	66.94	6.48	6.00	66.91	6.47	5.98
2b	68.00	6.93	5.66	67.77	6.87	5.72
2c	68.94	7.33	5.36	69.14	7.39	5.41
2d	69.79	7.69	5.09	69.78	7.68	5.09
3a	CHN Not Possible – See NMR (Figure 7.11)					
3b	CHN Not Possible – See NMR (Figure 7.12)					
3c	CHN Not Possible – See NMR (Figure 7.13)					
3d	CHN Not Possible – See NMR (Figure 7.14)					
4a	65.61	6.29	7.29	65.27	6.34	7.13
4b	66.32	6.58	7.03	65.97	6.95	6.91
4c	66.97	6.84	6.79	66.96	7.02	6.71
4d	67.59	7.09	6.57	67.98	7.17	6.21
5a • 1.5Na • 1H$_2$O	52.97	4.91	6.50	53.05	4.49	6.91
5b • 1.1Na • 0.9H$_2$O	55.36	5.29	6.45	55.46	4.89	6.55
5c • 1Na • 2H$_2$O	54.32	3.91	6.03	54.27	3.91	6.68
5d • 2Na • 2.5H$_2$O	51.66	5.91	5.48	51.74	5.69	5.75

SpinWorks 2.5:   SLM53

Figure 7.12. ^{1}H NMR of Compound **3a**.

SpinWorks 2.5:   SLM42 free base in CDCl3

Figure 7.13. ¹H NMR of Compound **3b**.

PPM   7.2   6.8   6.4   6.0   5.6   5.2   4.8   4.4   4.0   3.6   3.2   2.8   2.4   2.0   1.6   1.2   0.8   0.4   -0.0
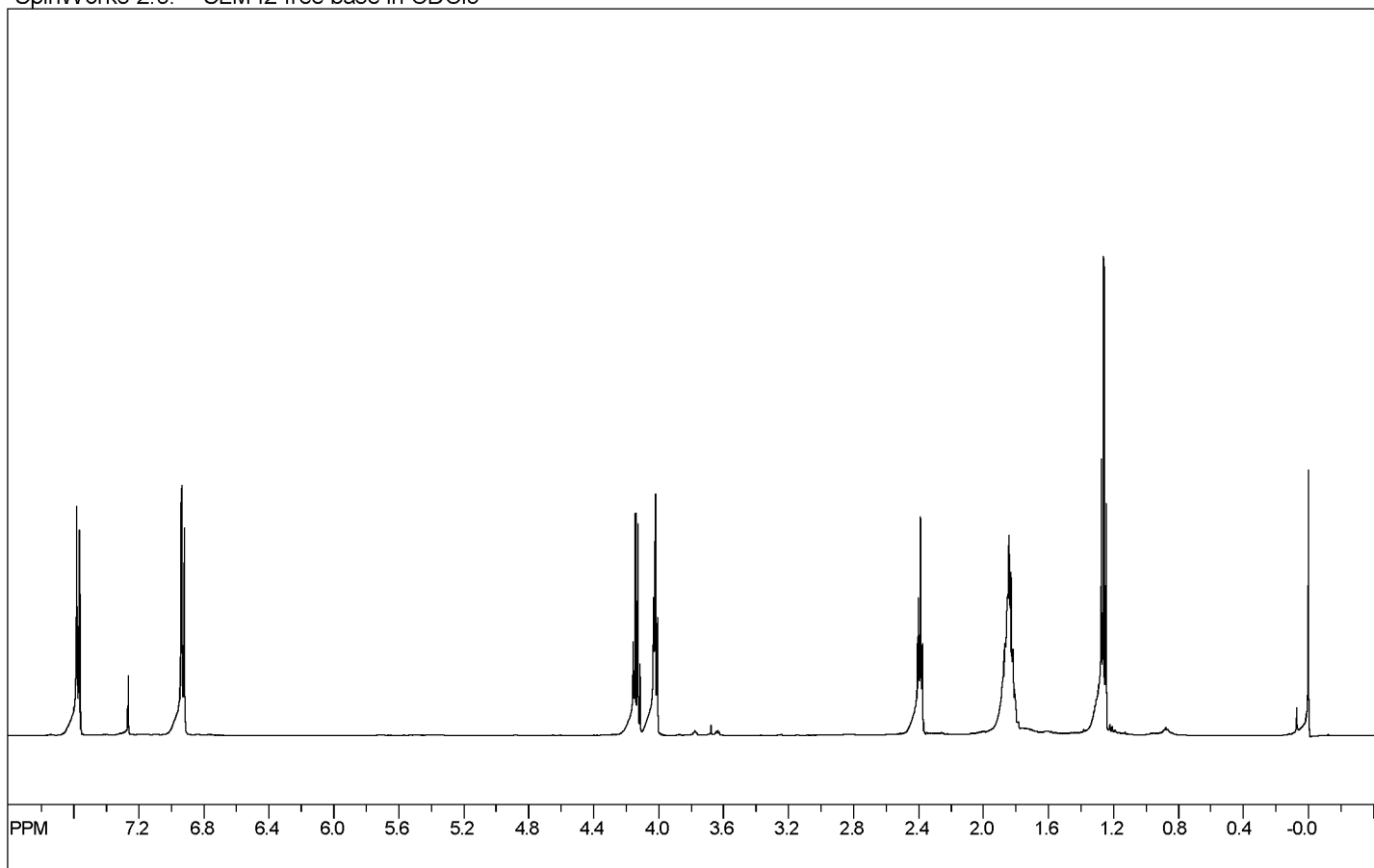
file: F:\NMR\SLM42fb_2006-08-21\PROTON_01.fid\fid block# 1 expt: "s2pul"
transmitter freq.: 499.751987 MHz
time domain size: 22706 points
width: 6000.60 Hz = 12.007156 ppm = 0.264274 Hz/pt
number of scans: 32

freq. of 0 ppm: 499.749517 MHz
processed size: 32768 complex points
LB: 0.000   GB: 0.0000

129

SpinWorks 2.5:   SLM59

Figure 7.14. ^{1}H NMR of Compound **3c**.

PPM   7.2   6.8   6.4   6.0   5.6   5.2   4.8   4.4   4.0   3.6   3.2   2.8   2.4   2.0   1.6   1.2   0.8   0.4
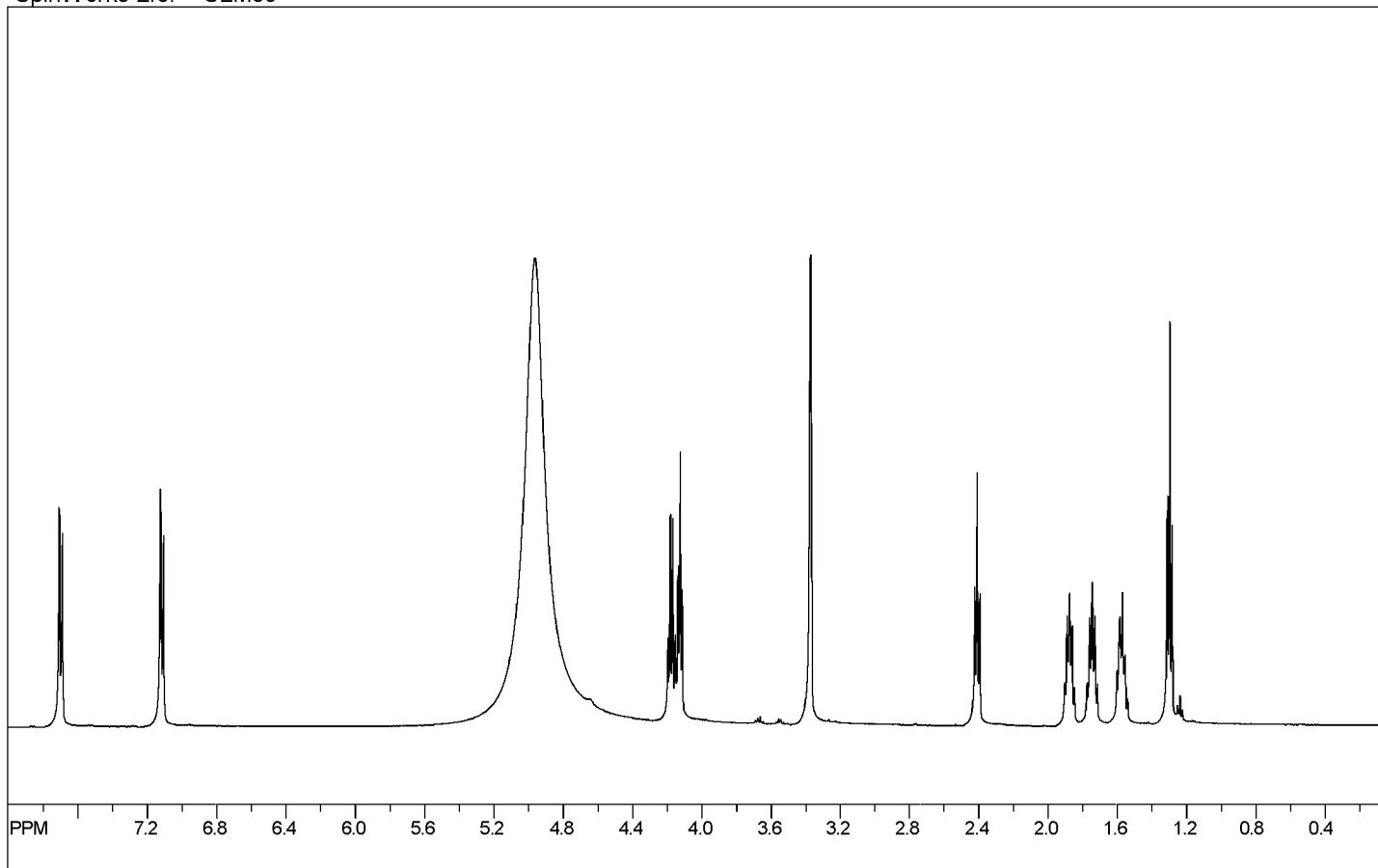
file: F:\NMR\SLM59_2006-11-14\PROTON_01.fid\fid block# 1 expt: "s2pul"
transmitter freq.: 499.753956 MHz
time domain size: 22706 points
width: 6000.60 Hz = 12.007109 ppm = 0.264274 Hz/pt
number of scans: 32

freq. of 0 ppm: 499.751457 MHz
processed size: 32768 complex points
LB: 0.000   GB: 0.0000

130

SpinWorks 2.5:   SLM65

Figure 7.15. ^{1}H NMR of Compound **3d**.

7.4.2. Fluorescence Binding Studies

The interaction between S100β and pentamidine was monitored in titrations of S100β into pentamidine (100 μM) and pentamidine fluorescence increases were measured at 345 nm intensity (λ_{ex} = 299 nm). The fluorescence data were collected on a Varian Cary Eclipse fluorescence spectrophotometer with the temperature maintained at 37°C using a circulating constant-temperature bath. All measurements were performed in quartz cuvettes with buffer containing 10 mM TES, pH 7.2, 15 mM NaCl, 100 mM KCl, and 0-10 mM $CaCl_2$.[216]

7.4.3 NMR Spectroscopy

Purified ^{15}N-labeled S100β was dialyzed against 0.1 mM TES buffer pH 7.2, 0.05 mM DTT, lyophilized, and hydrated in a small aliquot of ddH_2O and stored at -80 or -20 °C. The Ca^{2+}-loaded S100β-pentamidine NMR sample was prepared in a similar manner as previously described[217] and contained 0.5 mM S100β subunit concentration, 0.50-0.75 mM pentamidine, 0.34 mM NaN_3, 15 mM NaCl, 0-5% D_6-DMSO, 10-15 mM $CaCl_2$, 10% D_2O, 10 mM TES buffer, and adjusted to pH 7.2 with HCl.

Heteronuclear single quantum coherence (HSQC) NMR data were collected at 37°C with a Bruker Avance III 600 or with an Avance 800 US2 NMR spectrometer both equipped with pulsed-field gradients, four frequency channels, and triple resonance, z-axis gradient cryogenic probes.[218] Data were processed with NMRPipe, and proton chemical shifts were reported with respect to the H_2O or HDO signal taken as 4.658 ppm relative to external TSP (0.0 ppm). The ^{15}N chemical shifts were indirectly referenced as

previously described[219-221] using the following ratio of the zero-point frequency: 0.10132905 for ^{15}N to ^{1}H.[216]

Chapter 8

Summary

Morphine, a mu opioid receptor agonist, continues to be the primary drug of choice for the treatment of severe, chronic pain associated with surgery, cancer and AIDS due to its central analgesic effects. The use of opioids as analgesics, however, is accompanied by undesired side effects such as respiratory depression, nausea, constipation, and the development of tolerance and dependence, which limit clinical utility. The adverse constipation effect is primarily due to the peripheral effects of mu opioid agonists, and can be life threatening in severe situations. After repeated morphine administration, patients become tolerant to the central effects of morphine and therefore require greater doses to produce the same level of analgesia. Tolerance to the peripheral actions of morphine does not develop as rapidly as do the central effects, resulting in differential tolerance.

This differential tolerance results in increasing doses of morphine required to maintain analgesia, causing exponentially magnified constipatory effects. Receptor desensitization and internalization are mechanisms that produce tolerance at the receptor level; however, additional factors must be involved since tolerance development in the GI tract and the CNS do not coincide. The overall hypothesis is that one contributing mechanism to the differential tolerance to the analgesic effects of morphine is efflux transporter activity, specifically, P-gp at the BBB. Morphine is a known substrate for P-gp and P-gp expression in the BBB is up-regulated in morphine and oxycodone tolerant animals. Up-regulation of P-gp is therefore theorized to play a role in the development of differential tolerance by actively pumping morphine out of the CNS, resulting in relatively lower concentrations of morphine in the CNS.

Meperidine, a moderately potent mu opioid receptor agonist, has been reported to cause less constipation than morphine and is known to have a lower P-gp substrate activity than morphine. Meperidine therefore appears an excellent lead candidate to test our hypothesis, but there are serious problems with the chronic administration of meperidine. Meperidine is metabolized by two different pathways; the predominant pathway is hepatic carboxylesterase metabolism to meperidinic acid, an inactive metabolite, while the most clinically significant pathway is N-demethylation by the hepatic cytochrome P450 system to normeperidine, a non-opioid toxic metabolite, which has been reported to cause seizures. For these reason, we proposed to optimize meperidine by: 1) increasing potency, 2) increasing the duration of action, and 3) eliminating the toxic metabolite formation all while retaining low or further lowering P-gp substrate activity. These opioids with low or further reduced P-gp substrate activity were anticipated to be novel analgesics of similar potency to morphine, but do not give rise to differential tolerance and therefore represent excellent pharmacological tools to test our basic hypothesis.

A series of N-substituted meperidine analogs were synthesized based on standard opioid SAR to increase potency and analyzed for opioid and P-gp activity as described in Chapter 3. All analogs were found to be P-gp substrates using the P-gp-Glo assay with the exception of the N-phenylbutyl normeperidine analog. This analog was previously reported as having twice the potency of meperidine; however, when analyzed for P-gp activity *in vivo* it was determined that the analog was not twice as potent. The large dose (60 mg/kg) required for full antinociceptive activity caused seizures and eventual death

for the test animals and led to the discontinuation of *N*-phenylbutyl normeperidine as a lead compound.

Involvement in a similar project investigating a morphine series of compounds allowed for experience in both *in vitro* and *in vivo* analyses. 6-Desoxymorphine (6-DM) emerged as a lead candidate from the P-gp-Glo assay and was analyzed *in vivo* using a time course study; both analyses suggested that 6-DM was not a P-gp substrate. However, these results were inconclusive and an additional *in vivo* study was conducted. The dose-response study of 6-DM suggested that the analog was a P-gp substrate; therefore, further studies should be conducted to determine the true P-gp status of 6-DM. Another P-gp-Glo assay led to the discovery that oxymorphone, a potent mu opioid agonist, was not a P-gp substrate *in vitro*. To further investigate these results, an *in vitro* concentration dependent study was conducted on oxymorphone; serial dilutions allowed for investigation of oxymorphone at 0.97-500 uM, wherein all concentrations with the exception of 7.81 uM were not P-gp substrates. It is therefore concluded that oxymorphone is not a P-gp substrate *in vitro* and remains the best lead candidate for pursuing our hypothesis.

Chapter 4 describes the attempt to increase the duration of action of meperidine by making isosteric replacements of the 4-ester. A series of analogs were synthesized and evaluated in the P-gp-Glo assay to include the acid, amide, ester (meperidine), ketone, and nitrile analogs. The acid, amide, ketone, and ester analogs were not P-gp substrates; however, the most interesting results came from the introduction of a *m*-OH into the piperidine ring in a last attempt to increase potency. Addition of the *m*-OH dramatically increased the P-gp fold stimulation, which further supported previous

finding in our lab. These results along with the *N*-substituent work has allowed for development of SAR between the opioids and P-gp.

Introduction of steric hinderance into the piperidine ring of meperidine to <u>hinder *N*-dealkylation</u> as described in Chapter 5 is still under investigation. The added methyl groups have led to synthetic challenges as the chemistry did not proceed in a similar manner as the non-methylated synthetic schemes. Additional synthetic methods are described within the chapter. Completion of these analogs will provide a novel approach for introduction of alkyl groups into the 2- and 6-positions of the meperidine piperidine ring, providing future benefit in drug design and synthesis.

During the *N*-substituted meperidine analog synthesis, a series of nitrile intermediates were isolated and analyzed for opioid binding affinity; however, they were not opioids. Due to their structural similarity to <u>sigma</u> (σ, an ongoing stimulant project in the laboratory) ligands, the compounds were analyzed at σ_1 and σ_2 receptors and were found to be selective σ_1. Two *N*-substituted nitrile meperidine analogs, specifically *N*-crotyl and *N*-butyl were intentionally left out of the manuscript due to their binding affinities. The *N*-crotyl analog possessed a σ_1 K_i = 0.0018 nM $\pm$ 8.67^-5 and a σ_2 K_i = 69.64 nM $\pm$ 5.47, whereas the *N*-butyl analog had a σ_1 K_i = 0.13 nM $\pm$ 0.01 and a σ_2 K_i = 78.80 nM $\pm$ 2.13. Repetition of the *N*-crotyl analysis gave conflicting results, as the same and a higher K_i were prominent. Further analysis of these compounds is ongoing as σ_1 receptor subtypes are further explored, a potential cause for the variations in binding affinity.

Lastly, Chapter 7 describes an ongoing project in the laboratory in collaboration with Dr. David Weber in the University of Maryland, School of Medicine. A series of

compounds were designed and synthesized in order to investigate the optimal chain linker length necessary for a <u>dual profile inhibitor of S100β and p53</u> whose interaction leads to malignant melanoma as well as other cancers. A parallel series of compounds with chain lengths of 4-7 carbon atoms underwent binding and NMR perturbation studies. Preliminary results allow for a general conclusion that the six carbon chain length is optimal by NMR perturbation studies and it further appears that these compounds may bind at a novel site on the S100β protein. Further studies are required to more conclusively describe the results.

Appendices

Appendix A – Full Range Oxymorphone (OM) Concentration Dependent Study
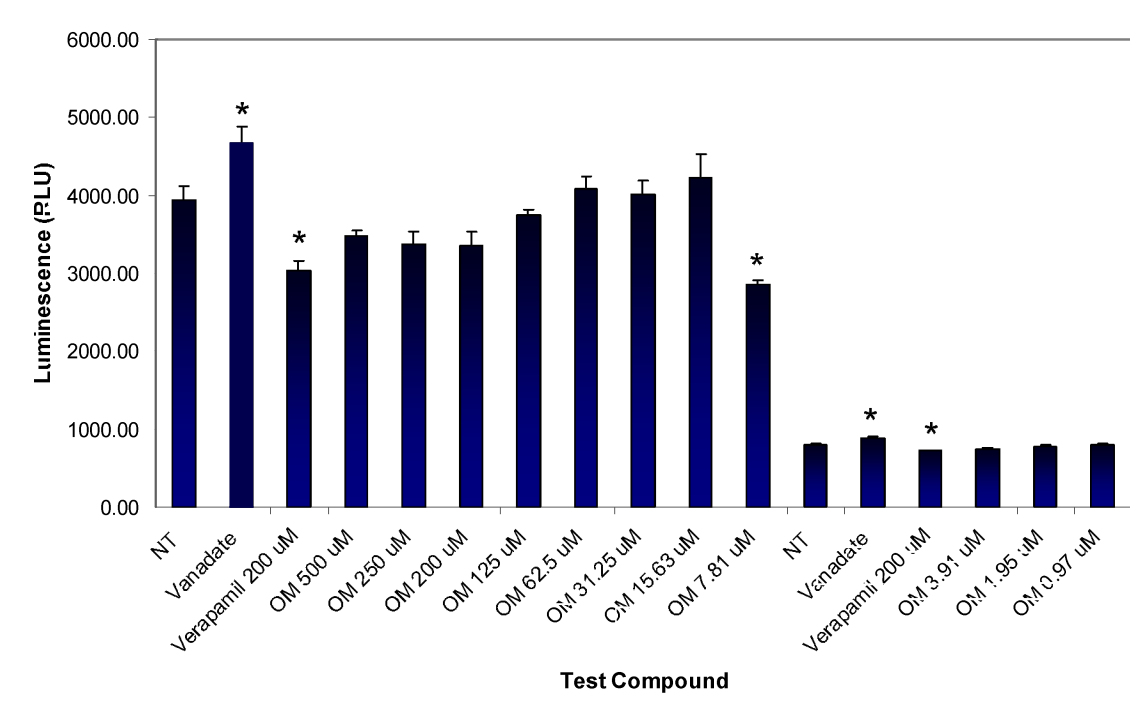
Results of various oxymorphone (OM) concentrations and standards in the P-gp-Glo assay system. Data are represented as mean $\pm$ SEM ($n = 4$). * Indicates significant difference from the control at $p < 0.05$ as indicated by the t-test. Concentrations 500 uM to 7.81 uM were initially run on one plate and all were non P-gp substrates with the exception of 7.81 uM. Since 7.81 uM OM was a substrate, additional concentrations of 3.91 uM to 0.97 uM were analyzed in a second experiment; none of which were substrates. Test concentrations must be compared against the controls they were run, due to the variance which exists in the basal level of P-gp activity in the controls. Overall, OM was found to be a non-P-gp substrate *in vitro* and 200 uM is an adequate concentration in which to test all subsequent compounds.

References

Reference List

1. McCartney, C. J.; Sinha, A.; Katz, J. A Qualitative Systematic Review of the Role of N-Methyl-D-Aspartate Receptor Antagonists in Preventive Analgesia. *Anesth. Analg.* **2004,** *98*, 1385-1400.

2. Boyd, R. E. Alpha2-Adrenergic Receptor Agonists as Analgesics. *Curr. Top. Med. Chem.* **2001,** *1*, 193-197.

3. Fox, A.; Bevan, S. Therapeutic Potential of Cannabinoid Receptor Agonists as Analgesic Agents. *Expert. Opin. Investig. Drugs.* **2005,** *14*, 695-703.

4. Kjaer, M.; Nielsen, H. The Analgesic Effect of the Gaba-Agonist Thip in Patients with Chronic Pain of Malignant Origin. A Phase-1-2 Study. *Br. J. Clin. Pharmacol.* **1983,** *16*, 477-485.

5. Decker, M. W.; Rueter, L. E.; Bitner, R. S. Nicotinic Acetylcholine Receptor Agonists: A Potential New Class of Analgesics. *Curr. Top. Med. Chem.* **2004,** *4*, 369-384.

6. Staats, P. S.; Yearwood, T.; Charapata, S. G.; Presley, R. W.; Wallace, M. S.; Byas-Smith, M.; Fisher, R.; Bryce, D. A.; Mangieri, E. A.; Luther, R. R.; Mayo, M.; McGuire, D.; Ellis, D. Intrathecal Ziconotide in the Treatment of Refractory Pain in Patients with Cancer or Aids: A Randomized Controlled Trial. *J. Amer. Med. Assoc.* **2004,** *291*, 63-70.

7. Fries, D. S., Opioid Analgesics. In *Foye's Principles of Medicinal Chemistry*, 5 ed.; **2002;** pp 453-479.

8. Mercadante, S. Opioid Rotation for Cancer Pain: Rationale and Clinical Aspects. *Cancer.* **1999,** *86*, 1856-1866.

9. Zieglgansberger, W.; Tolle, T.; Zimprich, A.; Hollt, V.; Spanagel, R. Endomorphins, Pain Relief, and Euphoria. *Pain and the Brain.* **1995,** *22*, 439-457.

10.   Quigley, C. The Role of Opioids in Cancer Pain. *Br. Med. J.* **2005,** *331,* 825-829.

11.   Williams, M.; Kowaluk, E. A.; Arneric, S. P. Emerging Molecular Approaches to Pain Therapy. *J. Med. Chem.* **1999,** *42,* 1481-1500.

12.   Breitbart, W.; Rosenfeld, B. D.; Passik, S. D.; McDonald, M. V.; Thaler, H.; Portenoy, R. K. The Undertreatment of Pain in Ambulatory Aids Patients. *Pain.* **1996,** *65,* 243-249.

13.   Kieffer, B. L.; Evans, C. J. Opioid Tolerance-in Search of the Holy Grail. *Cell.* **2002,** *108,* 587-590.

14.   von Zastrow, M.; Svingos, A.; Haberstock-Debic, H.; Evans, C. Regulated Endocytosis of Opioid Receptors: Cellular Mechanisms and Proposed Roles in Physiological Adaptation to Opiate Drugs. *Curr. Opin. Neurobiol.* **2003,** *13,* 348-353.

15.   White, J. M.; Irvine, R. J. Mechanisms of Fatal Opioid Overdose. *Addiction.* **1999,** *94,* 961-972.

16.   Aparasu, R.; McCoy, R. A.; Weber, C.; Mair, D.; Parasuraman, T. V. Opioid-Induced Emesis among Hospitalized Nonsurgical Patients: Effect on Pain and Quality of Life. *J. Pain Symptom Manage.* **1999,** *18,* 280-288.

17.   McNicol, E.; Horowicz-Mehler, N.; Fisk, R. A.; Bennett, K.; Gialeli-Goudas, M.; Chew, P. W.; Lau, J.; Carr, D. Management of Opioid Side Effects in Cancer-Related and Chronic Noncancer Pain: A Systematic Review. *J. Pain.* **2003,** *4,* 231-256.

18.   Cherny, N.; Ripamonti, C.; Pereira, J.; Davis, C.; Fallon, M.; McQuay, H.; Mercadante, S.; Pasternak, G.; Ventafridda, V. Strategies to Manage the Adverse Effects of Oral Morphine: An Evidence-Based Report. *J. Clin. Oncol.* **2001,** *19,* 2542-2554.

19.   Ossipov, M. H.; Lai, J.; King, T.; Vanderah, T. W.; Malan, T. P., Jr.; Hruby, V. J.; Porreca, F. Antinociceptive and Nociceptive Actions of Opioids. *J. Neurobiol.* **2004**, *61*, 126-148.

20.   Wang, J. B.; Johnson, P. S.; Persico, A. M.; Hawkins, A. L.; Griffin, C. A.; Uhl, G. R. Human Mu Opiate Receptor. Cdna and Genomic Clones, Pharmacologic Characterization and Chromosomal Assignment. *FEBS Lett.* **1994**, *338*, 217-222.

21.   Mansson, E.; Bare, L.; Yang, D. Isolation of a Human Kappa Opioid Receptor Cdna from Placenta. *Biochem. Biophys. Res. Commun.* **1994**, *202*, 1431-1437.

22.   Kieffer, B. L.; Befort, K.; Gaveriaux-Ruff, C.; Hirth, C. G. The Delta-Opioid Receptor: Isolation of a Cdna by Expression Cloning and Pharmacological Characterization. *Proc. Natl. Acad. Sci. U.S.A.* **1992**, *89*, 12048-12052.

23.   Evans, C. J.; Keith, D. E., Jr.; Morrison, H.; Magendzo, K.; Edwards, R. H. Cloning of a Delta Opioid Receptor by Functional Expression. *Science.* **1992**, *258*, 1952-1955.

24.   Kieffer, B. L. Opioids: First Lessons from Knockout Mice. *Trends Pharmacol. Sci.* **1999**, *20*, 19-26.

25.   Hasebe, K.; Kawai, K.; Suzuki, T.; Kawamura, K.; Tanaka, T.; Narita, M.; Nagase, H.; Suzuki, T. Possible Pharmacotherapy of the Opioid Kappa Receptor Agonist for Drug Dependence. *Ann. N Y Acad. Sci.* **2004**, *1025*, 404-413.

26.   Comer, S. D.; Hoenicke, E. M.; Sable, A. I.; McNutt, R. W.; Chang, K. J.; De Costa, B. R.; Mosberg, H. I.; Woods, J. H. Convulsive Effects of Systemic Administration of the Delta Opioid Agonist Bw373u86 in Mice. *J. Pharmacol. Exp. Ther.* **1993**, *267*, 888-895.

27.   De Luca, A.; Coupar, I. M. Insights into Opioid Action in the Intestinal Tract. *Pharmacol. Ther.* **1996**, *69*, 103-115.

28. Schug, S. A.; Zech, D.; Grond, S.; Jung, H.; Meuser, T.; Stobbe, B. A Long-Term Survey of Morphine in Cancer Pain Patients. *J. Pain Symptom Manage.* **1991,** *7*, 259-266.

29. Walsh, T. D. Prevention of Opioid Side Effects. *J. Pain Symptom Manage.* **1990,** *5*, 362-367.

30. Fallon, M. T.; Hanks, G. W. Morphine, Constipation and Performance Status in Advanced Cancer Patients. *Palliat. Med.* **1999,** *13*, 159-160.

31. Kurz, A.; Sessler, D. I. Opioid-Induced Bowel Dysfunction: Pathophysiology and Potential New Therapies. *Drugs.* **2003,** *63*, 649-671.

32. Corazziari, E. Role of Opioid Ligands in the Irritable Bowel Syndrome. *Can. J. Gastroenterol.* **1999,** *13 Suppl A*, 71A-75A.

33. Ericsson, C. D.; Johnson, P. C. Safety and Efficacy of Loperamide. *Am. J. Med.* **1990,** *88*, 10S-14S.

34. Wolff, B. G.; Michelassi, F.; Gerkin, T. M.; Techner, L.; Gabriel, K.; Du, W.; Wallin, B. A. Alvimopan, a Novel, Peripherally Acting Mu Opioid Antagonist: Results of a Multicenter, Randomized, Double-Blind, Placebo-Controlled, Phase III Trial of Major Abdominal Surgery and Postoperative Ileus. *Ann. Surg.* **2004,** *240*, 728-734.

35. Yuan, C. S. Clinical Status of Methylnaltrexone, a New Agent to Prevent and Manage Opioid-Induced Side Effects. *J. Support Oncol.* **2004,** *2*, 111-117.

36. FDA U.S. Food and Drug Administration - Center for Drug Evaluation and Research. www.accessdata.fda.gov (June 2, 2008).

37. Tamayo, A. C.; Diaz-Zuluaga, P. A. Management of Opioid-Induced Bowel Dysfunction in Cancer Patients. *Support Care Cancer.* **2004,** *12*, 613-618.

38.   Mancini, I.; Bruera, E. Constipation in Advanced Cancer Patients. *Support Care Cancer.* **1998,** *6*, 356-364.

39.   Palczewski, K.; Kumasaka, T.; Hori, T.; Behnke, C. A.; Motoshima, H.; Fox, B. A.; Le Trong, I.; Teller, D. C.; Okada, T.; Stenkamp, R. E.; Yamamoto, M.; Miyano, M. Crystal Structure of Rhodopsin: A G Protein-Coupled Receptor. *Science.* **2000,** *289*, 739-745.

40.   Williams, J. T.; Christie, M. J.; Manzoni, O. Cellular and Synaptic Adaptations Mediating Opioid Dependence. *Physiol. Rev.* **2001,** *81*, 299-343.

41.   Whistler, J. L.; Chuang, H. H.; Chu, P.; Jan, L. Y.; von Zastrow, M. Functional Dissociation of Mu Opioid Receptor Signaling and Endocytosis: Implications for the Biology of Opiate Tolerance and Addiction. *Neuron.* **1999,** *23*, 737-746.

42.   He, L.; Fong, J.; von Zastrow, M.; Whistler, J. L. Regulation of Opioid Receptor Trafficking and Morphine Tolerance by Receptor Oligomerization. *Cell.* **2002,** *108*, 271-282.

43.   Marinissen, M. J.; Gutkind, J. S. G-Protein-Coupled Receptors and Signaling Networks: Emerging Paradigms. *Trends Pharmacol. Sci.* **2001,** *22*, 368-376.

44.   Aquilante, C. L.; Letrent, S. P.; Pollack, G. M.; Brouwer, K. L. Increased Brain P-Glycoprotein in Morphine Tolerant Rats. *Life Sci.* **2000,** *66*, PL47-51.

45.   Hassan, H. E.; Myers, A. L.; Lee, I. J.; Coop, A.; Eddington, N. D. Oxycodone Induces Overexpression of P-Glycoprotein (Abcb1) and Affects Paclitaxel's Tissue Distribution in Sprague Dawley Rats. *J. Pharm. Sci.* **2007,** *96*, 2494-2506.

46.   Drewe, J.; Ball, H. A.; Beglinger, C.; Peng, B.; Kemmler, A.; Schachinger, H.; Haefeli, W. E. Effect of P-Glycoprotein Modulation on the Clinical Pharmacokinetics and Adverse Effects of Morphine. *Br. J. Clin. Pharmacol.* **2000,** *50*, 237-246.

47. King, M.; Su, W.; Chang, A.; Zuckerman, A.; Pasternak, G. W. Transport of Opioids from the Brain to the Periphery by P-Glycoprotein: Peripheral Actions of Central Drugs. *Nat. Neurosci.* **2001,** *4,* 268-274.

48. Xie, R.; Hammarlund-Udenaes, M.; de Boer, A. G.; de Lange, E. C. The Role of P-Glycoprotein in Blood-Brain Barrier Transport of Morphine: Transcortical Microdialysis Studies in Mdr1a (-/-) and Mdr1a (+/+) Mice. *Br. J. Pharmacol.* **1999,** *128,* 563-568.

49. Latta, K. S.; Ginsberg, B.; Barkin, R. L. Meperidine: A Critical Review. *Am. J. Ther.* **2002,** *9,* 53-68.

50. Dagenais, C.; Graff, C. L.; Pollack, G. M. Variable Modulation of Opioid Brain Uptake by P-Glycoprotein in Mice. *Biochem. Pharmacol.* **2004,** *67,* 269-276.

51. Casy, A. F.; Parfitt, R. T., *Opioid Analgesics.* Plenum Press: New York, **1986.**

52. Perrine, T. D.; Eddy, N. B. The Preparation and Analgesic Activity of 4-Carbethoxy-4-Phenyl-1-(2-Phenylethyl)Piperidine and Related Compounds. *J. Org. Chem.* **1956,** *21,* 125-126.

53. McLamore, S.; Ullrich, T.; Rothman, R. B.; Xu, H.; Dersch, C.; Coop, A.; Davis, P.; Porreca, F.; Jacobson, A. E.; Rice, K. C. Effect of N-Alkyl and N-Alkenyl Substituents in Noroxymorphindole,17-Substituted-6,7-Dehydro-4,5alpha-Epoxy-3,14-Dihydroxy-6,7:2',3'-Indolom Orphinans, on Opioid Receptor Affinity, Selectivity, and Efficacy. *J. Med. Chem.* **2001,** *44,* 1471-1474.

54. Redda, K. K.; Walker, C. A.; Barnett, G., *Cocaine, Marijuana, Designer Drugs: Chemistry, Pharmacology, and Behavior.* 5th ed.; CRC Press, Inc.: United States, **1989.**

55. Casy, A. F.; Chatten, L. G.; Khullar, K. K. Synthesis and Stereochemistry of 3-Methyl Analogues of Pethidine. *J. Chem. Soc. [Perkin 1].* **1969,** *18,* 2491-2495.

56.   Clark, R. F.; Wei, E. M.; Anderson, P. O. Meperidine: Therapeutic Use and Toxicity. *J. Emerg. Med.* **1995,** *13,* 797-802.

57.   Seifert, C. F.; Kennedy, S. Meperidine Is Alive and Well in the New Millennium: Evaluation of Meperidine Usage Patterns and Frequency of Adverse Drug Reactions. *Pharmacotherapy.* **2004,** *24,* 776-783.

58.   Janssen, P. A.; Eddy, N. B. Compounds Related to Pethidine-Iv. New General Chemical Methods of Increasing the Analgesic Activity of Pethidine. *J. Med. Pharm. Chem.* **1960,** *2,* 31-45.

59.   Casy, A. F.; Parfitt, R. T., Further Analgesics Based on Piperidine and Related Azacycloalkanes: Prodines, Promedols, Profadol, and Their Derivatives. In *Opioid. Analgesics: Chemistry and Receptors,* Plenum Press: New York, **1986**; pp 251-285.

60.   Bonjoch, J.; Casamitjana, N.; Bosch, J. A New Synthesis of 5-Phenylmorphans. *Tetrahedron.* **1988,** *44,* 1735-1741.

61.   Hennessy, M.; Spiers, J. P. A Primer on the Mechanics of P-Glycoprotein the Multidrug Transporter. *Pharmacol. Res.* **2007,** *55,* 1-15.

62.   Dean, M.; Hamon, Y.; Chimini, G. The Human Atp-Binding Cassette (Abc) Transporter Superfamily. *J. Lipid. Res.* **2001,** *42,* 1007-1017.

63.   Ambudkar, S. V.; Dey, S.; Hrycyna, C. A.; Ramachandra, M.; Pastan, I.; Gottesman, M. M. Biochemical, Cellular, and Pharmacological Aspects of the Multidrug Transporter. *Annu. Rev. Pharmacol. Toxicol.* **1999,** *39,* 361-398.

64.   Ambudkar, S. V.; Kimchi-Sarfaty, C.; Sauna, Z. E.; Gottesman, M. M. P-Glycoprotein: From Genomics to Mechanism. *Oncogene.* **2003,** *22,* 7468-7485.

65.   Schinkel, A. H. P-Glycoprotein, a Gatekeeper in the Blood-Brain Barrier. *Adv. Drug Deliv. Rev.* **1999,** *36,* 179-194.

66.   Raviv, Y.; Pollard, H. B.; Bruggemann, E. P.; Pastan, I.; Gottesman, M. M. Photosensitized Labeling of a Functional Multidrug Transporter in Living Drug-Resistant Tumor Cells. *J. Biol. Chem.* **1990,** *265,* 3975-3980.

67.   Higgins, C. F.; Gottesman, M. M. Is the Multidrug Transporter a Flippase? *Trends Biochem. Sci.* **1992,** *17,* 18-21.

68.   Wacher, V. J.; Wu, C. Y.; Benet, L. Z. Overlapping Substrate Specificities and Tissue Distribution of Cytochrome P450 3a and P-Glycoprotein: Implications for Drug Delivery and Activity in Cancer Chemotherapy. *Mol. Carcinog.* **1995,** *13,* 129-134.

69.   Schuetz, E. G.; Beck, W. T.; Schuetz, J. D. Modulators and Substrates of P-Glycoprotein and Cytochrome P4503a Coordinately up-Regulate These Proteins in Human Colon Carcinoma Cells. *Mol. Pharmacol.* **1996,** *49,* 311-318.

70.   Balayssac, D.; Authier, N.; Cayre, A.; Coudore, F. Does Inhibition of P-Glycoprotein Lead to Drug-Drug Interactions? *Toxicol. Lett.* **2005,** *156,* 319-329.

71.   Lin, J. H.; Yamazaki, M. Role of P-Glycoprotein in Pharmacokinetics: Clinical Implications. *Clin. Pharmacokinet.* **2003,** *42,* 59-98.

72.   Zhang, Y.; Bachmeier, C.; Miller, D. W. In Vitro and in Vivo Models for Assessing Drug Efflux Transporter Activity. *Adv. Drug Deliv. Rev.* **2003,** *55,* 31-51.

73.   Anderle, P.; Niederer, E.; Rubas, W.; Hilgendorf, C.; Spahn-Langguth, H.; Wunderli-Allenspach, H.; Merkle, H. P.; Langguth, P. P-Glycoprotein (P-Gp) Mediated Efflux in Caco-2 Cell Monolayers: The Influence of Culturing Conditions and Drug Exposure on P-Gp Expression Levels. *J. Pharm. Sci.* **1998,** *87,* 757-762.

74. Adachi, Y.; Suzuki, H.; Sugiyama, Y. Comparative Studies on in Vitro Methods for Evaluating in Vivo Function of Mdr1 P-Glycoprotein. *Pharm. Res.* **2001,** *18,* 1660-1668.

75. Evers, R.; Zaman, G. J.; van Deemter, L.; Jansen, H.; Calafat, J.; Oomen, L. C.; Oude Elferink, R. P.; Borst, P.; Schinkel, A. H. Basolateral Localization and Export Activity of the Human Multidrug Resistance-Associated Protein in Polarized Pig Kidney Cells. *J. Clin. Invest.* **1996,** *97,* 1211-1218.

76. Polli, J. W.; Wring, S. A.; Humphreys, J. E.; Huang, L.; Morgan, J. B.; Webster, L. O.; Serabjit-Singh, C. S. Rational Use of in Vitro P-Glycoprotein Assays in Drug Discovery. *J. Pharm. Exp. Ther.* **2001,** *299,* 620-628.

77. Schinkel, A. H.; Smit, J. J.; van Tellingen, O.; Beijnen, J. H.; Wagenaar, E.; van Deemter, L.; Mol, C. A.; van der Valk, M. A.; Robanus-Maandag, E. C.; te Riele, H. P.; et al. Disruption of the Mouse Mdr1a P-Glycoprotein Gene Leads to a Deficiency in the Blood-Brain Barrier and to Increased Sensitivity to Drugs. *Cell.* **1994,** *77,* 491-502.

78. Schinkel, A. H.; Mayer, U.; Wagenaar, E.; Mol, C. A.; van Deemter, L.; Smit, J. J.; van der Valk, M. A.; Voordouw, A. C.; Spits, H.; van Tellingen, O.; Zijlmans, J. M.; Fibbe, W. E.; Borst, P. Normal Viability and Altered Pharmacokinetics in Mice Lacking Mdr1-Type (Drug-Transporting) P-Glycoproteins. *Proc. Natl. Acad. Sci. U S A.* **1997,** *94,* 4028-4033.

79. Umbenhauer, D. R.; Lankas, G. R.; Pippert, T. R.; Wise, L. D.; Cartwright, M. E.; Hall, S. J.; Beare, C. M. Identification of a P-Glycoprotein-Deficient Subpopulation in the Cf-1 Mouse Strain Using a Restriction Fragment Length Polymorphism. *Toxicol. Appl. Pharmacol.* **1997,** *146,* 88-94.

80.   Callaghan, R.; Riordan, J. R. Synthetic and Natural Opiates Interact with P-Glycoprotein in Multidrug-Resistant Cells. *J. Biol. Chem.* **1993,** *268*, 16059-16064.

81.   Zong, J.; Pollack, G. M. Morphine Antinociception Is Enhanced in Mdr1a Gene-Deficient Mice. *Pharm. Res.* **2000,** *17*, 749-753.

82.   Dagenais, C.; Zong, J.; Ducharme, J.; Pollack, G. M. Effect of Mdr1a P-Glycoprotein Gene Disruption, Gender, and Substrate Concentration on Brain Uptake of Selected Compounds. *Pharm. Res.* **2001,** *18*, 957-963.

83.   Jette, L.; Beaulieu, E.; Leclerc, J. M.; Beliveau, R. Cyclosporin a Treatment Induces Overexpression of P-Glycoprotein in the Kidney and Other Tissues. *Am. J. Physiol.* **1996,** *270*, 756-765.

84.   Huwyler, J.; Drewe, J.; Gutmann, H.; Thole, M.; Fricker, G. Modulation of Morphine-6-Glucuronide Penetration into the Brain by P-Glycoprotein. *Int. J. Clin. Pharmacol. Ther.* **1998,** *36*, 69-70.

85.   Schinkel, A. H.; Wagenaar, E.; van Deemter, L.; Mol, C. A.; Borst, P. Absence of the Mdr1a P-Glycoprotein in Mice Affects Tissue Distribution and Pharmacokinetics of Dexamethasone, Digoxin, and Cyclosporin A. *J. Clin. Invest.* **1995,** *96*, 1698-1705.

86.   Letrent, S. P.; Pollack, G. M.; Brouwer, K. R.; Brouwer, K. L. Effect of Gf120918, a Potent P-Glycoprotein Inhibitor, on Morphine Pharmacokinetics and Pharmacodynamics in the Rat. *Pharm. Res.* **1998,** *15*, 599-605.

87.   Lotsch, J.; Tegeder, I.; Angst, M. S.; Geisslinger, G. Antinociceptive Effects of Morphine-6-Glucuronide in Homozygous Mdr1a P-Glycoprotein Knockout and in Wildtype Mice in the Hotplate Test. *Life Sci.* **2000,** *66*, 2393-2403.

88.   Bourasset, F.; Cisternino, S.; Temsamani, J.; Scherrmann, J. M. Evidence for an Active Transport of Morphine-6-Beta-D-Glucuronide but Not P-Glycoprotein-Mediated at the Blood-Brain Barrier. *J. Neurochem.* **2003,** *86,* 1564-1567.

89.   Thompson, S. J.; Koszdin, K.; Bernards, C. M. Opiate-Induced Analgesia Is Increased and Prolonged in Mice Lacking P-Glycoprotein. *Anesthesiology.* **2000,** *92,* 1392-1399.

90.   Crowe, A. The Influence of P-Glycoprotein on Morphine Transport in Caco-2 Cells. Comparison with Paclitaxel. *Eur. J. Pharmacol.* **2002,** *440,* 7-16.

91.   Wandel, C.; Kim, R.; Wood, M.; Wood, A. Interaction of Morphine, Fentanyl, Sufentanil, Alfentanil, and Loperamide with the Efflux Drug Transporter P-Glycoprotein. *Anesthesiology.* **2002,** *96,* 913-920.

92.   Skarke, C.; Jarrar, M.; Erb, K.; Schmidt, H.; Geisslinger, G.; Lotsch, J. Respiratory and Miotic Effects of Morphine in Healthy Volunteers When P-Glycoprotein Is Blocked by Quinidine. *Clin. Pharmacol. Ther.* **2003,** *74,* 303-311.

93.   Kharasch, E. D.; Hoffer, C.; Whittington, D.; Sheffels, P. Role of P-Glycoprotein in the Intestinal Absorption and Clinical Effects of Morphine. *Clin. Pharmacol. Ther.* **2003,** *74,* 543-554.

94.   Hamabe, W.; Maeda, T.; Fukazawa, Y.; Kumamoto, K.; Shang, L. Q.; Yamamoto, A.; Yamamoto, C.; Tokuyama, S.; Kishioka, S. P-Glycoprotein Atpase Activating Effect of Opioid Analgesics and Their P-Glycoprotein-Dependent Antinociception in Mice. *Pharmacol. Biochem. Behav.* **2006,** *85,* 629-636.

95.   Hamabe, W.; Maeda, T.; Kiguchi, N.; Yamamoto, C.; Tokuyama, S.; Kishioka, S. Negative Relationship between Morphine Analgesia and P-Glycoprotein Expression Levels in the Brain. *J. Pharmacol. Sci.* **2007,** *105,* 353-360.

96. Groenendaal, D.; Freijer, J.; de Mik, D.; Bouw, M. R.; Danhof, M.; de Lange, E. C. Population Pharmacokinetic Modelling of Non-Linear Brain Distribution of Morphine: Influence of Active Saturable Influx and P-Glycoprotein Mediated Efflux. *Br. J. Pharmacol.* **2007**.

97. Eap, C. B.; Buclin, T.; Baumann, P. Interindividual Variability of the Clinical Pharmacokinetics of Methadone: Implications for the Treatment of Opioid Dependence. *Clin. Pharmacokinet.* **2002,** *41*, 1153-1193.

98. Bouer, R.; Barthe, L.; Philibert, C.; Tournaire, C.; Woodley, J.; Houin, G. The Roles of P-Glycoprotein and Intracellular Metabolism in the Intestinal Absorption of Methadone: In Vitro Studies Using the Rat Everted Intestinal Sac. *Fundam. Clin. Pharmacol.* **1999,** *13*, 494-500.

99. Nanovskaya, T.; Nekhayeva, I.; Karunaratne, N.; Audus, K.; Hankins, G. D.; Ahmed, M. S. Role of P-Glycoprotein in Transplacental Transfer of Methadone. *Biochem. Pharmacol.* **2005,** *69*, 1869-1878.

100. Stormer, E.; Perloff, M. D.; von Moltke, L. L.; Greenblatt, D. J. Methadone Inhibits Rhodamine123 Transport in Caco-2 Cells. *Drug Metab. Dispos.* **2001,** *29*, 954-956.

101. Wang, J. S.; Ruan, Y.; Taylor, R. M.; Donovan, J. L.; Markowitz, J. S.; DeVane, C. L. Brain Penetration of Methadone (R)- and (S)-Enantiomers Is Greatly Increased by P-Glycoprotein Deficiency in the Blood-Brain Barrier of Abcb1a Gene Knockout Mice. *Psychopharmacology (Berl).* **2004,** *173*, 132-138.

102. Rodriguez, M.; Ortega, I.; Soengas, I.; Suarez, E.; Lukas, J. C.; Calvo, R. Effect of P-Glycoprotein Inhibition on Methadone Analgesia and Brain Distribution in the Rat. *J. Pharm. Pharmacol.* **2004,** *56*, 367-374.

103. Crettol, S.; Digon, P.; Golay, K. P.; Brawand, M.; Eap, C. B. In Vitro P-Glycoprotein-Mediated Transport of (R)-, (S)-, (R,S)-Methadone, Laam and Their Main Metabolites. *Pharmacology.* **2007,** *80*, 304-311.

104. Crowe, A.; Wong, P. Potential Roles of P-Gp and Calcium Channels in Loperamide and Diphenoxylate Transport. *Toxicol. Appl. Pharmacol.* **2003,** *193*, 127-137.

105. Bostrom, E.; Simonsson, U. S.; Hammarlund-Udenaes, M. Oxycodone Pharmacokinetics and Pharmacodynamics in the Rat in the Presence of the P-Glycoprotein Inhibitor Psc833. *J. Pharm. Sci.* **2005,** *94*, 1060-1066.

106. Somogyi, A. A.; Barratt, D. T.; Coller, J. K. Pharmacogenetics of Opioids. *Clin. Pharmacol. Ther.* **2007,** *81*, 429-444.

107. Kalvass, J. C.; Olson, E. R.; Pollack, G. M. Pharmacokinetics and Pharmacodynamics of Alfentanil in P-Glycoprotein-Competent and P-Glycoprotein-Deficient Mice: P-Glycoprotein Efflux Alters Alfentanil Brain Disposition and Antinociception. *Drug Metab. Dispos.* **2007,** *35*, 455-459.

108. Kharasch, E. D.; Hoffer, C.; Altuntas, T. G.; Whittington, D. Quinidine as a Probe for the Role of P-Glycoprotein in the Intestinal Absorption and Clinical Effects of Fentanyl. *J. Clin. Pharmacol.* **2004,** *44*, 224-233.

109. Mercer, S. L.; Hassan, H. E.; Cunningham, C. W.; Eddington, N. D.; Coop, A. Opioids and Efflux Transporters. Part 1: P-Glycoprotein Substrate Activity of N-Substituted Analogs of Meperidine. *Bioorg. Med. Chem. Lett.* **2007,** *17*, 1160-1162.

110. Casy, A. F.; Parfitt, R. T., Pethidine and Related 4-Phenylpiperidine Analgesics. In *Opioid Analgesics: Chemistry and Receptors*, Plenum Press: New York, **1986**; pp 229-249.

111. Cunningham, C. W.; Mercer, S. L.; Hassan, H. E.; Traynor, J. R.; Eddington, N. D.; Coop, A. Opioids and Efflux Transporters. Part 2: P-Glycoprotein Substrate Activity of 3- and 6-Substituted Morphine Analogs. *J. Med. Chem.* **2008,** *51*, 2316-2320.

112. Hassan, H. E.; Mercer, S. L.; Cunningham, C. W.; Coop, A.; Eddington, N. D. Evaluation of the P-Glycoprotein Affinity Status of a Series of Novel and Currently Available Morphine Analogs: Comparative Study with Meperidine Analogs to Identify Opioids with Minimal P-Gp Interactions. *Int. J. Pharm. Sci.* **2008,** *Accepted.*

113. Mercer, S. L.; Cunningham, C. W.; Eddington, N. D.; Coop, A. Opioids and Efflux Transporters. Part 3: P-Glycoprotein Substrate Activity of 3-Hydroxyl Addition to Meperidine Analogs. *Bioorg. Med. Chem. Lett.* **2008**, *18*, 3638-3640.

114. Tabakian, H. M. Update on Chronic Pain Management. *Mol. Med.* **2005,** *102*, 456-462.

115. Pasternak, G. W. Multiple Opiate Receptors: Deja Vu All over Again. *Neuropharmacology.* **2004,** *47 Suppl 1*, 312-323.

116. Hassan, H. E.; Myers, A. L.; Lee, I. J.; Coop, A.; Eddington, N. D. Oxycodone Induces Overexpression of P-Glycoprotein and Affects Paclitaxel's Tissue Distribution in Sprague Dawley Rats. *J. Pharm. Sci.* **2007,** *96*, 2494-2506.

117. Cunningham, C. W.; Mercer, S. L.; Hassan, H. E.; Traynor, J. R.; Eddington, N. D.; Coop, A. Opioids and Efflux Transporters. Part 2: P-Glycoprotein Substrate Activity of 3- and 6-Substituted Morphine Analogs. *J. Med. Chem.* **2008,** *51*, 2316-2320.

118. Eisleb, O. New Syntheses with Sodium Amide. *Chem. Ber.* **1941,** *74*, 1433-1450.

119. Elpern, B.; Gardner, L. N.; Grumbach, L. Strong Analgesics. The Preparation of Some Ethyl 1-Aralkyl-4-Phenylpiperidine-4-Carboxylates. *J. Am. Chem. Soc.* **1957,** *79*, 1951-1954.

120. Thorp, R. H.; Walton, E. New Analgesics. Ii. Further Homologs of Pethidine and the Pharmacology of These and Other Compounds. *J. Chem. Soc.* **1947**, 559-561.

121. Walton, E.; Green, M. B. New Analgesics. I. Homologues of Pethidine and Related Compounds. *J. Chem. Soc.* **1945**, 315-319.

122. Traynor, J. R.; Woods, J. H. Drug Evaluation Committee Report On: Evaluation of New Compounds for Opioid Activity (2006). *NIDA Res. Monogr.* **2007,** *187*, 113-132.

123. Drug Evaluation Committee Report On: Evaluation of New Compounds for Opioid Activity. *NIDA Res. Monogr.* **1965**.

124. Umans, J. G.; Inturrisi, C. E. Antinociceptive Activity and Toxicity of Meperidine and Normeperidine in Mice. *J. Pharmacol. Exp. Ther.* **1982,** *223*, 203-206.

125. Aceto, M.; Bowman, E.; Harris, L.; May, E. Dependence Studies of New Compounds in the Rhesus Monkey, Rat, and Mouse. *NIDA Res. Monogr.* **1998,** *178*, 363-407.

126. Aceto, M.; Bowman, E.; Harris, L.; Hughes, L.; Kipps, B.; Lobe, S.; May, E. Evaluation of New Compounds in the Rhesus Monkey, Rat and Mouse. *NIDA Res. Monogr.* **2007,** *187*, 136-164.

127. D'amour, F.; Smith, D. A Method for Determining Loss of Pain Sensation. *J. Pharmacol. Exp. Ther.* **1941,** *72*, 74-79.

128. Ross, F.; Wallis, S.; Smith, M. Co-Administration of Sub-Antinociceptive Doses of Oxycodone and Morphine Produces Marked Antinociceptive Synergy with Reduced CNS Side-Effects in Rats. *Pain.* **2000,** *84*, 421-428.

129. Nielsen, C.; Ross, F.; MT, S. Incomplete, Asymmetric, and Route-Dependent Cross-Tolerance between Oxycodone and Morphine in the Dark Agouti Rat. *J. Pharmacol. Exp. Ther.* **2000,** *295*, 91-99.

130. Kharasch, M. S.; Reinmuth, O., *Grignard Reactions on Nonmetallic Substances*. Prentice Hall: New York, **1954**; Chapter 10.

131. Rice, K. C. A Rapid, High-Yield Conversion of Codeine to Morphine. *J. Med. Chem.* **1977,** *20*, 164-165.

132. Seitner, P. G.; Martin, B. C. Survey of Analgesic Drug Prescribing Patterns. Washington, DC: The Drug Abuse Council. **1975**, 6-7.

133. Stambaugh, J. E.; Wainer, I. W. The Bioavailability of Meperidine Using Urine Assays for Meperidine and Normeperidine. *J. Clin. Pharmacol.* **1975,** *15*, 269-271.

134. Stambaugh, J. E.; Wainer, I. W.; Sanstead, J. K.; Hemphill, D. M. The Clinical Pharmacology of Meperidine--Comparison of Routes of Administration. *J. Clin. Pharmacol.* **1976,** *16*, 245-256.

135. Ellenhorne, M. J.; Barceloux, D. G., *Medical Toxicology*. Elsevier: New York, 1988.

136. Pond, S. M.; Tong, T.; Benowitz, N. L.; Jacob, P.; Rigod, J. Presystemic Metabolism of Meperidine to Normeperidine in Normal and Cirrhotic Subjects. *Clin. Pharmacol. Ther.* **1981,** *30*, 183-188.

137. Szeto, H. H.; Inturrisi, C. E.; Houde, R.; Saal, S.; Cheigh, J.; Reidenberg, M. M. Accumulation of Normeperidine, an Active Metabolite of Meperidine, in Patients with Renal Failure of Cancer. *Ann. Intern. Med.* **1977,** *86*, 738-741.

138. Klotz, U.; McHorse, T. S.; Wilkinson, G. R.; Schenker, S. The Effect of Cirrhosis on the Disposition and Elimination of Meperidine in Man. *Clin. Pharmacol. Ther.* **1974,** *16*, 667-675.

139. Odar-Cederlof, I.; Boreus, L. O.; Bondesson, U.; Holmberg, L.; Heyner, L. Comparison of Renal Excretion of Pethidine (Meperidine) and Its Metabolites in Old and Young Patients. *Eur. J. Clin. Pharmacol.* **1985,** *28*, 171-175.

140. Andrews, H. L. Cortical Effects of Demerol. *J Pharmacol Exp Ther.* **1942,** *76*, 89-94.

141. Hammelsbach, C. K. Studies of the Addiction Liability of Demerol (D-140). *J. Pharmacol. Exp. Ther.* **1942,** *75*, 64-68.

142. Kaiko, R. F.; Foley, K. M.; Grabinski, P. Y. Central Nervous System Excitatory Effects of Meperidine in Cancer Patients. *Ann. Neurol.* **1983,** *13*, 180-185.

143. Deneau, G. A.; Nakai, K. The Toxicity of Meperidine in the Monkey as Influenced by Its Rate of Absorption. *Bull. Drug Addict. Narcot.* **1961,** *6*, 2460-2469.

144. Jiraki, K. Lethal Effects of Normeperidine. *Am. J. Forensic Med. Pathol.* **1992,** *13*, 42-43.

145. Mather, L. E.; Meffin, P. J. Clinical Pharmacokinetics of Pethidine. *Clin. Pharmacokinet.* **1978,** *3*, 352-368.

146. Miller, J. W.; Anderson, H. H. The Effect of N-Demethylation on Certain Pharmacologic Actions of Morphine, Codeine, and Meperidine in the Mouse. *J. Pharmacol. Exp. Ther.* **1954,** *112*, 191-196.

147. Armstrong, P. J.; Bersten, A. Normeperidine Toxicity. *Anesth. Analg.* **1986,** *65*, 536-538.

148. Modica, P. A.; Temelhoffe, R.; White, P. F. Pro- and Anticonvulsant Effects of Anesthetics (Part I). *Anesth. Analg.* **1990,** *70*, 303-315.

149. Gilbert, P. E.; Martin, W. R. Antagonism of the Convulsant Effects of Heroin, D-Propoxyphene, Meperidine, Normeperidine and Thebaine by Naloxone in Mice. *J. Pharmacol. Exp. Ther.* **1975,** *192*, 538-541.

150. Tortella, F. C.; Cowan, A.; Alder, M. W. Studies on the Excitatory and Inhibitory Influence of Intracerebroventricularly Injected Opioids on Seizure Thresholds in Rats. *Neuropharmacology.* **1984,** *23*, 749-754.

151. Eisendrath, S. J.; Goldman, B.; Douglas, J.; Dimatteo, L.; Van Dyke, C. Meperidine-Induced Delirium. *Am. J. Psych.* **1987,** *144*, 1062-1065.

152. Clark, R. B.; Lattin, D. L. Metabolites of Meperidine in Serum. *Am. J. Obstet. Gynecol.* **1978,** *130*, 113-117.

153. Fries, D. S.; de Vries, J.; Hazelhoff, B.; Horn, A. s. Synthesis and Toxicity toward Nigrostriatal Dopamine Neurons of 1-Methyl-4-Phenyl-1,2,3,6-Tetrahydropyridine (Mptp) Analogs. *J. Med. Chem.* **1986,** *29*, 424-427.

154. Fortunato, J. M.; Ganem, B. Lithium and Potassium Trialkylborohydrides. Reagents for Direct Reduction of Alpha, Beta -Unsaturated Carbonyl Compounds to Synthetically Versatile Enolate Anions. *J. Org. Chem.* **1976,** *41*, 2194-2200.

155. Rapoport, H.; Bonner, R. M. Delta^7- and Delta^8- Desoxycodeine. *J. Am. Chem. Soc.* **1951,** *73*, 2872-2876.

156. Zhao, M.; Li, J.; Song, Z.; Desmond, R.; Tschaen, D. M.; Grabowski, E. J. J.; Reider, P. J. A Novel Chromium Trioxide Catalyzed Oxidation of Primary Alcohols to the Carboxylic Acids. *Tetrahedron Lett.* **1998,** *39*, 5323-5326

157. Taber, D. F.; Kong, S. Alkylation of Acetonitrile. *J. Org. Chem.* **1997,** *62*, 8575-8576.

158. Brown, H., *Boranes in Organic Chemistry.* Cornell University Press: Ithaca, NY, **1972**; p 209.

159. Cho, S.; Park, Y.; Kim, J.; Falck, J. R.; Yoon, Y. Facile Reduction of Carboxylic Acids, Esters, Acid Chlorides, Amides and Nitriles to Alcohols or Amines Using Nabh4/Bf3.Et2o. *Bull. Korean Chem. Soc.* **2004,** *25,* 407-409.

160. Davis, R.; Untch, K. G. Direct One-Step Conversion of Alcohols into Nitriles. *J. Org. Chem.* **1981,** *46,* 2985-2987.

161. Wolfrom, M. L.; Koos, E. W.; Bhat, H. B. Osage Orange Pigments. XVIII. Synthesis of Osajaxanthone. *J. Org. Chem.* **1967,** *32,* 1058-1060.

162. Martin, W. R.; Eades, C. G.; Thompson, J. A.; Huppler, R. E.; Gilbert, P. E. The Effects of Morphine- and Nalorphine- Like Drugs in the Nondependent and Morphine-Dependent Chronic Spinal Dog. *J. Pharmacol. Exp. Ther.* **1976,** *197,* 517-532.

163. Tam, S. W. Naloxone-Inaccessible Sigma Receptor in Rat Central Nervous System. *Proc. Natl. Acad. Sci. U S A.* **1983,** *80,* 6703-6707.

164. Matsumoto, R. R.; Liu, Y.; Lerner, M.; Howard, E. W.; Brackett, D. J. Sigma Receptors: Potential Medications Development Target for Anti-Cocaine Agents. *Eur. J. Pharmacol.* **2003,** *469,* 1-12.

165. Kawamura, K.; Ishiwata, K.; Tajima, H.; Ishii, S.; Shimada, Y.; Matsuno, K.; Homma, Y.; Senda, M. Synthesis and in Vivo Evaluation of [11c]Sa6298 as a Pet Sigma1 Receptor Ligand. *Nucl. Med. Biol.* **1999,** *26,* 915-922.

166. Kawamura, K.; Ishiwata, K.; Tajima, H.; Ishii, S.; Matsuno, K.; Homma, Y.; Senda, M. In Vivo Evaluation of [(11)C]Sa4503 as a Pet Ligand for Mapping Cns Sigma(1) Receptors. *Nucl. Med. Biol.* **2000,** *27,* 255-261.

167. Wolfe, S. A., Jr.; Culp, S. G.; De Souza, E. B. Sigma-Receptors in Endocrine Organs: Identification, Characterization, and Autoradiographic Localization in Rat Pituitary, Adrenal, Testis, and Ovary. *Endocrinology.* **1989,** *124*, 1160-1172.

168. Bouchard, P.; Quirion, R. [3h]1,3-Di(2-Tolyl)Guanidine and [3h](+)Pentazocine Binding Sites in the Rat Brain: Autoradiographic Visualization of the Putative Sigma1 and Sigma2 Receptor Subtypes. *Neuroscience.* **1997,** *76*, 467-477.

169. Walker, J. M.; Bowen, W. D.; Walker, F. O.; Matsumoto, R. R.; De Costa, B.; Rice, K. C. Sigma Receptors: Biology and Function. *Pharmacol. Rev.* **1990,** *42*, 355-402.

170. Hellewell, S. B.; Bruce, A.; Feinstein, G.; Orringer, J.; Williams, W.; Bowen, W. D. Rat Liver and Kidney Contain High Densities of Sigma 1 and Sigma 2 Receptors: Characterization by Ligand Binding and Photoaffinity Labeling. *Eur. J. Pharmacol.* **1994,** *268*, 9-18.

171. Newman, A. H.; Coop, A., Medicinal Chemistry: New Chemical Classes and Subtype-Selective Ligands. In *Sigma Receptors: Chemistry, Cell Biology and Clinical Implications*, Matsumoto, R. R.; Bowen, W. D.; Su, T. P., Eds. Springer: New York, **2007**; pp 25-44.

172. Maeda, D. Y.; Williams, W.; Kim, W. E.; Thatcher, L. N.; Bowen, W. D.; Coop, A. N-Arylalkylpiperidines as High-Affinity Sigma-1 and Sigma-2 Receptor Ligands: Phenylpropylamines as Potential Leads for Selective Sigma-2 Agents. *Bioorg. Med. Chem. Lett.* **2002,** *12*, 497-500.

173. Jung, D.; Floyd, J.; Gund, T. M. A Comparative Molecular Field Analysis (Comfa) Study Using Semiempirical, Density Functional, Ab Initio Methods and Pharmacophore Derivation Using Discotech on Sigma 1 Ligands. *J. Comput. Chem.* **2004,** *25*, 1385-1399.

174. Cratteri, P.; Romanelli, M. N.; Cruciani, G.; Bonaccini, C.; Melani, F. Grind-Derived Pharmacophore Model for a Series of Alpha-Tropanyl Derivative Ligands of the Sigma-2 Receptor. *J. Comput. Aided Mol. Des.* **2004**, *18*, 361-374.

175. Crawford, K. W.; Coop, A.; Bowen, W. D. Sigma(2) Receptors Regulate Changes in Sphingolipid Levels in Breast Tumor Cells. *Eur. J. Pharmacol.* **2002**, *443*, 207-209.

176. Matsumoto, R. R.; Shaikh, J.; Wilson, L. L.; Wang, J. J.; Coop, A. Ac927, a Selective Sigma Receptor Antagonist, Attenuates the Locomotor Stimulant and Neurotoxic Effects of Methamphetamine in Mice. *FASEB J.* **2007**, *21*, A777.

177. Shaikh, J.; Matsumoto, R. R. Effects of Sigma Receptor Antagonists, Bd1063 and Ac927, on Methamphetamine-Induced Dopamine Damage in Mouse Striatum. *FASEB J.* **2007**, *19*, A1081.

178. Matsumoto, R. R.; Pouw, B.; Mack, A. L.; Daniels, A.; Coop, A. Effects of Umb24 and (+/-)-Sm 21, Putative Sigma2-Preferring Antagonists, on Behavioral Toxic and Stimulant Effects of Cocaine in Mice. *Pharmacol. Biochem. Behav.* **2007**, *86*, 86-91.

179. Dewey, W. L., *National Institute on Drug Abuse Research Monograph Series.* U.S. Department of Health and Human Services, National Institutes of Health: Bethesda, MD, **2005**; Vol. 186.

180. Morrison, A.; Rinderknecht, H. Synthetic Analgesics. V. Compounds Related to Pethidine. *J. Chem. Soc.* **1950**, 1467-1469.

181. Thompson, D.; Reeves, P. C. Facile Synthesis of N-Substituted-4-Cyano-4-Phenylpiperidines Via Phase-Transfer Catalysis. *J. Heterocyc. Chem.* **1983**, *20*, 771-772.

182. Rehse, K.; Werner, U. Platelet Aggregation Inhibiting and Anticoagulant Effects of Oligoamines. I. N-(4-Piperidinyl)Methanamines. *Archiv. der Pharmazie.* **1986,** *319,* 505-515.

183. Daniels, A.; Ayala, E.; Chen, W.; Coop, A.; Matsumoto, R. R. N-[2-(M-Methoxyphenyl)Ethyl]-N-Ethyl-2-(1-Pyrrolidinyl)Ethylamine (Umb 116) Is a Novel Antagonist for Cocaine-Induced Effects. *Eur. J. Pharmacol.* **2006,** *542,* 61-68.

184. Ablordeppey, S. Y.; Glennon, R. A., Pharmacophore Models for Sigma-1 Receptor Binding. In *Sigma Receptors: Chemistry, Cell Biology and Clinical Implications,* Matsumoto, R. R.; Bowen, W. D.; Su, T. P., Eds. Springer: New York, **2007;** pp 71-98.

185. Mei, J.; Pasternak, G. W. Molecular Cloning and Pharmacological Characterization of the Rat Sigma1 Receptor. *Biochem. Pharmacol.* **2001,** *62,* 349-355.

186. McMahon, R. E.; Culp, H. W.; Cymerman, C. J.; Ekwuribe, N. Mechanism of the Dealkylation of Tertiary Amines by Hepatic Oxygenases. Stable Isotope Studies with 1-Benzyl-4-Cyano-4-Phenylpiperidine. *J. Med. Chem.* **1979,** *22,* 1100-1103.

187. Maeda, D. Y.; Coop, A. Studies into the Direct Conversion of Indolomorphinans to Their 4-Phenolic Derivatives. *Tetrahedron.* **2000,** *56,* 7399-7402.

188. Matsumoto, R. R.; McCracken, K. A.; Pouw, B.; Zhang, Y.; Bowen, W. D. Involvement of Sigma Receptors in the Behavioral Effects of Cocaine: Evidence from Novel Ligands and Antisense Oligodeoxynucleotides. *Neuropharmacology.* **2002,** *42,* 1043-1055.

189. Moore, B. W. A Soluble Protein Characteristic of the Nervous System. *Biochem. Biophys. Res. Commun.* **1965,** *19,* 739-744.

190. Donato, R. Intracellular and Extracellular Roles of S100 Proteins. *Microsc. Res. Tech.* **2003,** *60,* 540-551.

191. Heizmann, C. W. The Multifunctional S100 Protein Family. *Methods Mol. Biol.* **2002,** *172,* 69-80.

192. Santamaria-Kisiel, L.; Rintala-Dempsey, A. C.; Shaw, G. S. Calcium-Dependent and - Independent Interactions of the S100 Protein Family. *Biochem. J.* **2006,** *396,* 201-214.

193. Weber, D. J.; Rustandi, R. R.; Carrier, F.; Zimmer, D. B., Interaction of Dimeric S100b(Bb) with the Tumor Suppressor Protein: A Model for Ca-Dependent S100-Target Protein Interactions. In *The Molecular Basis of Calcium Action in Biology and Medicine,* Pochet, R., Ed. Kluwer Academic Publishers: Dordrecht, The Netherlands, **2000**; pp 469-487.

194. Zimmer, D. B.; Cornwall, E. H.; Landar, A.; Song, W. The S100 Protein Family: History, Function, and Expression. *Brain Res. Bull.* **1995,** *37,* 417-429.

195. Boni, R.; Heizmann, C. W.; Doguoglu, A.; Ilg, E. C.; Schafer, B. W.; Dummer, R.; Burg, G. Ca(2+)-Binding Proteins S100a6 and S100b in Primary Cutaneous Melanoma. *J. Cutan. Pathol.* **1997,** *24,* 76-80.

196. Hansson, L. O.; von Schoultz, E.; Djureen, E.; Hansson, J.; Nilsson, B.; Ringborg, U. Prognostic Value of Serum Analyses of S-100 Protein Beta in Malignant Melanoma. *Anticancer Res.* **1997,** *17,* 3071-3073.

197. Maelandsmo, G. M.; Florenes, V. A.; Mellingsaeter, T.; Hovig, E.; Kerbel, R. S.; Fodstad, O. Differential Expression Patterns of S100a2, S100a4 and S100a6 During Progression of Human Malignant Melanoma. *Int. J. Cancer.* **1997,** *74,* 464-469.

198. Camby, I.; Lefranc, F.; Titeca, G.; Neuci, S.; Fastrez, M.; Dedecken, L.; Schafer, B. W.; Brotchi, J.; Heizmann, C. W.; Pochet, R.; Salmon, I.; Kiss, R.; Decaestecker, C. Differential Expression of S100 Calcium-Binding Proteins Characterizes Distinct Clinical

Entities in Both Who Grade Ii and Iii Astrocytic Tumours. *Neuropathol. Appl. Neurobiol.* **2000,** *26*, 76-90.

199.   Camby, I.; Nagy, N.; Lopes, M. B.; Schafer, B. W.; Maurage, C. A.; Ruchoux, M. M.; Murmann, P.; Pochet, R.; Heizmann, C. W.; Brotchi, J.; Salmon, I.; Kiss, R.; Decaestecker, C. Supratentorial Pilocytic Astrocytomas, Astrocytomas, Anaplastic Astrocytomas and Glioblastomas Are Characterized by a Differential Expression of S100 Proteins. *Brain Pathol.* **1999,** *9,* 1-19.

200.   Davey, G. E.; Murmann, P.; Heizmann, C. W. Intracellular Ca2+ and Zn2+ Levels Regulate the Alternative Cell Density-Dependent Secretion of S100b in Human Glioblastoma Cells. *J. Biol. Chem.* **2001,** *276*, 30819-30826.

201.   Hauschild, A.; Engel, G.; Brenner, W.; Glaser, R.; Monig, H.; Henze, E.; Christophers, E. S100b Protein Detection in Serum Is a Significant Prognostic Factor in Metastatic Melanoma. *Oncology.* **1999,** *56*, 338-344.

202.   Hauschild, A.; Engel, G.; Brenner, W.; Glaser, R.; Monig, H.; Henze, E.; Christophers, E. Predictive Value of Serum S100b for Monitoring Patients with Metastatic Melanoma During Chemotherapy and/or Immunotherapy. *Br. J. Dermatol.* **1999,** *140*, 1065-1071.

203.   Hauschild, A.; Michaelsen, J.; Brenner, W.; Rudolph, P.; Glaser, R.; Henze, E.; Christophers, E. Prognostic Significance of Serum S100b Detection Compared with Routine Blood Parameters in Advanced Metastatic Melanoma Patients. *Melanoma Res.* **1999,** *9*, 155-161.

204.   Baudier, J.; Delphin, C.; Grunwald, D.; Khochbin, S.; Lawrence, J. J. Characterization of the Tumor Suppressor Protein P53 as a Protein Kinase C Substrate and a S100b-Binding Protein. *Proc. Natl. Acad. Sci. U.S.A.* **1992,** *89*, 11627-11631.

205. Delphin, C.; Ronjat, M.; Deloulme, J. C.; Garin, G.; Debussche, L.; Higashimoto, Y.; Sakaguchi, K.; Baudier, J. Calcium-Dependent Interaction of S100b with the C-Terminal Domain of the Tumor Suppressor P53. *J. Biol. Chem.* **1999,** *274,* 10539-10544.

206. Lin, J.; Yang, Q.; Yan, Z.; Markowitz, J.; Wilder, P. T.; Carrier, F.; Weber, D. J. Inhibiting S100b Restores P53 Levels in Primary Malignant Melanoma Cancer Cells. *J. Biol. Chem.* **2004,** *279,* 34071-34077.

207. Rustandi, R. R.; Baldisseri, D. M.; Weber, D. J. Structure of the Negative Regulatory Domain of P53 Bound to S100b(Betabeta). *Nat. Struct. Biol.* **2000,** *7,* 570-574.

208. Rustandi, R. R.; Drohat, A. C.; Baldisseri, D. M.; Wilder, P. T.; Weber, D. J. The Ca(2+)-Dependent Interaction of S100b(Beta Beta) with a Peptide Derived from P53. *Biochemistry.* **1998,** *37,* 1951-1960.

209. Wilder, P. T.; Lin, J.; Bair, C. L.; Charpentier, T. H.; Yang, D.; Liriano, M.; Varney, K. M.; Lee, A.; Oppenheim, A. B.; Adhya, S.; Carrier, F.; Weber, D. J. Recognition of the Tumor Suppressor Protein P53 and Other Protein Targets by the Calcium-Binding Protein S100b. *Biochim. Biophys. Acta.* **2006,** *1763,* 1284-1297.

210. Levine, A. J. P53 the Cellular Gatekeeper for Growth and Division. *Cell.* **1997,** *88,* 323-331.

211. Levine, A. J.; Momand, J.; Finlay, C. A. The P53 Tumour Suppressor Gene. *Nature.* **1991,** *351,* 453-456.

212. Markowitz, J.; Chen, I.; Gitti, R.; Baldisseri, D. M.; Pan, Y.; Udan, R.; Carrier, F.; MacKerell, A. D., Jr.; Weber, D. J. Identification and Characterization of Small Molecule Inhibitors of the Calcium-Dependent S100b-P53 Tumor Suppressor Interaction. *J. Med. Chem.* **2004,** *47,* 5085-5093.

213. Markowitz, J.; Mackerell, A. D., Jr.; Carrier, F.; Charpentier, T. H.; Weber, D. J. Design of Inhibitors for S100b. *Curr. Top. Med. Chem.* **2005,** *5,* 1093-1108.

214. Markowitz, J.; MacKerell, A. D., Jr.; Weber, D. J. A Search for Inhibitors of S100b, a Member of the S100 Family of Calcium-Binding Proteins. *Mini Rev. Med. Chem.* **2007,** *7,* 609-616.

215. Hisashi, T.; Akito, T.; Hiroyoshi, S.; Takatoshi, I. New Peptide Compound and a Process for the Preparation Thereof. EP 513675 A1, **1992.**

216. Charpentier, T. H.; Wilder, P. T.; Liriano, M. A.; Varney, K. M.; Pozharski, E.; MacKerell Jr., A. D.; Coop, A.; Toth, E. A.; Weber, D. J. Divalent Metal Ion Complexes of S100b in the Absence and Presence of Pentamidine. *J. Mol. Bio.* **2008,** in review.

217. Markowitz, J. S.; Chen, I.; Gitti, R.; Baldisseri, D. M.; Pan, Y.; Udan, R.; Carrier, F.; MacKerell Jr., A. D.; Weber, D. J. Identification and Characterization of Small Molecule Inhibitors of the Calcium-Dependent S100b-P53 Tumor Suppressor Interaction. *J. Med. Chem.* **2004,** *47,* 5085-5093.

218. Mori, S.; Abeygunawardana, C.; Johnson, M. O.; van Zijl, P. C. Improved Sensitivity of Hsqc Spectra of Exchanging Protons at Short Interscan Delays Using a New Fast Hsqc (Fhsqc) Detection Scheme That Avoids Water Saturation. *J. Magn. Reson. B.* **1995,** *108,* 94-98.

219. Edison, A. S.; Abildgaard, F.; Westler, W. M.; Mooberry, E. S.; Markley, J. L. Practical Introduction to Theory and Implementation of Multinuclear, Multidimensional Nuclear Magnetic Resonance Experiments. *Methods Enzymol.* **1994,** *239,* 3-79.

220. Live, D. H.; Davis, D. G.; Agosta, W. C.; Cowburn, D. Long Range Hydrogen Bond Mediated Effects in Peptides: ^{15}N NMR Study of Gramicidin S in Water and Organic Solvents. *J Am Chem Soc.* **1984,** *106,* 1939-1941.

221. Spera, S.; Bax, A. Empirical Correlation between Protein Backbone Conformation and C(Alpha) and C(Beta)/13-C Nuclear Magnetic Resonance Chemical Shifts. *J. Am. Chem. Soc.* **1991,** *113,* 5490-5492.